Research in AGRICULTURAL ENGINEERING

Czech Academy of Agricultural Sciences

VOLUME 60
Special Issue
Prague 2014
ISSN 1212-9151 (Print)
ISSN 1805-9376 (On-line)

Research in AGRICULTURAL ENGINEERING

formerly ZEMĚDĚLSKÁ TECHNIKA since 1955 to 1999

An international peer-reviewed journal published by the Czech Academy of Agricultural Sciences and financed by the Ministry of Agriculture of the Czech Republic

Aims and scope: The journal of RAE publishes original research papers devoted to all scientific and applied aspects of Agricultural Engineering including those laying on the border with other scientific disciplines, for example mechatronics, IT, robotics, ecology, energetics, economy, ergonomic, applied physics, biochemistry, biotechnology, bionics and waste management. Special at attention is devoted to new technologies with respect to their environmental aspects and agricultural products quality control. Papers are published in English (British spelling).

Abstracts are comprised in:
- Agrindex of AGRIS/FAO database
- CAB Abstracts
- Czech Agricultural and Food Bibliography
- SCOPUS

Periodicity: 4 issues per year, volume 60 appearing in 2014.

Editorial Office

Research in Agriculture Engineering, Ing. Eva Karská, Executive Editor, Czech Academy of Agricultural Sciences, Slezská 7, 120 00 Prague 2, Czech Republic, phone: + 420 227 010 606, fax: + 420 227 010 116, e-mail: rae@cazv.cz

Subscription information

Subscription orders can be entered only by calendar year and should be sent to: Czech Academy of Agricultural Sciences, Slezská 7, 120 00 Prague 2, Czech Republic. Subscription price is 155 USD (subscribers from the Czech Republic can apply for special rates).

Electronic access

Full papers from Vol. 48 (2002), instructions to authors and information on all journals edited by the Czech Academy of Agricultural Sciences are available at http://agriculturejournals.cz/web/rae.htm

Online Manuscript Submission

All manuscripts must be submitted to the journal website (http://agriculturejournals.cz/web/rae.htm). Authors are requested to submit the text, tables, and artwork in electronic form to this web address. Authors unable to submit an electronic version should contact by e-mail the Editorial Office.
Both the dates of the receipt of the manuscript and of the acceptance by the Managing Editorial Board for publishing will be indicated in the printed contribution.

MK ČR E 6698

Research in **AGRICULTURAL ENGINEERING**

formely ZEMĚDĚLSKÁ TECHNIKA

Volume 60 **2014**

Research in AGRICULTURAL ENGINEERING

Volume *60*, 2014, Special Issue

CONTENTS

Go to the website for information about Research in Agricultural Engineering:
http://www.agriculturejournals.cz/web/RAE.htm

Effect of irrigation machines on soil compaction

J. Jobbágy, P. Findura, F. Janík

Department of Machines and Production Systems, Faculty of Engineering, Slovak University of Agriculture in Nitra, Nitra, Slovak Republic

Abstract

Jobbágy J., Findura P., Janík F., 2014. **Effect of irrigation machines on soil compaction**. Res. Agr. Eng., *60* (Special Issue): S1–S8.

The analysis of soil compaction with chassis of a wide-span irrigation machine Valmont was determined. The sprinkler had 12 two-wheeled chassis (size of tyre 14.9" × 24"). During the evaluation of soil compaction, we monitored the values of penetration resistance and soil moisture during the operation of the sprinkler. Considering the performance parameters of the pump, the sprinkler was only half of its length (300 m) in the technological operation. In this area, also field measurements were performed in 19 monitoring points spaced both in tracks and outside the chassis tracks. The analysis showed the impact of compression with sprinkler wheels. The correction of obtained results of penetration resistance was applied in connection with soil moisture (mass) values according to Act No. 220/2004 (Lhotský et al. 1985). The results of average resistance ranged from 1.2 to 3.26 MPa. The values of the max. resistance ranged from 2.3 to 5.35 MPa. The results indicated a shallow soil compaction; however, it is not devastating.

Keywords: penetration resistance; soil moisture; sprinkler; soil

Soil compaction is a serious problem that adversely affects the productivity of crops, while crop yields are significantly reduced. It is a process of soil particles relocation, which reduces soil porosity, thereby causing an aeration decrease and an increase in volume density and soil strength (Al-Adawi, Reeder 1996; Hillel 1998; Brady, Weil 1999).

Soil compaction greatly affects the physical condition of the soil profile, especially with the pressure of agricultural machinery in cultivation and harvest. The result of this pressure is a technological or secondary compaction of the soil profile, defined with critical values of physical soil properties, particularly with a high volumetric density and low porosity (Fulajtár 2005).

An overview of the spatial distribution of compacted soil layers can be obtained by measuring the soil penetration resistance, which depends on volumetric density and soil moisture. For a precise definition of the extent of compacted soil layers, it is important to determine its vertical and horizontal spatial distribution. The critical value of soil compaction for plant growth is dependent on soil type and soil moisture (Schuler, Woods 1992).

In terms of soil particle size, compacted sandy soils have little or no ability of spontaneous recovery, while for heavier soils, there are factors that allow reversible processes (regeneration of soil structure) (Mašek 2005).

Soil properties characterize the operating conditions of tractors and influence the load of hydraulic and transmission systems. Therefore, we have to determine the soil properties in operating conditions of a tractor (Majdan et al. 2011). Interaction between the tyre and soil affects the exploitation of

Supported by the Scientific Grant Agency VEGA of the Ministry of Education of the Slovak Republic and the Slovak Academy of Sciences, Grant No. 1/0407/11.

machinery in agriculture (Šesták et al. 1998; Rédl 2009).

Soil compaction increases soil strength and decreases soil physical fertility through decreasing storage and supply of water and nutrients, which leads to additional fertiliser requirement and increasing production cost (Hamza, Anderson 2005).

There are environmental effects of soil compaction. The effect of compacted soil on the emissions released from soil into the atmosphere were observed for N_2O (Šima et al. 2013) and CO_2 (Šima, Dubeňová 2013).

MATERIAL AND METHODS

The main objective was to investigate the effect of soil compaction with the axles of a wide-span irrigation machine and to evaluate the acquired knowledge and outcomes of the measurement. To meet these objectives, in 2011 some field measurements were made in conditions of a farm Kovacs Agro, s.r.o., Hronovce, Slovak Republic. The arrangement of monitoring points was performed according to Fig. 1. These points were located not only in tracks of the chassis but also outside them. The number of monitoring points was 19. Field experiments also included the measurement of soil moisture content (WET sensor; DELTA-T Devices Ltd., Cambridge, UK; HH2 logger; DELTA-T Devices Ltd., Cambridge, UK) and penetration resistance (Penetrologger Eijkelkamp; Eijkelkamp, Giesbeek, Netherlands; Fig. 2). The experiments were conducted at certain soil moisture during the operation of the irrigation machine. Penetration resistance was measured simultaneously with the measurement of soil moisture. We used a conical tip with an angle of 30°, which is recommended by the ASAE Standard S313.2 (1994) for heavy and medium soils. The measurement of soil penetration resistance requires a uniform pressing of the cone into the soil (about 3 cm/s). The penetrologger's measuring range is 0–10 MPa. This device allows recording the soil profile to a depth of 0.8 m, with a depth resolution of 10 mm. During the penetration, depth is sensed with an internal ultrasound sensor. When measuring the penetration resistance, each measurement consisted of three measurements. The depth of measurements was up to a 40 cm depth. Measured values of penetration resistance were corrected by obtained values of soil moisture (in percentage by weight). This was determined by a gravimetric method. Measuring the moisture with the WET sensor was carried out for each monitoring point three times.

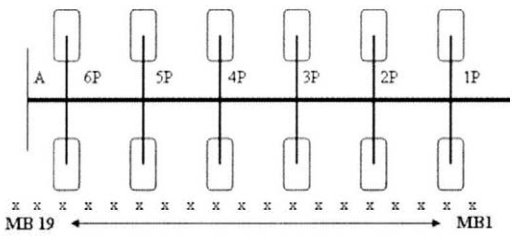

Fig. 1. Principe of measurement of soil parameters

A – centre of wide range irrigation machine, P – tower, x – monitoring points, MB – monitoring point

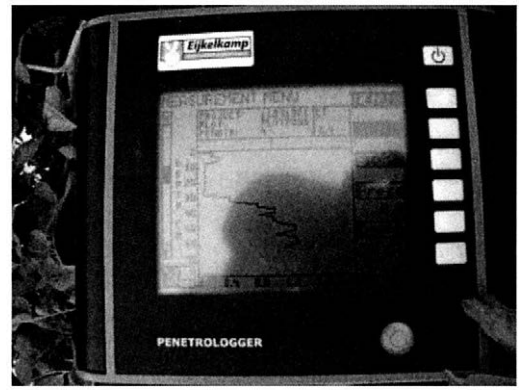

Fig. 2. Penetrologger Eijkelkamp – measurement

Field measurements were performed for the sprinkler Valley (Valley Irrigation, Holdrege, USA; Fig. 3), linear type, with a length of 594.59 m and the number of chassis 12 (Table 1). Besides the central tower (4 wheels), each chassis was equipped with two wheels. Only a half was always in operation (300 m, the entire irrigation machine moved, but only half sprayed water). A problem was the performance parameters of the pump, which would not cover a reliable technological operation of irrigation equipment for a length of 600 m. A water-pumping station was used as a water source.

The effect of the sprinkler chassis on soil compaction was investigated by monitoring the compaction level in wheel tracks and outside them. Measurements were corrected and evaluated according to the Slovak Act No. 220/2004. When the soil moisture was above the correction interval, soil resistance was actually lower, and we had to add

Fig. 3. Linear irrigation machines Valley Valmont, 600 m: (a) machine and (b) tyre

0.25 MPa per each percentage by weight outside the interval. If soil moisture was below the correction interval, it was necessary to deduct 0.25 MPa per each percentage by weight outside the interval. In terms of our research, in clay soils this interval was 18–16% of soil moisture (percentage by weight). Therefore, data were corrected according to LHOTSKÝ et al. (1985), and the correction of the results is defined as follows:

$$PO_{KL} = (PO \pm 0.25z) \quad (1)$$

where:

PO – measured penetration resistance (MPa)

PO_{KL} – corrected penetration resistance according to LHOTSKÝ et al. (1985) (MPa)

z – difference between the prescribed and measured moisture; its sign depends on whether it is above or below the range

Table 1. Technical characteristic of wide range irrigation machine (Valley, Valmont)

Parameter	Value
Sprinkler spacing	192 cm
Number of two-wheeled chassis	12
System length	594.59 m
Type of wheels	high float 14.9" × 24"
Width of wheels	37.8 cm
Power supply	480 V/60 Hz
Maximum speed of system travel	123.6 m/h
Approx. weight (with water), length of section 49.12 m	2,814 kg
Approx. weight (with water), length of section 54.86 m	3,080 kg
Required run power	20 kW
Type of guidance	below ground – shielded
Length of guidance cable	5,608 m

RESULTS AND DISCUSSION

The selected field is included in BPEJ 0039002. It is a very warm, dry and lowland region, Haplic Chernozem and Luvi-Haplic Chernozem on loess, slope 0–1°, a plane without surface water erosion, medium (loamy) soil, according to the granularity code. The total area of the field was 181.31 ha, of which the irrigated area was 180.14 ha, which means a 99.35 % coverage.

Variability of soil moisture

Soil moisture is a key feature of the soil for crop irrigation regime. Measurements were conducted at 19 monitoring points in wheel tracks of the sprinkler and outside them. Table 2 shows the descriptive statistics of measurements before the application of irrigation rates. The average value of soil moisture was 10.11% vol. However, the value of the coefficient of variation was high (31.55%). After irrigation, values of soil moisture increased on average by 20.83% vol. The value of the coefficient of variation in measuring the volumetric soil moisture decreased to 17.86%. In this case, there was a positive effect of irrigation and more balanced soil moisture across the whole width of the irrigation machine (Fig. 4).

Variability of penetration resistance

In determining the variability of penetration resistance, measurements were performed before irrigation. After irrigation, measurements of penetration resistance were sufficiently affected by soil moisture because all values are outside of the range defined by LHOTSKÝ et al. (1985). Therefore, a cor-

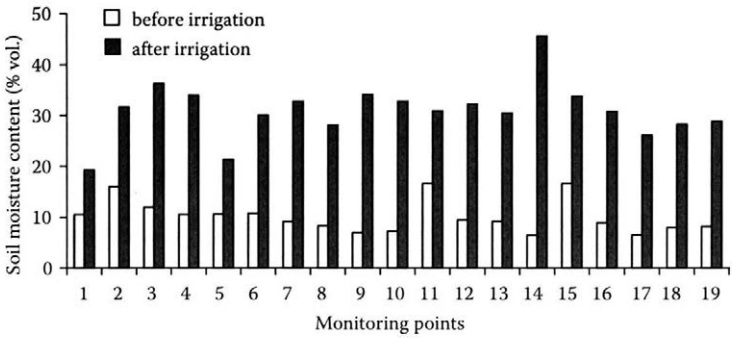

Fig. 4. Soil moisture content before and after irrigation

rection factor of humidity was used, and all data were corrected according to the Act No. 220/2004 on the conservation and use of agricultural land. Values of penetration resistance were corrected to 18–16% vol. soil moisture.

It follows from the collected data that the farm extensively applies the principles preventing an undesired impact of agricultural machinery on the soil on the monitored field, since the average value of penetration resistance ranged from 1.2 to 3.26 MPa (Fig. 5a). The max. values of penetration resistance ranged from 2.3 to 5.35 MPa (Fig. 5b). The limit value for the max. soil penetration resistance was exceeded at two monitoring points (P5 and P6).

According to the ASAE Standard EP542 (2004), 2 MPa is the value of penetration resistance which already limits the development of the root system of plants; however, this standard does not distinguish between soil types. The variability of penetration resistance is given by the variability of moisture conditions and passes of machines, too.

When comparing the data obtained, we concluded that penetration resistance increased in wheel tracks of the irrigation machine. The graphical representation shows that penetration resistance in wheel tracks after machine passes is higher than outside of tracks. Fig. 6 shows the secondary compaction which is significant especially in the depth of up to 10 cm.

Determining the effect of soil moisture on penetration resistance

To illustrate the effect of soil moisture on penetration resistance (Fig. 7), we used average values of penetration resistance and soil moisture. The reliability coefficient R^2 has a value of 0.0074. By transfering the obtained dependence with a trendline penetration resistance rises slightly with increasing soil moisture. On the basis of values of the coefficient R^2 trial there was no dependence of penetration resistance on soil moisture. Fig. 8 also

Table 2. Measured data, soil moisture content, percentage by volume and by weight before and after irrigation

Parameter	Soil moisture content (% wt.)		Soil moisture content (% vol.)	
	before irrigation	after irrigation	before irrigation	after irrigation
Average	8.44	25.78	10.11	30.94
Median	7.76	25.49	9.20	30.90
Modus	8.78	–	10.53	32.80
Standard deviation	2.66	4.74	3.19	5.52
Variance	7.08	22.49	10.20	30.52
Difference max-min	8.47	22.39	10.16	26.30
Minimum	5.39	15.82	6.47	19.30
Maximum	13.86	38.21	16.63	45.60
Sum	160.27	489.83	192.12	587.80
Sample size	19.00	19.00	19.00	19.00
Coefficient of variation	31.54	18.39	31.55	17.86

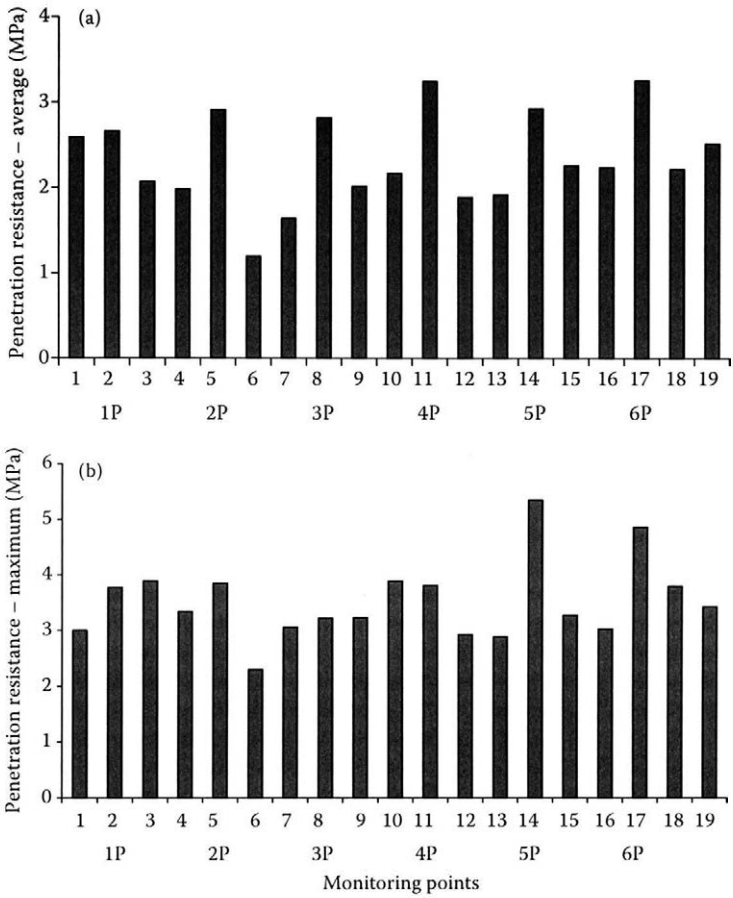

Fig. 5. Penetration resistance of soil (a) average and (b) maximum
P – tower

shows the extreme values of penetration resistance in several measuring points. After application of irrigation depth the value of penetration resistance decreased depending on the depth measurement (Fig. 8). Soil compaction with the impact machine passes is a specific phenomenon that is becoming even more a current topic in our conditions due to a constant modernization of machinery.

Based on the obtained literatures (HILLER 1998; DUIKER 2004; FULAJTÁR 2005), it can be concluded that it is necessary to evaluate the soil compaction always with respect to current humidity conditions, the presence of a particular crop, soil types, and used machinery. Soil compaction is caused by effects of increasingly heavy machinery on soil as well as tillage and passes under an improper soil moisture. Increasing compaction is affected not only by tractors and harvesters but also by other self-propelled, trailer and semi-trailer machines. In general, shallow soil compaction is attributed to pressure in the "tyre-soil" area, while deep soil compaction refers to the effects of the total axle load on soil (DUIKER 2004).

When using the wide-span irrigation machine with selected tyres, an effect of the chassis on shallow soil compaction was confirmed. The values of penetration resistance ranged from 0 to 3.13 MPa in tracks and outside them. The highest changes were demonstrated in the tracks of the second chassis (tower). However, it is possible to state that the irrigation machine with its total mass divided into individual chassis does not cause devastating compaction. It is rather only a local and shallow soil compaction which can be removed with appropriate tillage. The soil moisture content is an important factor for passes of machines. The soil moisture content is determined from a disturbed soil sample. Another factor is the total weight of the machine and the total contact area. The number of machine passes on the soil is needed to be

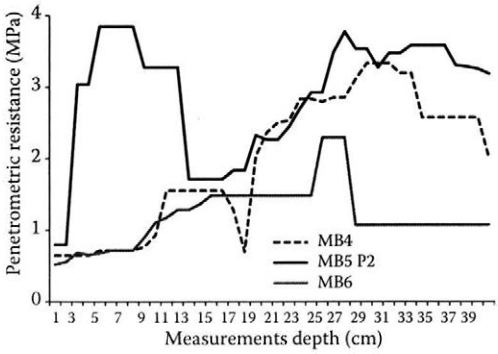

Fig. 6. Relationship between penetration resistance and measurement depth in monitoring points

MB4, MB6 – monitoring point outside of chassis; MB5 – monitoring point within the chassis (tower 2P)

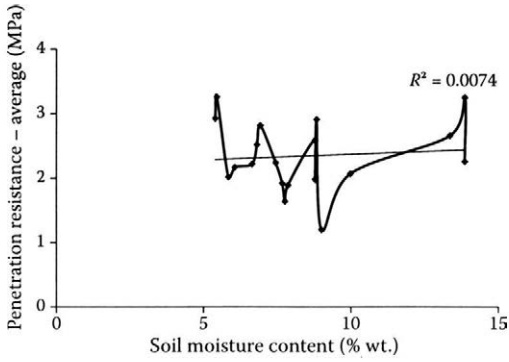

Fig. 7. Relationship between penetration resistance and soil moisture content

monitored and reduced. Joining certain operations can contribute to reducing soil compaction.

VÁCHAL et al. (1983) recommend the reduction of passes after sub-soiling in the first year, to merge machines into aggregates, and to grow deep-rooted crops at least two years after intervention. All the performed measures must lead to creating an optimal soil structure and its protection.

Machine passes on the soil can cause its compression; they can reduce the soil porosity and create barriers to water and air movement in the soil and roots penetration in the soil. Soil compaction is determined by several methods. Most of them require soil sampling, time necessary for laboratory analyses, or a long period of field preparation where holes are prepared for ditch sensors.

Probably, the fastest way to determine soil compaction is the measuring of penetration resistance. The results of penetration resistance on the monitored field confirmed a higher soil resistance in wheels tracks of the irrigation machine. CARRARA et al. (2003) state that there are a lot of examples where penetration resistance is used for monitoring the soil compaction.

During the year, the soil responds to machine passes in different ways. Soil resistance to compaction decreases with increasing soil moisture. Humid and light soils have a very low resistance during seedbed preparation and sowing when passes cause compaction of the topsoil and subsoil, which affects the crop grown during the whole growing season. Other risky periods occur during autumn field operations when loaded machines compact the soil into a high depth (HŮLA 1989). Our values were evaluated in conformance with the values introduced in the Act No. 220/2004. The results have shown a clear effect of irrigation machine wheels on compaction.

The presented act specifies the limit values of corrected penetration resistance ranging from 3.7 to 4.2 MPa at the moisture of 18–16% wt. for clayey soil. Our results have not exceeded these limit values. It means that compaction values harmful for plant growth were not exceeded. However, there was a higher compression in wheels tracks of the irrigation machine.

Solving this issue in relation to soil compaction has focused mainly on a new design of tyres and weight reduction of machines. Before new design of tyres got into production, it was recommended to use double wheels to reduce soil compaction with

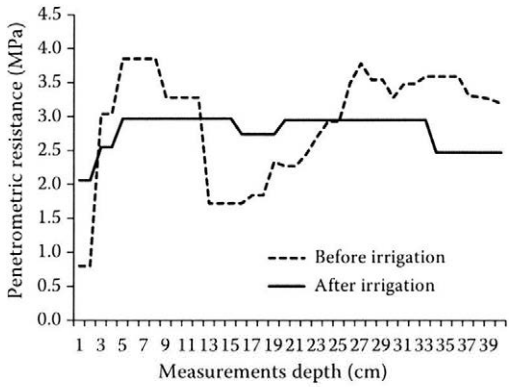

Fig. 8. Relationship between penetration resistance and measurement depth in monitoring point MB5, tower 2, before and after irrigation

contact pressures. Controlled underinflated tyres of machines also appear to be suitable for driving on fields. However, new constructions of low-pressure tyres are currently dominating (JAVŮREK, VACH 2008). The model of tyres used on the irrigation machine Valmont was also radial on all the axles due to a lower compaction in their tracks.

According to ABEDIN and HETTIARATCHI (2002), the incidence of compacted layers in the soil profile is usually possible to detect only in the spring when the soil profile is evenly moistened. Measurement in summer and in autumn is unreliable because the soil profile can show large moisture differences, which are reflected in the values of soil penetration resistance.

CONCLUSION

Soil compaction caused by machinery is a specific phenomenon that is becoming even more a current topic in our conditions due to a constant modernization of machines. In examining the variability of penetration resistance in dependence on the monitoring point, we found that in wheel tracks of the irrigation machine, penetration resistance is higher than outside of tracks. Based on the results, we can say that due to a lower weight of the whole machine in comparison with other machines, there was only a shallow soil compaction. In our case, penetration resistance increased with depth. At some monitoring points, penetration resistance reached the max. value of 5 MPa. Measurement results were corrected with soil moisture according to LHOTSKÝ et al. (1985) and Act No. 220/2004. We would recommend to map the entire field and to determine the variability of penetration resistance throughout the field.

References

ABEDIN M.Z., HETTIARATCHI D.R.P., 2002. State parameter interpretation of cone penetration tests in agricultural soils. Biosystems Engineering, *83*: 469–479.

Act No. 220/2004 on the Conservation and Use of Agricultural Land. Available at www.zbierka.sk/sk/predpisy/220-2004-z-z.p-7816.pdf (accessed January 28, 2013)

AL-ADAWI S.S., REEDER R.C., 1996. Compaction and subsoiling effects on corn and soybean yields and soil physical properties. Transactions of the ASABE, *39*: 1641–1649.

ASAE Standards, 1994. Soil Cone Penetrometer. ASAE S312.3. Standards Engineering Practices Data. St. Joseph, ASAE.

ASAE Standards, 2004. EP542 Procedures for using and reporting data obtained with the soil cone penetrometer. 50th Ed. St. Joseph, ASAE.

BRADY N.C., WEIL R.R., 1999. The Nature and Properties of Soil. New Jersey, Prentice Hall: 881.

CARRARA M., COMPARETTI A., FEBO P., MORELLO G., ORLANDO S., 2003. Mapping soil compaction measuring cone penetrometer resistance. In: Proceedings from 4th European Conference on Precision Agriculture, Wageningen, Wageningen Academic Publishers: 176.

DUIKER S.W., 2004. Avoiding soil compaction. Available at http://pubs.cas.psu.edu/freepubs/pdfs/uc186.pdf (accessed February 17, 2013).

HAMZA M.A., ANDERSON W.K., 2005. Soil compaction in cropping systems: A review of the nature, causes and possible solutions. Soil and Tillage Research, *82*: 121–145.

HILLEL D., 1998. Environmental Soil Physics. San Diego, Academic Press, Division of Harcourt Brace and Company: 771.

HŮLA J., 1989. Vliv přejezdů techniky na půdní prostředí a možnosti minimalizace negativního působení. [Impact of machine passes on soil and possibilities of minimizing negative effects.] In: Vplyv techniky na pôdu. [Impact of Machinery on Soil.] Banská Bystrica, Dom techniky ČSVTS: 54–61.

FULAJTÁR E., 2005. Fyzikálne vlastnosti pôdy. [Physical Properties of Soil.] Bratislava, VÚPOP: 142.

JAVŮREK M., VACH M., 2008. Negativní vlivy zhutnění půd a soustava opatření k jejich odstranění. [Negative Effects of Soil Compaction and Measures for their Elimination.] Prague, VURV: 24.

LHOTSKÝ J. et al., 1985. Vztah penetračního odporu k objemové hmotnosti a vlhkosti zhutněných půd. [Relationship Between Penetration Resistance and Bulk Density and Humidity of Soil Compaction.] Prague, VÚZZP: 24–33.

SCHULER R.T., WOOD R.K., 1992. Soil compaction. Conservation Tillage Systems and Management. Ames, Iowa State University: 69–76.

MAŠEK J., 2005. Technologie zpracování půdy. [Technology of soil cultivation.] Mechanizace zemědělství, *54*: 50–55.

MAJDAN R., TKÁČ Z., KOSIBA J., CVÍČELA P., DRABANT Š., TULÍK J., STANČÍK B., 2011. Zisťovanie súboru vlastností pôdy z dôvodu merania prevádzkových režimov traktora pre aplikáciu ekologickej kvapaliny. [Soil properties determination by reason of measuring the tractor operating regimes for biodegradable fluid application.] In: Technika v technológiách agrosektora 2011. Nitra, SUA in Nitra: 71–75.

ŠESTÁK J., RÉDL J., RYBAN G., 1998. K niektorým otázkam odvaľovania kolesa s pneumatikou. [To some questions of tyred wheel rolling.] In: Kvalita a spoľahlivosť strojov. Nitra, SUA in Nitra: 250–253.

Šima T., Nozdrovický L., Dubeňová M., Krištof K., Krupička J., 2013. Effect of the crop residues on nitrous oxide flux in the controlled traffic farming system during the soil tillage by LEMKEN Rubin 9 disc harrow. Agronomy Research, *11*: 103–110.

Šima T., Dubeňová M., 2013. Effect of crop residues on CO_2 flux in the CTF system during soil tillage by a disc harrow Lemken Rubin 9. Research in Agricultural Engineering, *59* (Special Issue): S15–S21.

Rédl J., 2009. Pružnosť a pevnosť. [Mechanics of Materials.] Nitra, SUA in Nitra: 106.

Váchal J., Ehrlich P., Lhotský J., Chábera V., Simota J., 1983. Zásady komplexního zúrodňování težkých a zhutnělých půd s porušenou strukturou a stavbou. [Methods of Improving Heavy and Compacted Soils.] České Budějovice, Dům techniky ČSVTS: 31–60.

Received for publication April 12, 2013
Accepted after corrections October 14, 2013

Corresponding author:

Ing. Ján Jobbágy, PhD., Slovak University of Agriculture in Nitra, Faculty of Engineering, Department of Machines and Production Systems, Tr. A. Hlinku 2, 949 76 Nitra, Slovak Republic, phone: + 421 376 414 796, e-mail: jan.jobbagy@uniag.sk

Elimination of ecological fluids contamination in agricultural tractors

R. Majdan[1], Z. Tkáč[1], B. stančík[1], R. Abrahám[1], I. Štulajter[1], P. Ševčík[2], M. Rášo[2]

[1]*Department of Transport and Handling, Faculty of Engineering, Slovak University of Agriculture in Nitra, Nitra, Slovak Republic*
[2]*Slovnaft, a.s., Bratislava, Slovak Republic*

Abstract

Majdan R., Tkáč Z., Stančík B., Abrahám R., Štulajter I., Ševčík P., Rášo M., 2014. **Elimination of ecological fluids contamination in agricultural tractors**. Res. Agr. Eng., *60* (Special Issue): S9–S15.

This contribution presents the elimination of pollution for ecological fluids of UTTO (universal tractor transmission oils) type in agricultural tractors. The common oil filling of the transmission and hydraulic system is polluted by residues of old fillings from attachments such as ploughs, trailers, etc. In the tractor Zetor Forterra 114 41, a newly developed synthetic ecological fluid HEPR (VDMA 24568) was applied. The oil showed pollution limits after completing 900 engine hours. For this reason, a filtration device was designed to clean mainly biodegradable fluids UTTO. On the basis of fluid application evaluation and performed filtration, it can be concluded that a simple and affordable filtration system reduces the concentration of the most dangerous contamination particles (particles lager than 14 μm) by up to 30%.

Keywords: ecological oil; cleanliness level; filtration; viscosity; hydraulic pump

Considering the character of agricultural production, the transport in agriculture significantly affects the economic effectiveness as well as environmental pollution (Korenko, Žitňák 2008; Žitňák, Korenko 2008). Mineral oils designed for hydraulic and transmission systems of agricultural tractors reliably meet all the requirements of operating conditions in most cases. Properties of mineral oils are verified by many years of use. Machine manufacturers have rich experience with mineral and synthetic oils and therefore they widely use them at present. Sloboda and Sloboda (2002), Jobbágy et al. (2003), Ileninová et al. (2008) and Tóth et al. (2012) confirm this fact in their works. However, a slow but steady move towards the use of environmentally friendly or more readily biodegradable lubricant fluids has taken place during the last decade. Biodegradability has become one of the most important design parameters both in the selection of base fluids and in the overall formulation of the finished lubricant (Mendoza et al. 2011).

Because of frequent accidents at a working place, ground contamination with liquid lubricants is very probable. For these reasons, constructions of rotating components and systems make an effort to lubricate with biolubricants (Rédl et al. 2012).

Universal tractor transmission oils (UTTO) are designed for hydraulic and transmission systems of agricultural tractors. These fluids provide lubrication functions in the gear box and transmission of energy in the hydraulic system of the tractor. Currently, tractor hydraulic systems are quite complicated. These systems use mainly gear or piston hydraulic pumps and motors which transform

Supported by the Scientific Grant Agency VEGA of the Ministry of Education of the Slovak Republic and the Slovak Academy of Sciences, Grant No. 1/0857/12.

pressure energy into mechanical work. Besides the energy transfer, universal oils must lubricate, dissipate heat, and they must be compatible with sealing materials and metal components of the system.

It was reported that over 60% of all lubricants end up in soil and water. Hydraulic line breaks are extremely common. If not attended to, these releases can cause contamination of the soil, ground and surface water. Many equipment operators do not clean up spills, thereby introducing pollutants to the environment. Using a fluid that is biodegradable reduces the cost of clean-up as well as the potential for polluting the environment (CAUFFMAN et al. 2006).

The UTTO requires care and monitoring of operating parameters such as every part of the agricultural tractor. That applies even more in case of ecological fluids. Ecological fluids are more sensitive to a change in operating conditions compared with mineral oils. Fluid cleanliness is one of the most important features. Often, the cleanliness and technical condition of the UTTO are frequent causes of failures of the transmission and mainly hydraulic system of the tractor. A contaminated fluid creates a risk to the machine in terms of wear and failure. Pollution is dangerous because it accelerates the degradation and oxidation processes in the fluid. If the fluid is contaminated with dirt above the permitted level, it must be replaced. The fluid needs to be replaced even if it has good physical and chemical properties expressed by viscosity or acid number. However, in the case of expensive ecological fluids, such a solution is not economical. Therefore, the elimination of pollution from fluid by using filtration is an ecological as well as economical solution.

MATERIAL AND METHODS

The newly developed biodegradable synthetic oil-base fluid HEPR according to VDMA 24568 (1999) was applied in the agricultural tractor Zetor Forterra 114 41 (Zetor, a.s., Brno, Czech Republic). The fluid was developed by Slovnaft, a.s., a member of the MOL group, Hungary. The fluid was tested under laboratory conditions. It was cyclically loaded under a nominal pressure of 20 MPa. Laboratory testing conditions and practices of the biodegradable fluid mentioned above were described by DRABANT et al. (2010), HUJO et al. (2012a,b), and KOSIBA et al. (2012a,b). The fluid was loaded by cyclic pressure at temperature 65°C, which was measured during the tractor operation as stated by KOSIBA et al. (2010). After successful tests, the fluid was used in the agricultural tractor. The physical and chemical properties and pollution of the fluid were evaluated during the operation test. A filtration device was designed and tested due to exceeding the pollution limits of the fluid. The filtration device was designed to ensure a reliable operation of the tractor with ecological fluids.

Filtration device. The main parts of the filtration device (developed by Department of transport and handling, Faculty of engineering, Slovak University of Agriculture in Nitra) are the filter housing with a filter element. The filtration device is connected to the implement hydraulic circuit of the tractor by hoses (Fig. 1). The tractor hydraulic pump pumps the universal transmission and hydraulic oil through the filtration device. Thus, the filtration device does not need to be equipped with a pump, making its construction easier. In this case, a low-pressure filter housing was used (up to 0.2 MPa) of FS 02 type (Kovolis Hedvikov, a.s., Hedvikov, Czech Republic). The filtration device needs to have the flow adjusted to ensure a low pressure. The tractor Zetor Forterra 114 41 does not have a regulating hydraulic pump so it is not possible to set the desired flow rate in the hydraulic circuit. Consequently, a measuring device (6) HT 50 A (XPS Corporation, Owatonna, USA) was connect-

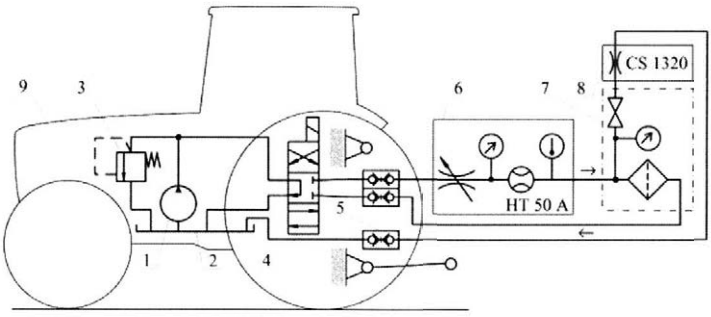

Fig. 1. Connection scheme of filtration device

1 – tractor hydraulic pump; 2 – gear and hydraulic oil supply; 3 – pressure relief valve; 4 – hydraulic valve; 5 – quick couplings of implement hydraulic circuit; 6 – measuring device; 7 – filtration device; 8 – device for measuring cleanliness level; 9 – tractor

ed to the filtration device in series. Flow value of 0.2 dm^3/s was set using a throttle valve of this device. The measuring device HT 50A was used for hydraulic heating of the tractor oil fill before filtration and for setting the desired flow during filtration. The measuring device mentioned above can be replaced with a simple throttle valve and flow meter. The filtration efficiency was monitored by measuring the cleanliness level of the oil that enters the filter. A part of the oil entering the filter flows through the measuring device CS 1320 (Hydac Ltd., Sulzbach, Germany), which measures the cleanliness level according to the ISO 4406 (1999). To measure the cleanliness level, a low oil flow was only used. The low flow rate was set by a jet in this device.

The filtration device was designed so that it can be made using different types of filter housings, which are available in a particular farm (Fig. 2). The advantage of the device is its connection by quick couplers to the implement hydraulic circuit of the tractor. Connection does not need additional assembly, which is characterized by simplicity. It is universally applicable to different types of tractors. The design of the low-pressure filter housing required setting a relatively low flow rate through the filtration device (0.2 dm^3/s); the throttle valve has thus to be used to set the required flow rate (Fig. 1). This throttle valve was placed to the measuring device. The flow meter EVS 31000 (Hydac Ltd., Sulzbach, Germany) was installed to check the right value of flow rate during the filtration. One filtering of the whole oil fill (in our case 120 dm^3) took about 10 minutes. We filtered the oil fill two times to improve the quality of filtration. If pressure filter housing designed to the hydraulic pump flow of a given tractor type is used, it would be possible to filtrate the oil fill without the flow control valve. The filtering system would be simplified and filtration time shortened.

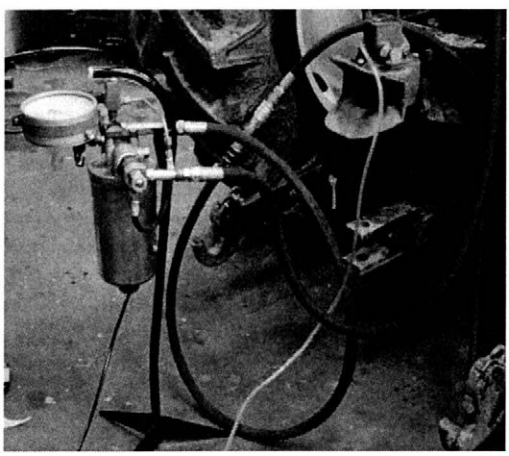

Fig. 2. Filtration device connected to the tractor

The filtration capability of a paper element was 10 μm. The filter cartridge was placed in an aluminium housing of the filtration device. The filtration device was made by simply placing the filter housing on the stand with hoses adapters for connecting; it was designed at the Department of Transport and Handling, Faculty of Engineering, Slovak University of Agriculture in Nitra, Slovak Republic. The filtration device is connected to the implement hydraulic circuit by pressure hoses and quick coupling.

Evaluation of the technical condition of ecological fluid. The technical condition of the monitored fluid was necessary to be evaluated before filtration. The following parameters were evaluated:

- kinematic viscosity at 40°C,
- concentration of additives on the basis of the chemical elements content (Ca, P and Zn) (ICP spectrometry method was used),
- depletion of antioxidants on the basis of FTIR spectroscopy.

These parameters were analysed from oil samples in an accredited laboratory (Wearcheck, Hungary).

Kinematic viscosity is evaluated based on the positive or negative tolerance of the measured values in comparison with the value of new oil. Therefore, the kinematic viscosity of new oil must be evaluated. The deviation of kinematic viscosity is calculated by using the formula:

$$\Delta V = \frac{\nu_N - \nu_U}{\nu_N} \times 100 \quad (\%) \tag{1}$$

where:

ΔV – deviation of kinematic viscosity (%)

ν_N – kinematic viscosity of the new oil (mm^2/s)

ν_U – kinematic viscosity of the used oil (mm^2/s)

Additives concentration was monitored on the basis of relevant content of chemical elements (Ca, P and Zn). A decrease in the content of these elements in an oil sample is calculated by using the following formula:

$$\Delta A = \frac{A_N - A_U}{A_N} \times 100 \quad (\%) \tag{2}$$

where:

ΔA – decrease of chemical elements representing the additives (%)

A_N – content of chemical elements representing the additives in new oil (mg/kg)

A_U – content of chemical elements representing the additives in used oil (mg/kg)

The filtration of oil filling of the tractor transmission and hydraulic system was evaluated according to the following procedure:

- Online monitoring of the pollution decrease on the basis of the filtered oil cleanliness level during filtration. The device CS 1320 was used to evaluate the pollution on the basis of the Standard ISO 4406 (1999).
- Offline pollution assessment on the basis of analyses of oil samples after filtration. This was done in the accredited laboratory Wearcheck (Almásfüzitö, Hungary). Pollution was evaluated according to the concentration of chemical elements Fe, Cu, Si, Al, Pb, Ag, Ni and Mn. The contents of these chemical elements were analysed by inductively coupled plasma (ICP) atomic emission spectrometry.

A decrease in the content of the chemical elements which represent fluid contamination is calculated on the basis of information on polluted and filtered oil. Impurity content represents fluid contamination. A decrease in the content of chemical elements which represent fluid contamination is calculated by using the formula:

$$\Delta Z = \frac{Z_U - Z_F}{Z_U} \times 100 \quad (\%) \qquad (3)$$

where:

ΔZ – decrease in chemical elements content representing pollution (%)

Z_U – content of chemical elements representing pollution in used oil (mg/kg)

Z_F – content of chemical elements representing oil pollution after filtration (mg/kg)

Oil samples were taken after completing 150, 450, 900 engine hours during the tractor operation and after filtration. A representative sample of new oil was taken before filling the tractor transmission and hydraulic system with oil. This sample was marked as 0 engine hours.

RESULTS AND DISCUSSION

The cleaning of the transmission and hydraulic system oil fill makes sense only if the fluid parameters meet the prescribed technical limits. Lubricating properties of fluids can be best evaluated on the basis of kinematic viscosity which has a decisive influence on the formation of an oil film. Fig. 3 shows the course of the kinematic viscosity of oil during the tractor operation.

Kinematic viscosity is a parameter that can decrease or increase during operation. In this case, the decrease in kinematic viscosity was calculated $\Delta V = 6.89\%$ according to Eq. (1), based on the value of new oil $\nu_N = 58$ mm^2/s and value of used oil after 900 engine hours $\nu_U = 54$ mm^2/s. The decrease of kinematic viscosity does not exceed the limit of 10% which is prescribed for the UTTO. Kinematic viscosity was thus within the prescribed limits before the planned filtration.

Fig. 4 shows the FTIR spectrum of ecological oil used in the agricultural tractor. The FTIR analysis can detect the depletion of antioxidants that protect the oil from degradation. In the case of antioxidants depletion, the oil must be replaced or depleted antioxidants must be added. Therefore, it was necessary to carry out the measurement of antioxidants. The wavenumber of 3,650 cm^{-1} and 3,620 cm^{-1} is typical for phenolic antioxidants and

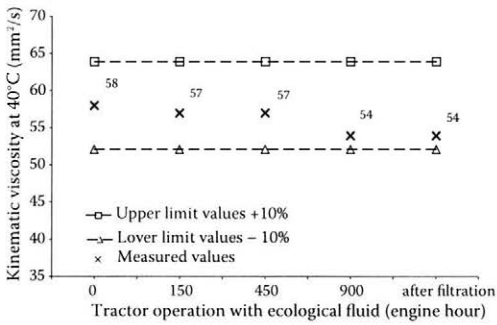

Fig. 3. Kinematic viscosity of oil during the tractor operation

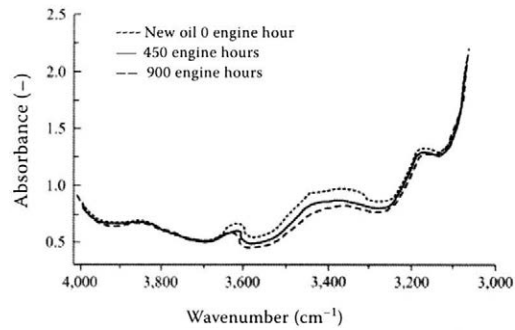

Fig. 4. Determination of antioxidant concentration using FTIR spectroscopy

Table 1. Concentration of chemical elements (mg/kg) representing the additives

Chemical element	Time of tractor operation (engine hours)				ΔA (%)
	0	150	450	900	
Ca	3,171	3,245	2,615	2,488	21.54
P	1,276	1,119	1,114	1,105	13.41
Zn	1,381	1,364	1,129	1,264	8.48

ΔA – decrease of chemical elements representing the additives (%)

the wavenumber of 1,437 cm^{-1} for amine antioxidants. Fig. 4 shows a slight decrease in the concentration of both types of antioxidants. Therefore, there is a gradual depletion of antioxidants in the oil. The remaining concentration of antioxidants can also protect the oil from degradation. Therefore, it was possible to clean the oil from mechanical impurities by using filtration.

Information on the technical condition of the tractor transmission and hydraulic oil fill after completing 900 engine hours are supplemented by information on the quantity of additives that improve the properties of used fluid.

Table 1 shows the three base elements that characterize the complex of additives, namely calcium, phosphorus and zinc. The concentration of these chemical elements decreases due to a gradual depletion of additives in the oil. A decrease in the concentration of chemical elements that represent additives ΔA was calculated according to Eq. (2). The largest decrease was observed in the measuring of calcium at 21.54%. In the monitored oil only a slight decrease was recorded in additives concentration.

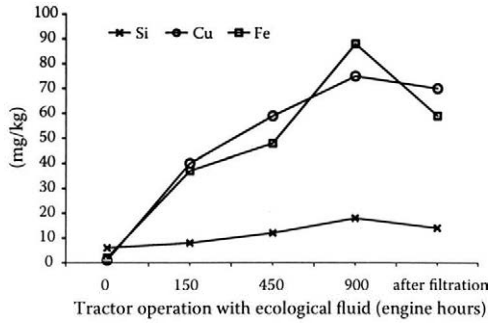

Fig. 5. Concentration (mg/kg) of iron, copper and silicon in oil samples during the tractor operation

The physical and chemical properties of the ecological oil UTTO, as the quality evaluation parameters, were monitored during the tests performed by VIŽINTIN and KRŽAN (2003). The authors focused on the kinematic viscosity, additive content and oxidative stability. Based on these parameters, they evaluated the properties of the sunflower oil-base fluid UTTO with AW and EP additives. MENDOZA et al. (2011) present the results of using the ecological fluid in the agricultural tractor Agria, model 9100. In operating tests, they did not notice any exceeding of limits in the physical and chemical parameters of the used oil Biogir-06. KUČERA et al. (2008) evaluated the kinematic viscosity of the ecological oil NAPRO-HO. This oil did not exceed the limit viscosity value of 10% during tests.

Table 2 and Fig. 5 show an increase in the concentration of pollution particles in oil during the tractor operation. The contamination which exceeded the permitted concentrations of iron and copper was observed after completing 900 engine hours. Therefore, filtration was performed with the designed fil-

Table 2. Concentration (mg/kg) of chemical elements characterizing the mechanical contaminants

Chemical element	Time of tractor operation (engine hours)				After filtration	ΔZ (%)
	0	150	450	900		
Fe	2	37	48	88	59	32.95
Cu	1	40	59	75	70	6.66
Si	6	8	12	18	14	22.23
Al	1	1	2	6	4	33.34
Pb	3	2	7	7	7	–
Ag	2	1	2	1	1	–
Ni	< 1	< 1	< 1	1	1	–
Mn	< 1	< 1	< 1	1	< 1	–

ΔZ – decrease in chemical elements content representing pollution (%)

Table 3. Cleanliness level during the oil filtration

No.	Cleanliness level according to ISO 4406 (1999)					
	> 4 μm		> 6 μm		> 14 μm	
	ISO class	particles/0.1 dm^3	ISO class	particles/0.1 dm^3	ISO class	particles/0.1 dm^3
1	24	8,000,000	23	4,000,000	10	500–1,000
2	24	–	23	-	9	250–500
3	24	16,000,000	23	8,000,000	8	130–250

No. – measurement number

tration device. Fig. 5 shows a decrease in the concentration of major polluting chemical elements such as iron, copper and silicon after filtration.

Table 3 shows the results of cleanliness level measurements using the device CS 1320, which was connected to the filtration device during filtration. During filtration, a decrease in the concentration of pollution occurred in three stages. They are identified in Table 3 as the measurements Nos 1, 2 and 3. Measurement results of the cleanliness level show a reduction in the largest pollution particles (> 14 μm) which are the most dangerous for transmission and hydraulic system of the tractor.

CONCLUSION

This contribution deals with the application and pollution of the ecological fluid UTTO in the transmission and hydraulic system of the tractor. Design and use of filtration devices designated to ensure a reliable operation of the ecological fluid in agricultural tractors are presented. The designed filtration system ensures a clean fluid during its operation in the tractor. The filtration device can be simply used for different types of tractors because it is connected to the implement hydraulic circuit. It can be made from the filter housing and filter element, which are available in most farms. Based on the measurements, we can conclude that the designed filtration system is suitable for cleaning ecological fluids used in tractors. The manufacturing of the filtration system is simple and affordable. Table 2 shows the progress of fluid contamination up to the limit level after completing 900 engine hours. Table 3 shows a reduction in iron up to 30% after filtering. A positive filtration effect was shown during the cleanliness level measurement, too. This was reflected in a decrease in the cleanliness level for particles larger than 14 μm in two categories.

Monitoring of oil contamination is the main parameter for filtering or change of oils in tractor hydraulic and gear system. In actual practice the high quality oils with very good physical and chemical properties are used in tractors. Therefore the oil contamination is the main indicator for filtering. The producers of oil state the limits for contamination according to oil and tractor type.

References

Cauffman G., Holland L., Perez J., Lloyd W., Boehman A., Richard T., Buffington D., 2006. Penn state and green hydraulic fluids. Available at http://www.research.psu.edu /capabilities/documents/ biohydraulic.pdf

Drabant Š., Kosiba J., Jablonický J., Tulík J., 2010. The durability test of tractor hydrostatic pump type UD 25 under operating load. Research in Agricultural Engineering, *56*: 116–121.

Hujo Ľ., Kosiba J., Jablonický J., Tulík J., 2012a. Load characteristics of three-point tractor linkage. In: Naučni trudove – zemedelska technika i technologii, agrarni nauki i veterinarna medicina, remont i nadeždnosť. October 26–27, 2012. Rousse, University of Rousse: 172–176.

Hujo Ľ., Kosiba J., Jablonický J., Drabant Š., 2012b. Teoretický návrh laboratórneho skúšobného zariadenia na testovanie traktorovej hydrauliky. [Theoretical design of a laboratory test device for the testing of tractor hydraulics.] In: Technics in Agrisector Technologies 2012, November 5, 2012. Nitra, SUA in Nitra: 68–73.

Ileninová J., Mihalčová J., Košťáliková D., 2008. Hodnotenie vlastností hydraulických kvapalín v leteckých motoroch. [Evaluation of hydraulic fluid properties in aero-engine.] In: REOTRIB 2008, May 28–30, 2008. Prague, Institute of Chemical Technology Prague: 118–122.

ISO 4406, 1999. Hydraulic fluid power – Fluids – Method for coding the level of contamination by solid particles. Geneva, International Organization for Standardization.

Jobbágy J., Petranský I., Simoník J., 2003. Tlakové režimy v hydraulike traktorov ZTS v súprave s poľnohospodárskym

náradím. [Pressure regimes in hydraulics of tractors ZTS in set agricultural implements.] In: International Student's Scientifics Conference, April 1–2, 2003. Nitra, SUA in Nitra: 94–101.

Kosiba J., Drabant Š., Jablonický J., Tulík J., 2010. Meranie teplotného režimu hydrauliky traktora. [Measurement of temperature regimes of tractor hydraulics.] In: XXIX. Setkání kateder mechaniky tekutin a termomechaniky June 23–25, 2010. Ostrava, VŠB – Technical University of Ostrava: 141–144.

Kosiba J., Hujo Ľ., Angelovič M., Šinský V., 2012a. Zisťovanie prevádzkových parametrov poľnohospodárskych traktorov. [Detection of operating parameters of agricultural tractors.] In: Technics in Agrisector Technologies 2012. November 5, 2012. Nitra, SUA in Nitra: 80–85.

Kosiba J., Varga F., Mojžiš M., Bureš Ľ., 2012b. Záťažové charakteristiky traktora Fendt 926 Vario pre simuláciu na experimentálnom zariadení. [Load characteristics of tractor Fendt 926 Vario for simulation on experimental bench.] Acta Facultatis Technicae, *17:* 63–72.

Korenko M., Žitňák M., 2008. Využitie strojov pri zbere a prepave balíkov slamy na energetické účely. [Machines utilization during harvest and transport of straw bales for energetic purpose.] In: Perspective in Education Process at Universities with Technical-Orientation in Visegrad Countries: International Science Conference. Nitra, SUA in Nitra: 275–279.

Kučera M., Rousek M., 2008. Evaluation of thermooxidation stability of biodegradable recycled rapeseed-based oil NAPRO-HO 2003. Research in Agricultural Engineering, *54:* 163–169.

Mendoza G., Igartua A., Fernandez-Diaz B., Urquiola F., Vivanco S., Arguizoniz R., 2011. Vegetable oils as hydraulic fluids for agricultural applications. Grasas y Aceites, *62:* 29–38.

Rédl J., Váliková V., Kročko M., 2012. Mathematical model of sliding couple lubricated with biolubricants. Acta Technologica Agriculturae, *15:* 46–52.

Sloboda A. Jr., Sloboda A., 2002. Využitie tribotechnickej diagnostiky z pohľadu bezpečnosti prevádzky pre núdzový hydraulický okruh lietadla. [Use of tribotechnical diagnostic from view of safe operation for emergency hydraulic system of aeroplane.] Acta Mechanica Slovaca, *3:* 107–113.

Tóth F., Rusnák J., Kadnár M., 2012. Monitoring of geometric cylindricity tolerance changes on a test sliding pair using the oils Madit PP 80 and Mobil Mobilube SHC. Acta Technologica Agriculturae, *15:* 100–102.

VDMA 24568, 1999. Fluidtechnik Biologisch schnell abbaubare Druckflüssigkeiten – Prüfung der Einwirkung auf Legierungen aus Buntmetallen. Frankfurt am Main, VDMA.

Vižintin J., Kržan B., 2003. Tribological properties of vegetable based universal tractor transmission oil. In: Rotrib 2003, September 24–26, 2003. Galati, Dunarea de Jos University of Galati: 221–227.

Žitňák M., Korenko M. 2008. Výkonnosť a energetická náročnosť dopravných prostriedkov pri zbere a preprave balíkov slamy. [Performance and energetic demandingness of vehicles during harvest and transport of straw bales.] In: Vozidlá 2008: Nové trendy v konštrukcii a exploatácii vozidiel. Nitra, SUA in Nitra: 181–185.

Received for publication April 12, 2013
Accepted after corrections, June 17, 2014

Corresponding author:

Ing. Radoslav Majdan, PhD., Slovak University of Agriculture in Nitra, Faculty of Engineering, Department of Transport and Handling, Tr. A. Hlinku 2, 949 76 Nitra, Slovak Republic
phone: + 421 904 198 433, e-mail: radoslav.majdan@gmail.com

Assessment of risks in implementing automated satellite navigation systems

M. Žitňák, M. Macák, M. Korenko

Department of Structures, Faculty of Engineering, Slovak University of Agriculture in Nitra, Nitra, Slovak Republic

Abstract

Žitňák M., Macák M., Korenko M., 2014. **Assessment of risks in implementing automated satellite navigation systems**. Res. Agr. Eng., *60* (Special Issue): S16–S24.

One of the ways of increasing the efficiency and safety of work is the implementation of navigation systems in agricultural practice. Satellite navigation as a means of reducing the unit costs and increasing the safety can have a significant economic impact on a company when properly used. The objective of measurement was to assess the accuracy of a satellite system AutoTrack working with a correction signal SF2. Its provider specifies an accuracy of ± 5 cm for this signal type. The accuracy of machine work was compared for two scenarios, i.e. with and without satellite navigation. Further, the navigation of machines focused predominantly on AgGPS EZ-Guide Plus and AutoTrac Universal. The FMEA method was used to determine the risk of probable failures that can occur on machines while working. This work describes the individual failures that can occur on navigation systems of machines and analyses their impact on operator's safety.

Keywords: assisted steering; operator's safety; navigation accuracy; FMEA analysis

Occupational health and safety is an inseparable part of working and production activities. Safety is often perceived as a prevention of accidents, as measures leading to the elimination of accidents and health damage. However, a modern insight into this field is much broader. It defines a 'human factor', gives priority to a human being and his protection with respect to all the aspects associated with work (Hrubec et al. 2009). In connection with the protection of employees, it is required to deal with such factors as stress, workload, work monotony, working conditions, working relationships, etc.

Risk management is one of the tools, by means of which it is possible to increase the safety margin of various processes and specific activities. It enables the identification, assessment and reduction of risks (Pačiová et al. 2009).

When working with machines in agricultural practice, it is possible to encounter several aspects having an impact on safety. Individual types of threat that occur can influence not only operator's safety but can also have an environmental impact. At the same time, it need not be a sudden impact, but a progressive that occurs with failing to observe the basic rules, standards or laws (Macák, Žitňák 2010).

Frohman and Švarda (2010) describe the use of satellite navigation and RTK corrections in subsoiling. They indicate that using such operations within an effort to maintain competitiveness on the market appears to be more effective than the policy of buying larger machines and acquiring a larger area of agricultural land. McMahon (2003) describes the structure and benefits of assisted steering. He especially deals with the wireless transmission of

Supported by Ministry of the Education, Research, Science and Sports of the Slovak Republic within the framework of the European Union Operational Programme Research and Development, Project No. ITMS 26220220014.

application maps and recorded data directly from a field into a central computer. When determining the accuracy of satellite navigation of a tractor with implement, EHSANI et al. (2002) used an average error and standard deviation of machine trajectory error calculated from differences between an actual machine position in the field and a calculated (theoretical) position. They considered the efficiency comparison of six navigation systems with RTK GPS, as the theoretically most accurate system, to be the most reliable system of determining the accuracy of navigation systems.

An FMEA is an inductive (forward logic) failure analysis and is a core task in reliability engineering, safety engineering and quality engineering (PRÍSTAVKA et al. 2011). A successful FMEA activity helps to identify potential failure modes based on experience with similar products and processes or based on common physics of failure logic (BUJNA et al. 2012). It is widely used in development and manufacturing industries in various phases of the product life cycle (BUJNA, PRÍSTAVKA 2012). An effects analysis refers to studying the consequences of those failures on different system levels.

The objective of this work was to assess the risks associated with implementing the automated satellite navigation systems into a company by means of Failure Mode and Effects Analysis (FMEA). To make assessment the most effective, it was necessary to consider the accuracy of selected satellite navigation systems AutoTrack Universal and AgGPS EZ-Guide Plus. Subsequently, on the basis of the performed measurements and observed experience of operators and service workers, risks were assessed by means of the said FMEA.

MATERIAL AND METHODS

The assessment of AgGPS EZ-Guide Plus and AutoTrack Universal (both Deere & Company, Moline, USA) was performed on the basis of monitoring these systems when working in practical conditions. Based on practical experience and available manufacturer's guides, a network diagram with individual basic elements of a GPS receiver (StarFire iTC; Deere & Company, Moline, USA) (Fig. 1) was prepared. The network diagram was used as a background for creating the analysis of risk by means of FMEA.

The individual system elements (Fig. 1) were analysed using the FMEA method. After determining probable errors and reporting their impact on individual parts of the navigation system, we have searched for possible consequences and causes of these errors. The following part contained the determination of importance, probability and detectability of errors. After having determined the MR/P value (level of risk/priority), suitable corrective measures were suggested, and the risk number MR/P was specified again.

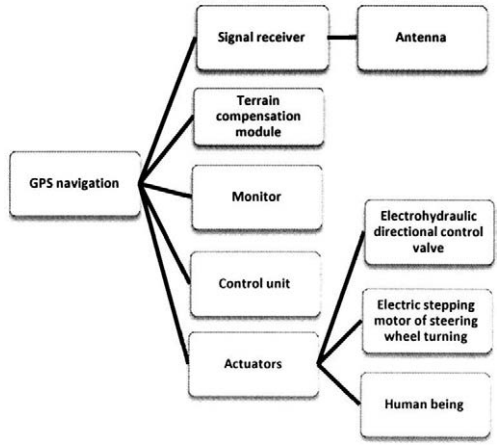

Fig. 1. Navigation system elements where failures are possible to occur

The table of FMEA analysis (Table 1) contains individual numerical values representing the risk number MR/P (*Vz* – severity, *Vy* – occurrence, *Od* – detection). The values *Vz*, *Vy*, and *Od* were determined according to the tables in STN ISO 9000 (2005).

To identify the risks, we have performed a number of measurements to determine the accuracy of navigation and to monitor the problems of operators with the navigation system as well as the benefits resulting from its implementation.

One of the said practical experiments was carried out in a field belonging to PD Rastislavice (farming cooperative), Slovak Republic. We measured there the accuracy of work of the automated satellite navigation system during soil loosening by a disc tiller. In this field, an experimental part was selected having an area of 9.51 ha, on which 213 monitoring points were distributed.

The machine (Kuhn Discovery XM 40; KUHN S.A., Saverne, France) performed shallow tillage after previous subsoiling and harvest of sugar beet. The basic technical parameters of the tractor and tiller Kuhn Discovery XM 40 are shown in Table 2.

The steering system is controlled by a steering system unit (SSU) (Deere & Company, Moline,

Table 1. FMEA form for assessment of failures

Serial No.	Failure location	Failure mode	Failure cause	Q	S	E	Consequences	*Vy*	*Vz*	*Od*	*MR/P*	Measures	*Vy*	*Vz*	*Od*	*MR/P*
1	signal receiver	short-term loss of signal	shielding of satellite signal	Y	N	Y	downtime, stress	6	5	3	90	maintenance of wind barriers	5	5	3	75
2	signal receiver	signal disturbance	effect of high voltage line	Y	N	Y	signal drop-out, worker's fatigue	4	4	3	48	working perpendicularly to line	3	4	2	24
3	signal receiver	neither differential nor correction signal	licence for differential signal expired	Y	N	N	no signal, downtime, stress	2	5	3	30	regular renewal of licence rights	1	5	3	15
4	terrain compensation module	position is occupied to the right or to the left	MTK is not calibrated	Y	Y	Y	error in navigation position	7	7	3	147	regular calibration	5	7	2	70
5	mobile processor	memory error	internal memory error	Y	N	N	system is unable to work	4	7	5	140	regular service and inspection of hardware	2	7	4	56
6	compensation module	MTK is unable to compensate changes in terrain	speed sensor does not respond	Y	Y	Y	inaccuracy of travels, effect on safety	6	7	4	168	regular service inspections	4	6	3	72
7	compensation module	MTK is able to correct neither position nor angle	heeling sensor is beyond range	Y	N	Y	inaccuracy of travels, effect on safety	6	6	6	216	regular inspection	4	6	3	72
8	monitor	parallel tracking system is slow or sluggish	incorrect update	Y	Y	Y	downtime, fatigue	4	6	5	120	setting of device	3	6	3	54
9	monitor	audible alarm does not sound	failure	N	Y	Y	late machine reversal by operators	4	3	3	36	inspection	3	3	3	27
10	monitor	display is blank or poorly visible	interrupted voltage	Y	Y	Y	reduced performance	3	6	4	72	inspection	2	6	3	36
11	monitor	display is not functioning correctly	problem with hardware	N	Y	N	reduced system safety	3	7	3	63	regular hardware tests	2	5	3	30
12	antenna	no communication with GPS receiver	GPS receiver or light bar are faulty	Y	Y	N	limitation of works, stress	4	7	3	84	using quality devices only	2	7	3	42
13	pc card	problem with data card	erroneous data card	N	N	N	delay of works	3	6	2	36	using quality memory media only	2	6	2	24
14	signal receiver	no communication with display	problem with can bus	Y	N	Y	device is unable to communicate with display	3	7	3	63	inspections	2	7	2	28

Table 1 to be continued

Serial No.	Failure location	Failure mode	Failure cause	Q	S	E	Consequences	*Vy*	*Vz*	*Od*	*MR/P*	Measures	*Vy*	*Vz*	*Od*	*MR/P*
15	mobile processor	device fails to accept the licence code	error in re-programming the product on card	N	Y	N	downtime, stress	4	7	4	112	training	2	7	2	28
16	monitor	overloaded display	absence of operator's knowledge	Y	Y	N	short-term system failure	3	4	4	48	increasing the awareness of operators	2	4	3	24
17	power supply	device is not activated after starting	damage of power supply due to vibrations	Y	Y	N	disabled works, stress	4	3	4	48	service inspections	2	3	3	18
18	control unit	vehicle deviates from travel direction	erroneous signal evaluation	Y	Y	Y	reduced quality of work	3	4	5	60	using a quality correction signal	2	4	5	40
19	electric stepping motor	steering wheel is skipping with automated guidance	rearrangement of drive on the steering wheel	Y	Y	Y	failure of automated guidance	3	6	4	72	using quality devices only	2	6	3	36
20	light bar	only one diode is shining on the bar	incorrect temperature in driver's cabin	Y	Y	Y	downtime, device damage	2	7	3	42	training	2	2	2	28

E –environment; S– safety; Q – quality; Y – yes, N – no; *Vy* – occurrence; *Vz* – severity; *Od* – detection; *MR/P* – risk number/priority; MTK – terrain compensation module

USA). This control unit collects information from individual components of the system, and signals pass from there into an electrohydraulic control valve ensuring tractor steering (turning of steering wheels). The substance of steering is in the fact that the electrohydraulic control valve doses the oil to double-action hydraulic cylinders so that the required direction of movement is maintained.

After passing of the machine, initial monitoring points were marked using marking pegs, from which the actual machine working width was measured using a metric gauge.

Navigation inaccuracies were recorded by measuring the implement width on worked soil after three passes of the machine, by which overlaps and skips were obtained, representing inaccuracies caused by a double navigation of the machine. In evaluation with this method, overlaps and double working width, which was set for navigation 4.8 m (Fig. 2a) and 5.2 m, were subtracted. Accuracy without satellite navigation was also measured. In that case, the machine was navigated based on experience and skills of operators. The measuring procedure with this method was identical with the previous one. With respect to the measuring method used, negative numerical values representing skips are actually overlaps (positive values).

RESULTS AND DISCUSSION

The disc tiller Kuhn Discovery XM 40 consists of two disc sections. The rear section of discs is wider than the front section by 0.35 m on each side. For the 4.8 m value set for navigation, multiple tillage was performed in certain parts of the field. Fig. 2a indicates that the navigated machine worked the dimensioned widths of right and left margins three times (i.e. in two passes, the area was worked once by the front section and two times with the rear section), thus creating an overlap of 0.7 m. For the given machine in this operation, the value of 5.15 m (Fig. 2b) represents an ideal value of spacing between neighbouring tramlines, which is entered into the satellite navigation system. There are no multiple overlaps, and an ideal areal machine capacity is ensured. For an optimum tillage with more plant residues (stubble etc.), it would be necessary to set the satellite navigation value to 5.00–5.10 m.

Fig. 3 illustrates a box-and-whisker plot representing the values of skips and overlaps for three passes of the machine with satellite navigation (Fig. 2). This

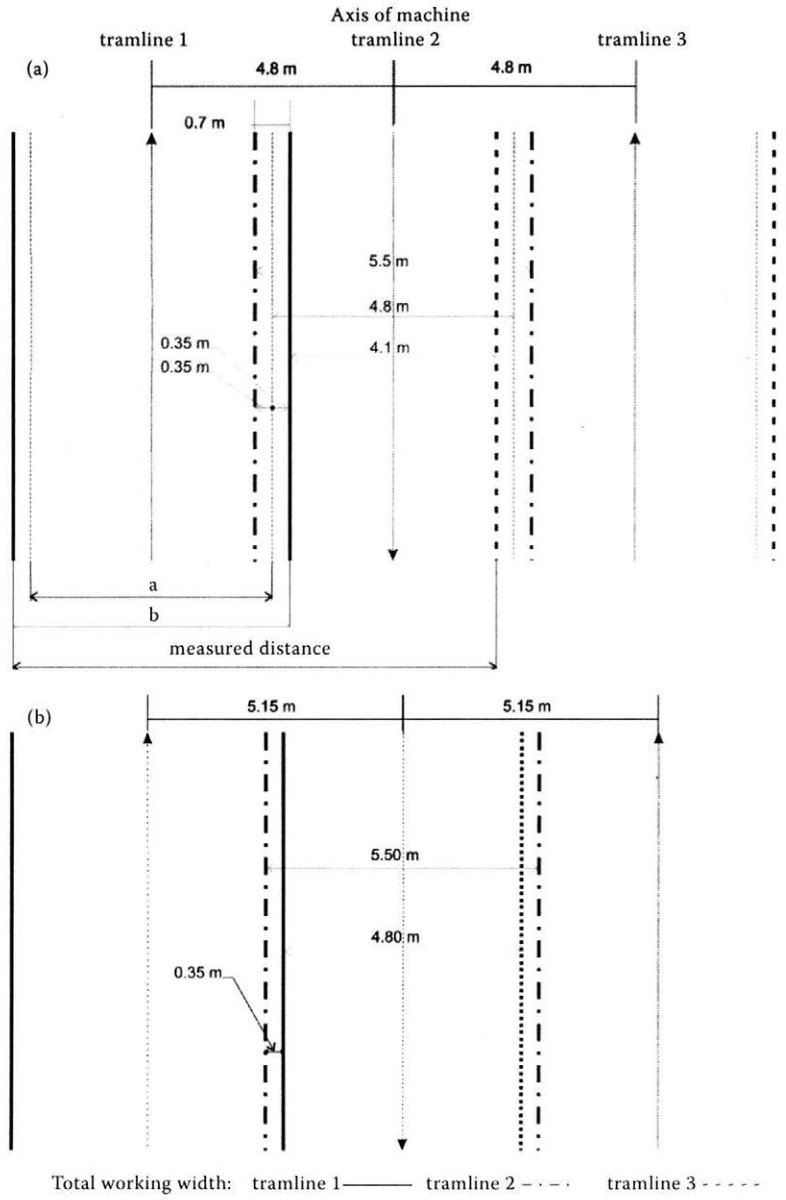

Fig. 2. Scheme of machine tramlines for navigation at (a) 4.8 m and (b) at 5.15 m
a –working width of first disc section; b – working width of second disc section (total working width of machine)

plot indicates a negative value of median equal to –0.06 m, which represents the mean value of the measured data. The plot further indicates the values of the upper and lower quartile; its interval of skips ranges from –0.01 m to –0.11 m. Without satellite navigation of the machine, half the values of skips ranged from –0.75 m to –0.93 m (Fig. 3).

With respect to the used measuring method, it should be noted that the presented results with a negative value actually represent a positive value, i.e. overlap.

For the performed field operation, it is possible to state that the used satellite navigation AutoTrack with the correction signal SF2 is sufficient in terms

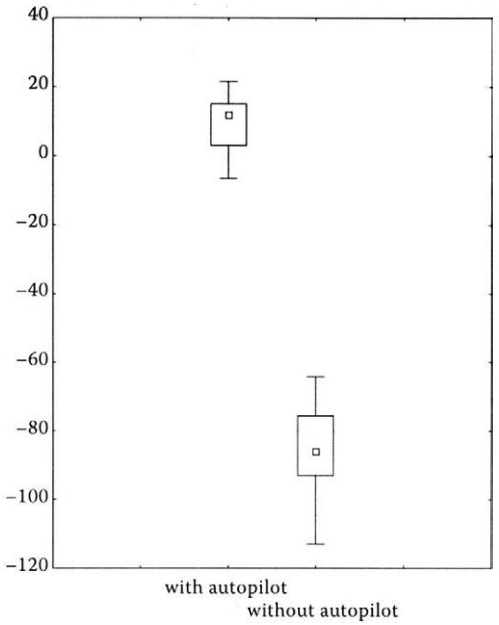

Fig. 3. Skips and overlaps with and without using the AutoTrack guidance system negative values mean overlaps, positive values mean skips

of agronomical requirements on tillage. An unnecessary large overlap occurred due to setting an incorrect value of working width for the satellite navigation system. Based on such experiments and failures recorded by machine operators and service workers, we determined the risks associated with using satellite navigation systems.

Procedure of FMEA application

After becoming sufficiently familiar with functions and work of machines using navigation systems, we used the FMEA analysis according to relevant criteria and consultations, and according to the selected methodology:

- identification of risks;
- identification of risks consequences;
- identification and analysis of risks causes;
- identification of risk level (quantifying the risk);
- determining corrective measures and re-quantifying the risk.

Evaluation of FMEA results (AgGPS EZ-Guide Plus and AutoTrack Universal)

By using the FMEA method, we were able to significantly reduce the value of risk on the examined navigation systems. After determining the importance, probability and detectability of a failure, and after subsequently quantifying the MR/P value, we have drawn the following conclusions.

The analysis gives us an overview of possible demonstrations and causes of failure that can occur when working with the navigation system. A significant point of the whole analysis was a proposal of safety measures to improve the existing situation. Before the evaluation of risks when working with the navigation of machines, it was necessary to know all the factors that can influence the safety of operators as well as legal regulations to be met by the system.

By determining the correct selection of safety measures, we reduced the most of revealed threats to an acceptable risk level. For the application of a similar analysis in practice, the implementation of this principle means a great success in terms of operators' safety at work. We found that exceeding values of risk are influenced especially by the absence of trained staff, regular renewal of licence agreements, regular maintenance and inspection of hardware and software, and using quality components of equipment. Every year, navigation systems bring new functions meaning a large obstacle for untrained staff. If operators do not know the system and there is an unexpected, banal, e.g. electronic or mechanical error that is easy to be removed and operators are unable to respond promptly, there is

Table 2. Basic technical parameters of machine

DISCOVER tiller XM 40		JOHN DEERE tractor 7820	
Working width (m)	4.75	engine output rating (ECE) (kW)	136
Max. working depth (mm)	220	max. engine output (ECE) (kW)	145
No. of discs (pcs)	40	transport Boost (ECE) (kW)	157
Disc diameter (mm)	660	No. of cylinders/volume (cm^3)	6TI/6,800
Working speed (km/h)	8–12	torsion moment flexibility (%)	45
Machine weight (kg)	4,290	max. speed (km/h)	40.0/50.0
Machine transport width (m)	2.45	power take-off (1/min)	540/540E/1,000
Required tractor power (kW)	132	hydraulics max. piston force (kN)	90.0

a time stress. In the long term, stress can have unfavourable effects on health and it is currently very underestimated. Last but not least, we shall not forget physical and sensory threats that were identified when assessing. Physical threats especially occur during the assembly of individual navigation components. An example can be mounting the receiver on the tractor's roof. Furthermore, there are various effects such as slipping when boarding, which is not directly connected with navigation but influences the safety of operators in terms of working environment. We shall not forget the sensory load which employees are constantly subjected to even though employers often pay no attention to that. Finally, there are other significant risks such as risk arising due to an incorrect ergonomy of workplace (worker is in an unfavourable position when spraying a high crop stand, causing spinal column pain). In the long term, these effects can be a starter of occupational diseases. Therefore, organizations should pay attention to possibilities of improving the process of farm machinery navigation. Individual manufacturers, such as, e.g. the Norac company (Saskatoon, Canada), offer technical solutions reducing the level of risk in certain threats.

Table 3. Highest values of risk number/priority (*MR/P*)

Failure location	Failure mode	*MR/P* before corrective measures	*MR/P* after corrective measures
MTK	position is occupied to the right or to the left	147	70
MTK	unable to compensate changes in terrain	168	84
MTK	able to correct neither position nor angle	216	72
Monitor	parallel tracking system is slow and sluggish	120	54
Mobile processor	device fails to accept the licence code	112	28
Mobile processor	memory error	140	56

MTK – terrain compensation module

In the prepared forms (Table 1), there are several indicators that show the resulting values of risk for individual components of the examined system. According to the evaluation, the highest risk level occurred in the terrain compensation module (MTK), which is the most important component to cover the undesired overlaps and skips on steep land. This error is often difficult to reveal; therefore, the value of the highest risk on this component represents number 216 (Table 3). The relevant corrective measures (Table 1) give an overview of how to avoid the individual failures.

Table 3 contains the system components with the highest risk number. It is possible to see how the risk value declined on the most risky parts of the system. The risk value was reduced by about one half, and this value can be considered a controllable risk. With these navigation system components, a high risk level before measures was and often is caused by absence of knowledge. The problem of a company that decides to use the satellite navigation of machines is especially the absence of perfectly qualified personnel.

In our case, failures with the highest risk number represent 30% of the total possible examined components on which failures of a certain extent are possible to occur. The remaining 70% are negligible failures because their values do not exceed risk number 100. However, also with these negligible failures were we able to reduce the risk by one half. That can be considered as very successful in practical applications.

In conclusion, it can be stated that using navigation in machines has a positive effect on the facilitation of work and reduction of fatigue; however, an efficient management of work is necessary.

Our analysis focused on failures of GPS navigation, by which we obtained valuable information on possible failures and the mode of their detection. When applying the FMEA method, a too high risk number forced us to consider suitable corrective measures.

As already mentioned, the individual forms contain described consequences such as safety, stress, fatigue, which are directly or indirectly influenced by navigation itself. When working with mobile machines and energy sources, operators are influenced primarily by the working environment. The role of navigation is to alleviate some negative consequences of the working environment; however, not always are we able to reduce these consequences by GPS.

When performing the individual working operations, operators are under sensory stress which is caused by a continuous monitoring of display and control elements. Sensory stress can best be seen in the system working on the principle of a light bar, where the vision of operators is loaded with monitoring the diodes on the panel of the light bar. Therefore, such being the case, the use of automated navigation with a stepping motor appears to be a better solution. An important factor for operator's comfort is the distribution of individual display and control elements of navigation. This issue is described in the Decree No 542/2007 on details of occupational health protection against physical stress, mental stress and sensory stress.

Using navigation, operators can be under a considerable stress. That occurs when operators are not trained and have not a perfect knowledge of controlling the system. There is often a failure that cannot be easily and quickly removed, and service workers must be called. By waiting on service workers, working hours can be extended, and the total downtime can be prolonged, which is undesirable for operators, especially when they are paid according to output. The reduction of negative impacts of stress on operators and working process can be achieved by preventive maintenance.

After reviewing the said facts, it can be stated that the use of navigation systems appears to be a suitable method for facilitating the work. To maintain this trend and in order for the operator not to be under an excessive mental stress, the suitability of using the above-mentioned FMEA is at the right place, especially when the objective is to save time and investments that are not negligible when implementing the GPS navigation.

CONCLUSION

This contribution focuses on the safety of navigation systems in a company. The use of navigation systems and navigation equipment in mobile machines working in fields appears to be the right response to increase the safety and reduce the potential environmental impacts. The implementation of satellite navigation increases the overall productivity of work and reduces the fatigue of workers. We know that the current market is enriched by growing complexities of machines and technologies, by which the probability of risk increases. Therefore, it is important that attention is paid to occupational health and safety. The responsibility for the concept and policy of occupational health and safety lies on the employer. The thing that matters and which the employer must not forget is training. In order to increase the overall efficiency of using navigation systems, the worker must be provided with relevant information on possible failures of navigation systems.

When using navigation, it is necessary to be aware of individual unfavourable impacts on operators such as a poor organisation of work and failing to observe the preventive maintenance. Decision to use GPS and apply the FMEA method can positively influence the whole farm. By a preventive application of FMEA, it is possible to avoid problems that often occur when applying new technologies.

The result of function of the entire system is a more accurate and comfort control of driving direction, which leads to reduction of the load, fatigue and stress of operators. That contributes to increasing safety of working with machines, which was confirmed by a driver of the measured machine, too. Other benefits of satellite navigation systems with an autopilot are the possibility of working at night, in fog, and in dusty conditions, i.e. by observing the required spacing of tramlines, increased quality of work (overlaps, skips, headlands, etc.), and limiting the environmental damage.

References

Bujna M., Kotus M., Prístavka M., Földešiová D., 2012. Analýza ohrozenia metódou FMEA. [Analysis of hazard using FMEA.] In: Technika v technológiách agrosektora 2012. Nitra, SUA in Nitra: 32–35.

Bujna M., Prístavka M., 2012. Analýza ohrozenia metódou FMEA. [Analysis of hazard using FMEA.] In: Kvalita a spoľahlivosť technických systémov. Nitra, SUA in Nitra: 36–40.

EHSANI M.R., SULLIVAN M., WALKER J.T., ZIMMERMAN T.L., 2002. A method of evaluating different guidance systems. An ASAE meeting paper No. 021155, St. Joseph, ASAE: 9.

Decree No 542/2007. Vyhláška č. 542/2007 Z. z. o podrobnostiach o ochrane zdravia pred fyzickou záťažou pri práci, psychickou pracovnou záťažou a senzorickou záťažou pri práci. [On details of occupational health protection from physical stress, mental stress and sensory stress.]

FROHMAN E., ŠVARDA R., 2010. Využitie satelitnej navigácie a polohových systémov GPS v poľnohospodárstve. [Using satellite navigation and GPS positioning systems in agriculture.] TechPark. Available at www.techpark.sk/technika-782009/vyuzitie-satelitnej-navigacie-a-polohovych-systemov-gps-v-polnohospodarstve.html (accessed January 15, 2013).

HRUBEC J. et al., 2009. Integrovaný manažérsky system. [Integrated Management System.] Nitra, SUA in Nitra: 543.

MACÁK M., ŽITŇÁK M., 2010. Efektívne využitie satelitnej navigácie v podmienkach presného poľnohospodárstva. [Effective use of satellite navigation in precision agriculture.] Nitra, SUA in Nitra: 125.

MCMAHON K., 2003. Assisted driving. Farm Industry News, 38. Available at http://proquest.umi.com/pqdweb?did=293373431&sid=13&Fmt=4&clientId=70242&RQT=309&VName=PQD

PAČIOVÁ H., SINAY J., GLATZ J., 2009. Bezpečnosť a riziká technických systémov. [Safety and risks of technical systems.] Košice, Technical University: 246.

PRÍSTAVKA M., HRUBEC J., BUJNA M., KOTOROVÁ M., 2011. Quality control in production processes. In: Toyotarity. Control in Organizations. Dnipropetrovsk, Yurii V. Makovetsky: 121–129.

STN ISO 9000, 2005. Systémy manažérstva kvality. Základy a slovník. [Quality management systems. Basis and vocabulary.] Bratislava, Slovak Office of Standards, Metrology and Testing.

Received for publication April 15, 2013
Accepted after corrections July 29, 2013

Corresponding author:

Ing. MIROSLAV ŽITŇÁK, PhD., Slovak University of Agriculture in Nitra, Faculty of Engineering, Department of Structures, Tr. A. Hlinku 2, 949 76 Nitra, Slovak Republic
phone: +421 37 641 5692, e-mail: miroslav.zitnak@uniag.sk

Research of journal bearings for using in agricultural mobile machines

M. Kadnár[1], J. Rusnák[1], M. Bujna[1], J. Valíček[2,3], M. Kušnerová[2,3], P. Tököly[4]

[1]*Department of Machine Design, Faculty of Engineering, Slovak University of Agriculture in Nitra, Nitra, Slovak Republic*
[2]*Institute of Physics, Faculty of Mining and Geology, VŠB–Technical University of Ostrava, Ostrava, Czech Republic*
[3]*Regional Materials Science and Technology Centre, Faculty of Metallurgy and Materials Engineering, VŠB – Technical University of Ostrava, Ostrava, Czech Republic*
[4]*Department of Technical mechanics and Machine parts, Faculty of Special Techniques, Alexander Dubček University of Trenčín, Trenčín, Slovak Republic*

Abstract

Kadnár M., Rusnák J., Bujna M., Valíček J., Kušnerová M., Tököly P., 2014. **Research of journal bearings for using in agricultural mobile machines**. Res. Agr. Eng., *60* (Special Issue): S25–S30.

The competitive environment forces producers in agricultural machine industry to decrease the costs. Producers as well as sub-suppliers need to find possible savings. The paper presents results of laboratory experiments with real journal bearings made of bimetallic alloy performed to find out possible replacement of a rolling bearing by a journal bearing. An important correlation between the results of laboratory experiments with a model of tribological system and the real journal node can be achieved by a maximum approach of simulation features by real running conditions. Thus, the given experiment conditions result from the chosen application, i.e. a steering servo unit in mobile machines. The experiments were performed on the Tribotestor M'06" testing machine.

Keywords: bearings; bimetallic alloy; tribological experiment; Tribotestor M'06"

Nowadays, the experimental determining of tribological features is performed via devices with different configurations. It is very common that experiment parameters are always chosen based on needs and demands. Each experiment is influenced by several factors, whereas the weight of factors is different, and each of them is determined to solve a partial tribological task (Mang, Dresel 2001; Bayer 2004; Ünlü, Atik 2007; Kučera, Pršan 2008a). The data obtained from experiments have an important influence on interpreting the results where friction and wear are measured. The development of microtribology and nanotribology influences the parameters of experimental testing devices. There is a trend of using devices with low surface speed and low load. In most situations, the real friction node is replaced by a line contact or a spot contact; however, the reached friction coefficient cannot be compared with values of real journal nodes (Žiačik et al. 1995; Kučera 2008). There also exist minimum experimental devices which are able to perform an experiment with real journal node during real running conditions as they are usually used to provide durability tests (Bayer 2004; Kučera, Pršan 2008b; Kadnár et al. 2011). According to the simple design of existing devices, the minimum possibility of changing the parameters during the experiment may be seen as their disadvantage.

MATERIAL AND METHODS

Test Rig. In experiments with real journal bearings, the Tribotestor M'06 testing machine (Slovak University of Agriculture in Nitra, Nitra, Slovak Republic) allows:

- to use the most modern measuring technology,
- to influence the range of running parameters,
- to provide modification easily,
- to provide several lubrication modes, etc.

When the journal node is loaded by normal force F_N, there is friction between the shaft and bearing, represented by friction force F_T effecting the rotation movement of the shaft. Friction also causes the transmission of torsion moment to the head of the testing machine (Fig. 1). The transmitted torsion moment is defined by friction force $F_T' = F_T$ and the radius (diameter) of the shaft r_H.

The friction coefficient is determined by the formula:

$$\mu = \frac{F_t a}{F_N r_H} \quad (1)$$

where:

F_t – force at the end of teasting head's arm (N)
a – length of testing head's arm (mm)
F_N – normal force (N)
r_H – radius (diameter) of the testing shaft (mm)

Material. For the producer of the steering servo unit, the experiments with different kinds of journal bearings were elaborated for the purpose of replacing the rolling bearing by the journal bearing. The reason of the purpose was an expected saving. Bimetallic bearings are made by curling bimetallic strips with different sliding materials. The active layer is represented by a sliding material which is coated on a steel base in the form of powder and is compressed by rolling. The smooth structure is considered to be the main advantage because the bearings of these materials are usable also within the critical friction. The structure of the materials is illustrated in Table 1.

The B10 material is a metal-polymer composite material with excellent friction features also without lubrication. The required shaft roughness can-

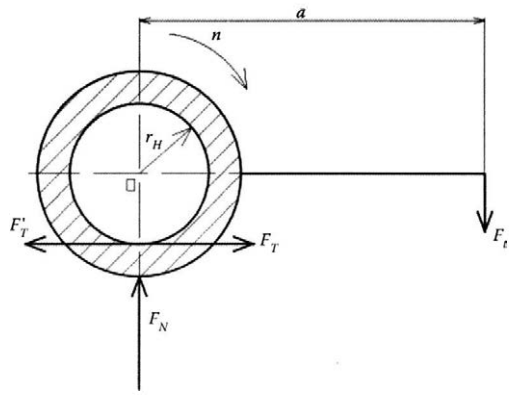

Fig. 1. Diagram of Tribotestor M'06 testing machine

F_T' – transmitted torsion moment force; F_N – normal load; F_T – friction force; F_t – force at the end of teasting head's arm; n – revolutions; a – length of testing head's arm, r_H – radius of the testing shaft

not exceed 0.4 μm, the shaft hardness must be over 200 HB. B30 is a bimetallic material with bronze alloy (both Kajo Metal, Dolní Kubín, Slovak Republic). The required shaft features are the same as for the B10 material. The basic features of the B10 and B30 materials are illustrated in Table 2.

Experiments. The following conditions were followed during the experiments for friction measurement:

- shaft of Φ 10, cemented, hardened and edged – material ČSN 14 220/EN 16MnCr5 – common material for the selected application (each shaft used only for one measurement),
- bearing clearance of 0.02 mm,
- six tested samples of each materials,
- no lubrication.

Kadnár (2009) illustrates the selection of experiment parameters. Based on the parameters, the complex mode of the experiment for friction measurement was determined. The mode included several partial phases which are illustrated in Table 3. Before the experiment, each sliding node was exposed by a test run of 600 s with the revolutions of 2,000 min^{-1} and load of 150 N. The phase was considered to be a preparatory phase, and reached results are not taken into consideration further.

Table 1. Chemical structure of materials (% wt.)

Material	Cu	Pb	Sn	Zn	P	Fe	Ni	Sb	Other
B10 CuPb10Sn10	rest	9–11	9–11	≤ 0.5	≤ 0.1	≤ 0.7	≤ 0.5	≤ 0.2	≤ 0.5
B30 CuPb30	rest	26–33	≤ 0.5	≤ 0.5	≤ 0.1	≤ 0.7	≤ 0.5	≤ 0.2	≤ 0.5

Table 2. Basic features of B10 and B30 materials

Material	Chemical structure	Tensile strength (MPa)	Max. load in static stress (MPa)	Max. load in dynamic stress (MPa)	Max. operation temp. (°C)
B10	CuPb10Sn10	230–280	200	120	250
B30	CuPb30	90–107	120	40	160

Table 3. Phases of the experiment for friction measurement

Phase	Time (s)	Duration (s)	Load (N)	Revolutions (rpm)
Sliding node stabilisation	0	20	20	2,000
Measurement with constant speed	20	120	100	2,000
	140	120	150	2,000
	260	120	200	2,000
	380	120	250	2,000
Sliding node stabilisation	500	20	20	4,000
Measurement with constant speed	520	120	150	4,000
	640	120	150	500
Supporting measurement for checking of measuring device	760	30	100	0
	790	30	150	0
	820	30	200	0
	850	30	250	0

After the test run, each node was stabilised, i.e. loaded by 20 N with the revolutions of 2,000 min^{-1}. Consequently, the measurement with the revolutions of 2,000 min^{-1} was performed with the load of 100, 150, 200 and 250 N. Each measurement lasted 120 seconds. Before the measurement with constant load, each node undertook another stabilisation which lasted 20 s loaded by 20 N with the revolutions of 4,000 min^{-1}.

The measurement with constant load was undertaken with the load of 150 N and revolutions of 4,000 min^{-1} or 500 min^{-1}. Both measurements lasted 120 s. The diagram of load and rotational frequency depending on time is illustrated in Fig. 2.

There are many statistical interpretations of friction measurement. For an application in tribology, table data are used rather than additional information (Bhushan 2002; Bayer 2004; Ünlü, Atik 2009; Kadnár et al. 2011). The most important information is that in the unfiltered record during friction force measurement, the measured data generally reflect the reality in a tribological node. Further processed information in a table or figure is only its interpretation. Thus, we have decided for a compromise, i.e. for a figure interpretation with illustrating the average value of measurement and the statistical interval of 95%. The idea is supported by the fact that the total friction coefficient is not

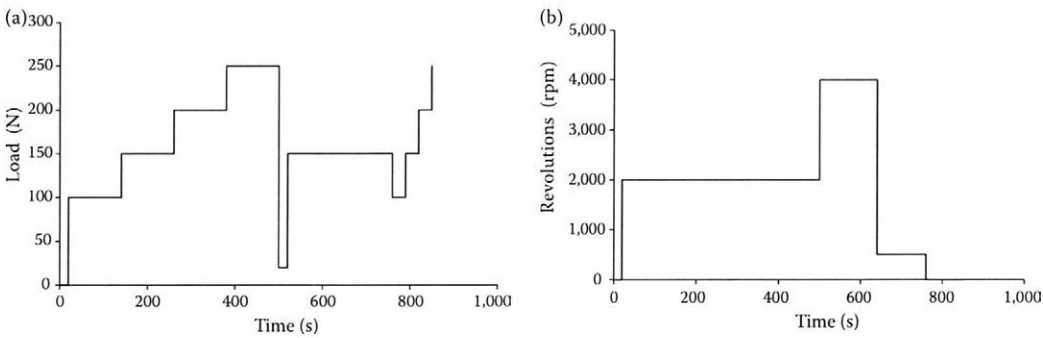

Fig. 2. Load (a) and rotational frequency (b) depending on time

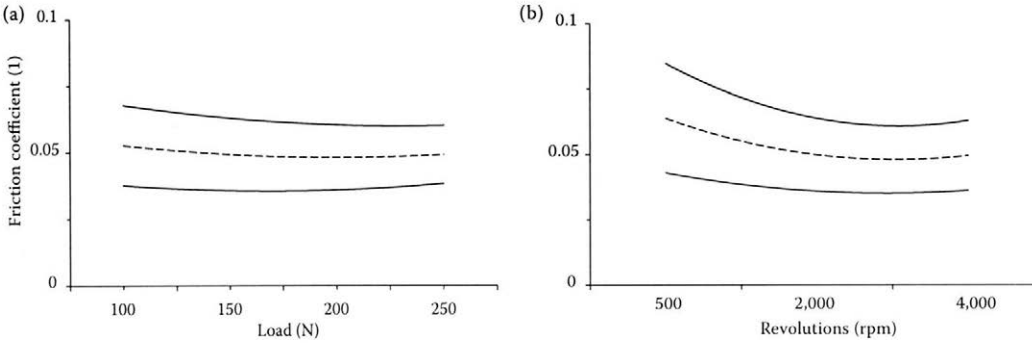

Fig. 3. B10 material – friction coefficient depending (a) on load and (b) on rotational frequency with 95% interval of confidence

a measured value but a calculated one. At the same time, rotational frequency was used rather than the surface speed concerning the features of the steering servo unit (PÁLTIK et al. 2007; PONIČAN, KORENKO 2008).

RESULTS AND DISCUSSION

Within the sliding node, the B10 material had stable features in connection with variable load or variable rotational frequency. No important vibrations were recorded during test run and experiments themselves. The diagram of friction coefficient within constant rotational frequency, i.e. depending on variable load, is illustrated in Fig. 3a.

At the load of 100 N, the friction coefficient was 0.05. When decreasing the load, there were only little differences in friction coefficient. The temperature was practically the same, i.e. 42°C. At the load of 250 N, the friction coefficient was 0.05. Thus, the sliding node of B10 material can be evaluated to be favourable. At the load of 150 N, there was only a little decrease in friction coefficient.

At the rotational frequency of 500 min^{-1}, the lubrication mode can be considered to be mixed. However, the friction coefficient did not exceed the limit of 0.1. During the experiment, the friction coefficient ranged from 0.06 to 0.07. The diagram of friction coefficient with constant load and variable rotational frequency is illustrated in Fig. 3b.

At the frequency of 4,000 min^{-1}, the friction coefficient decreased to 0.05. Thus, it is possible to conclude that the sliding node of B10 material is considered to have stable features. Despite the conclusion, the bearing surface had little wear, a local wear of thin film, i.e. a sliding layer on the surface of the material (Fig. 4).

Regarding the surface of the journal bearing of B10 material, the separation of surface was recorded. In some parts, there was a visible subsurface layer of sintered bronze. Based on the results, the wear resistance of B10 material towards the chosen application is not sufficient. The weight loss of B10 material ranged from 9 to 14 mg (Fig. 5).

The test run or experiments themselves when using the B30 material recorded more important vibrations. Fig. 6a illustrates the diagram of fric-

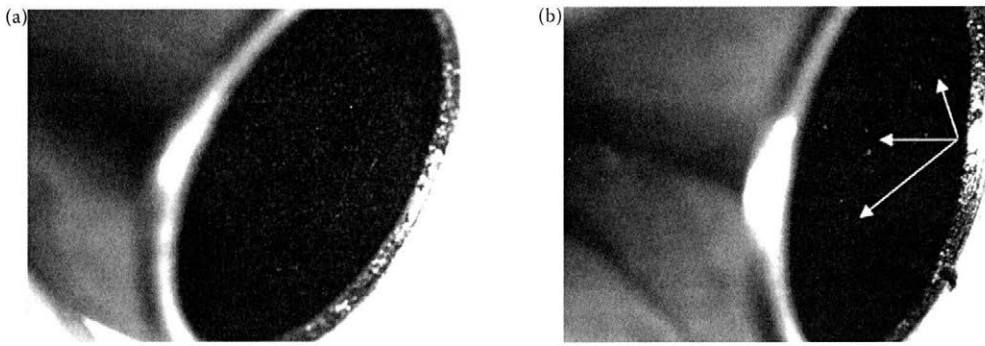

Fig. 4. B10 material – surface before (a) and after (b) the measurement

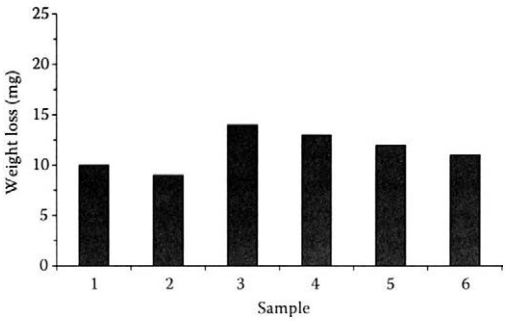

Fig. 5. B10 material – weight loss

tion coefficient depending on variable load. At the load from 100 to 200 N, the friction coefficient was 0.08. At the load of 250 N, the friction coefficient decreased to 0.07. The temperature was not more than 43°C.

At the load of 150 N and lower frequencies, the friction coefficient decreased to 0.10. It resulted from conditions in the sliding node which corresponds to the area of mixed friction.

The diagram of friction coefficient with constant load and variable frequency is illustrated in Fig. 6b. At the frequency of 4,000 min^{-1}, the friction coefficient decreased to 0.08.

According to the high value of friction coefficient, the B30 material is considered to be less favourable. The surface of sliding material had local wear (Fig. 7). A higher rate of noise and vibrations were also recorded. The sliding node had only average features regarding friction and wear, and therefore the bearings after the test can be considered to be damaged. Based on the experiment results, the wear resistance of B30 material is evaluated to be not sufficient.

The weight loss within the B30 material ranged from 11 to 16 mg (Fig. 8).

CONSLUSION

As the literature confirms, high values of friction coefficient were recorded within dry friction. The tested bearings were stable depending on load as

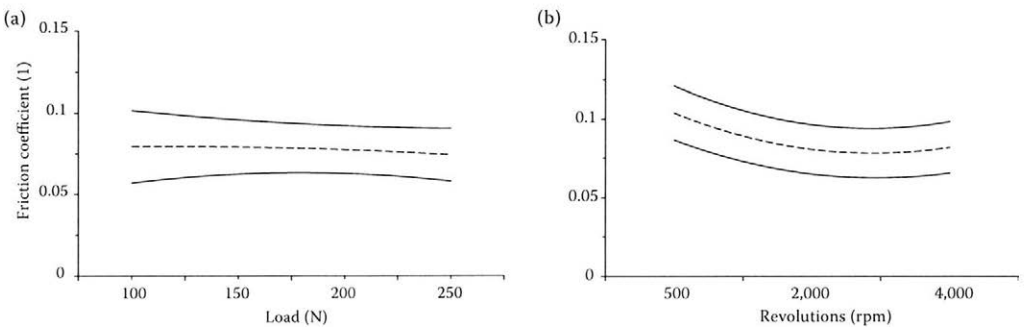

Fig. 6. B30 material – (a) friction coefficient depending on load and (b) on frequency with 95% interval of confidence

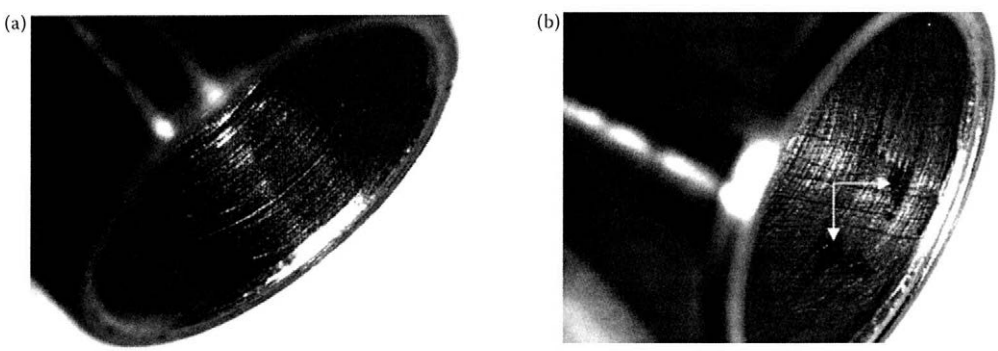

Fig. 7. B30 material – surface before (a) and after (b) the measurement

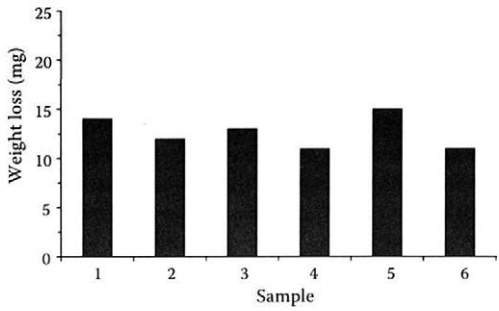

Fig. 8. B30 material – weight loss

well as frequency. For the chosen application, the tested bearings are considered not to be suitable. In the future, it is possible to verify tribological features of tested bearings also within hydrodynamic friction, whereas the structure of the testing head allows the circulation of lubricant and an additional influence of sliding node temperature, which helps to simulate real conditions better.

References

Bayer G.R., 2004. Mechanical Wear Fundamentals and Testing. New York, Marcel Dekker: 399.

Bhushan B., 2002. Introduction to Tribology. New York, John Wiley & Sons: 752.

Kadnár M., Rusnák J., Kučera M., Kročko M., 2009. Selection of sliding node for steering servo unit. In: 50th International Scientific Conference of Departments of Machine Design. Žilina, EDIS.

Kadnár M., Kadnár J., Hloch S., Valíček J., Rusnák J., 2011. The design and verification of experimental machine for real journal bearing testing. Tehnički vjestnik, *18*: 95–98.

Kučera M., 2008. Prediction of characteristics for pairs of materials in condition of limit friction. Acta Technologica Agriculturae, *11*: 11–15.

Kučera M., Pršan J., 2008a. Analysis of friction marks and wear products. Acta Technologica Agriculturae, *11*: 43–49.

Kučera M., Pršan J., 2008b. Tribologic properties of selected materials. Technical Sciences, *11*: 228–241.

Mang T., Dresel W., 2001. Lubricants and Lubrication. New York, Wiley: 790.

Páltik J., Findura P., Maga J., Korenko M., Angelovič M., 2007. Agricultural Machinery: Testing, Construction, Usage (1st part). Nitra, SUA in Nitra: 190.

Poničan J., Korenko M., 2008. Plant Production Machinery: Collecting Machinery for Crops, Grains, Flax, Potatoes, Vegetables and Fruit. Nitra, SUA in Nitra: 248.

Ünlü S.B., Atik E., 2007. Determination of friction coefficient in journal bearings. Materials & Design, *28*: 973–977.

Ünlü S.B., Atik E., 2009. Tribological properties of journal bearings manufactured from particle reinforced al composites. Materials & Design, *30*: 1381–1385.

Žiačik A., Bronček J., Šiška V., 1995. The sliding properties of the bearings with polymer lining. In: Faculty of Mechanical Engineering. 2nd Scientific Conference. Žilina, University of Žilina: 40–44.

Received for publication April 15, 2013
Accepted after corrections July 27, 2013

Corresponding author:

Doc. Ing. Milan Kadnár, PhD., Slovak University of Agriculture in Nitra, Faculty of Engineering, Department of Machine Design, Tr. A. Hlinku 2, 949 76 Nitra, Slovak Republic
phone: + 421 376 414 107, e-mail: milan.kadnar@uniag.sk

Fuzzy control of temperature and humidity microclimate in closed areas for poultry breeding

M. Olejár, V. Cviklovič, D. Hrubý, L. Tóth

Department of Electrical Engineering, Automation and Informatics, Faculty of Engineering, Slovak University of Agriculture in Nitra, Nitra, Slovak Republic

Abstract

Olejár M., Cviklovič V., Hrubý D., Tóth L., 2014. **Fuzzy control of temperature and humidity microclimate in closed areas for poultry breeding**. Res. Agr. Eng., *60* (Special Issue): S31–36.

This contribution describes the ways of temperature and humidity microclimate control in breeding areas using a fuzzy controller. It is focused on poultry, whereby the most important parameters for optimal breeding are temperature and humidity. The main aim was to evaluate the control process according to control quality in the controller's steady state and the power consumption of the system. The used control algorithm was designed in the Matlab application, and it was practically verified in a closed thermodynamic system. Practical measurements have shown that with an increasing number of fuzzy controller's interference rules a better control quality in steady states and lower power consumption of the system is achieved.

Keywords: fuzzy algorithm; control quality; thermoregulation

With a classical insight into control and automation everything is based on the controller's dominance in a control circuit. The majority of analyses and criteria evaluating the results of control are subordinate to that. A number of methods used in practice have been existing for more than 50 years. However, there are a number of new methods that enrich the existing control theory. One of such methods is fuzzy control, the main advantage of which is a high-performance computing and possibility to control several physical variables at the same time. On the basis of described advantages, fuzzy control is applied to control systems where conventional methods of technological process control have been used to date.

One of applications is the maintenance of thermal and humidity microclimate in closed areas for poultry breeding. The role of control is to ensure conditions for a healthy and good organism growth, high utility with respect to basic needs of the species and category of poultry. One of other important conditions is to minimize the power consumption in order to achieve the lowest cost of breeding.

MATERIAL AND METHODS

The creation of optimal conditions for poultry is especially important in the first few days after hatching, when the chicken's body is not fully developed. Immediately after hatching and drying, a chicken can ingest the food, but is not able to compensate the temperature fluctuation because its thermoregulation is not fully developed. For this reason, it is necessary to ensure a relatively high temperature in the breeding area in the first weeks, as shown in Table 1. Temperature stabilization for adult hens occurs on approximately the fourteenth day of age. Thermoregulation is fully developed after the fourth week of age. Thermoregulation in halls is especially important in relation to the development of the chicken's body. Higher or lower

Table 1. Microclimate conditions for poultry breeding

Age (weeks)	Heating by local sources (°C)		Full-area heating (°C)	Relative humidity (%)
	in the hall	below the source		
1	24–25	33	33	70–75
2	21–22	28	28	
3	20	25	25	65
4	18	23	23	55–70

temperatures negatively affect the feed consumption, growth, activity of chickens and consequently the health. One of the indicators of a suitable microclimate in halls is also animal mortality during the laying breeding (GÁLIK 2004). At the same time, thermal and humidity regime is automatically regulated in halls. Relative humidity is considered always in relation to temperature. For higher temperatures, the relative humidity is lower, which causes drying of mucous membranes (and that supports infectious diseases), reduces the growth and increases the dust level. When the relative humidity falls below 30%, there is an increase in susceptibility to infections, which is related to the fact that microorganisms survive in dry air for a longer time. A high relative humidity, which is usually at lower temperatures, reduces the insulation ability of feathers, causes the wetting of bedding materials, which increases the production of ammonia and hydrogen sulphide (SKŘIVAN et al. 2000). Therefore, a good development of chickens requires a higher relative humidity during the first weeks, and then it falls as shown in Table 1.

One of the ways to ensure suitable microclimatic conditions in poultry breeding is the use of fuzzy control. The advantage of this control in comparison with conventionally used controls is the ability to control several independent physical quantities. A characteristic feature of fuzzy control is the possibility to use human's empirical knowledge about the controlled process, which is referred to as the base of data. The base of data is represented by information on steady states and intervals that include values of input and output variables, their limits, including the verbally defined control strategy by means of which it is possible to perform the control. The fuzzy controller's structure is shown in Fig. 1.

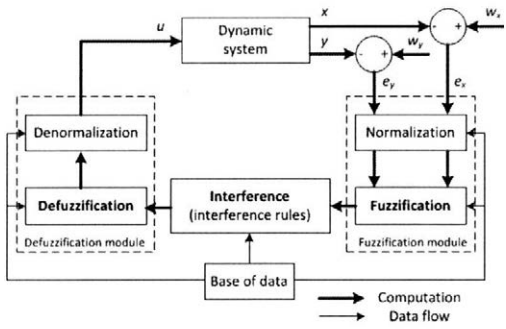

Fig. 1. Block diagram of the fuzzy controller

u – control variable; y – process variable 1; x – process variable 2; e_x – controller error variable x; e_y – controller error variable y; w_x – set point variable x; w_y – set point variable y

In the fuzzification block, there are converted data that are measured for fuzzy sets. Each fuzzy set is represented by membership function. These functions determine the degree by which the measured value is included in the fuzzy set. Values can range from 0 (measurement is not included in the fuzzy set) to 1 (measurement is included in the fuzzy set). Fuzzy sets are described by linguistic variables, which are expressions of a certain language such as, for example water is "cold", "warm" and "hot". Examples of three fuzzy sets, which are represented by linguistic variables $LP1$, $LP2$ and $LP3$, are shown in Fig. 2.

The fuzzification block can be preceded by a normalization block for conversion of physical values to normalized values. In the interference block, which forms the main part of the fuzzy controller, output fuzzy sets are obtained from input fuzzy sets on the base of interference rules. In our case, input variables are temperature and humidity x, y and one actuating variable u. These variables are described by several fuzzy sets represented by linguistic variables. The method of obtaining the output fuzzy sets from input fuzzy sets is as follows:

$$\alpha_1 = m_{LP1}(x) \wedge m_{LP1}(y) = \min\{m_{LP1}(x), m_{LP1}(y)\} \quad (1)$$

$$\alpha_2 = m_{LP2}(x) \wedge m_{LP1}(y) = \min\{m_{LP2}(x), m_{LP1}(y)\} \quad (2)$$

where

α_1 – degree of membership function $m_{LP1}(u)$ of linguistic variable $LP1$ of actuating variable u

α_2 – degree of membership function $m_{LP2}(u)$ of linguistic variable $LP2$ of actuating variable u

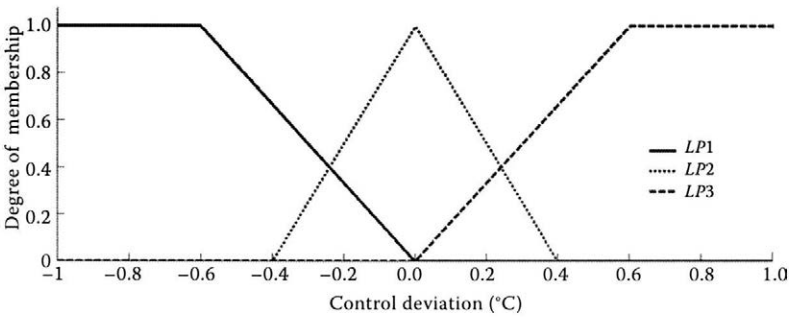

Fig. 2. Membership function for fuzzy sets of control deviation represented by the linguistic variables *LP*1, *LP*2 and *LP*3

$m_{LP1}(x)$ – membership function of linguistic variable *LP1* of input variable x

$m_{LP1}(y)$ – membership function of linguistic variable *LP1* of input variable y

$m_{LP2}(x)$ – membership function of linguistic variable *LP2* of input variable x

Fuzzy sets of the actuating variable u are determined as follows:

$$^*m_{LP1}(u) = \alpha_1 \wedge m_{LP1}(u) = \min \{\alpha_1, m_{LP1}(u)\} \quad (3)$$

$$^*m_{LP2}(u) = \alpha_2 \wedge m_{LP2}(u) = \min \{\alpha_2, m_{LP2}(u)\} \quad (4)$$

where:

$m_{LP1}(u)$ – membership function of linguistic variable *LP*1 of actuating variable u

$m_{LP2}(u)$ – membership function of linguistic variable *LP*2 of actuating variable u

$^*m_{LP1}(u)$ – fuzzy set of membership function $m_{LP1}(u)$

$^*m_{LP2}(u)$ – fuzzy set of membership function $m_{LP2}(u)$

The resulting fuzzy set is determined by unification of fuzzy sets $^*m_{LP1}(u)$ and $^*m_{LP2}(u)$:

$$^*m_{CEL}(u) = \max \{^*m_{LP1}(u), ^*m_{LP2}(u)\} \quad (5)$$

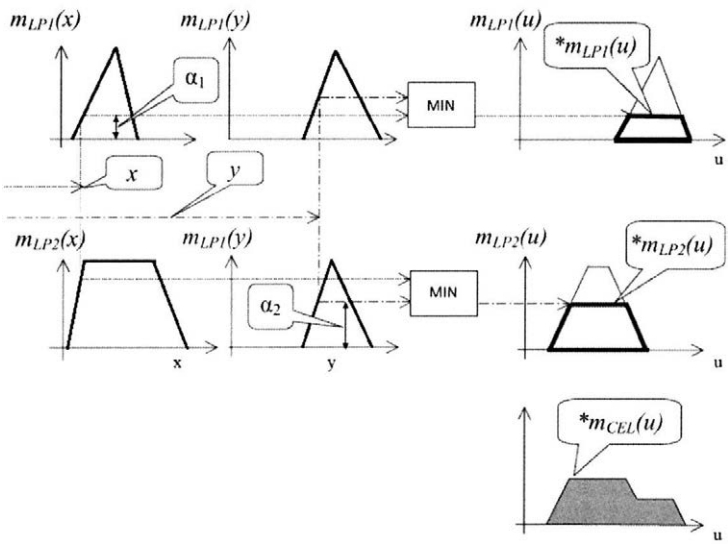

Fig. 3. Determination of output fuzzy sets for two output variables x, y (Modrlák 2004)

α_1 – degree of membership function $m_{LP1}(u)$ of linguistic variable *LP*1 of actuating variable u; α_2 – degree of membership function $m_{LP2}(u)$ of linguistic variable *LP*2 of actuating variable u; $m_{LP1}(x)$ – is membership function of linguistic variable *LP1* of input variable x, $m_{LP1}(y)$ – membership function of linguistic variable *LP*1 of input variable; $m_{LP2}(x)$ – membership function of linguistic variable *LP*2 of input variable x; $m_{LP1}(u)$ – membership function of linguistic variable *LP*1 of actuating variable u; $m_{LP2}(u)$ – membership function of linguistic variable *LP*2 of actuating variable u; $^*m_{LP1}(u)$ – fuzzy set of membership function $m_{LP1}(u)$; $^*m_{LP2}(u)$ – fuzzy set of membership function $m_{LP2}(u)$; $^*m_{CEL}(u)$ – resulting fuzzy set is determined by unification of fuzzy sets $^*m_{LP1}(u)$ and $^*m_{LP2}(u)$

Graphical representation of determining the output fuzzy set is shown in Fig. 3. The relationship between input and output fuzzy sets that are represented by linguistic variables is determined by decision rules. Generally, it is a simple logical operation, the form of which for two input variables and one output variable is as follows:

IF (x belongs to $LP1$) **AND** (y belongs to $LP1$) **THEN** (u belongs to $LP1$)

IF (x belongs to $LP2$) **AND** (y belongs to $LP2$) **THEN** (u belongs to $LP2$)

The number of interference rules is determined by multiplying the number of input fuzzy sets. The last task of the fuzzy controller is to assign the actuating variable value to the output fuzzy set. This process of linking is named as defuzzification. There are many defuzzification methods which are based on the methods of determining the centre of gravity or methods for determining the maximum, as shown in Fig. 4. For the first method, the output value of action is determined as the coordinate of the resulting area of fuzzy set. The methods of determining the maximum are based on determining the most significant maximum of the resulting fuzzy set located on the left (LoM), on the right (RoM), or in the centre (MoM) (Modrlák 2004). After the defuzzification block, there can be a denormalization block where conversion of the output variable to the physical output variable is performed. We have used the centre of gravity method for defuzzification.

RESULTS AND DISCUSSION

In the control of microclimate temperature and humidity conditions in the breeding area, two physical variables are controlled. This type of control is demanding in terms of fuzzy controller selection and its setup. A standard PSD controller does not support a concurrent control of more variables due to their different behaviour. This is related to different setting of controller parameters for individual controlled variables. For such applications, it is therefore preferable to use a fuzzy controller that is independent of the number of input and output variables. A detailed mathematical description of the controlled system is not needed because the fuzzy controller uses human empirical knowledge on the controlled process. This feature simplifies the implementation of the fuzzy controller into real conditions of poultry breeding. The block diagram of the control algorithm is shown in Fig. 5.

Input variables of the fuzzy controller are temperature control deviation e_t and relative humidity control deviation e_h. The output variable is the actuating variable u that controls the heating and ventilation system. The closed breeding area represented an isolated thermodynamic system with dimensions 100 × 50 × 50 cm. A fuzzy controller with 9 and 49 interference rules was used for temperature and humidity control in order to assess the impact of the rules count on quality control. After defining all the fuzzy controller parameters, we have obtained the resulting control areas, which are shown in Fig. 6. These control areas determine the basic control strategy, the result of which is the waveform of temperature and humidity in the closed breeding space. Whereas the entire breeding is time-consuming, time was shortened to 18 h, which represents 3 weeks of breeding. This time is sufficient for evaluating the basic statistical parameters. As regards temperature control, we have focused on the required temperature values for full-area heating that are shown in Table 1.

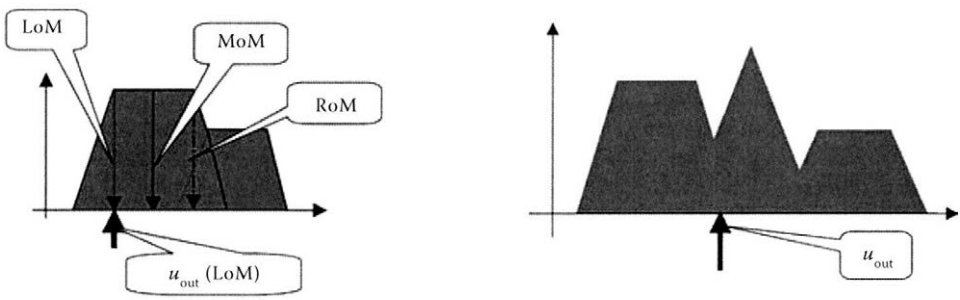

Fig. 4. Ways of defuzzification: (a) using the method of determining the most significantly located maximum on the left (LoM), on the right (RoM), or in the centre (MoM), (b) using the method of determining the centre of gravity (u_{out} – output actuating variable) (Modrlák 2004)

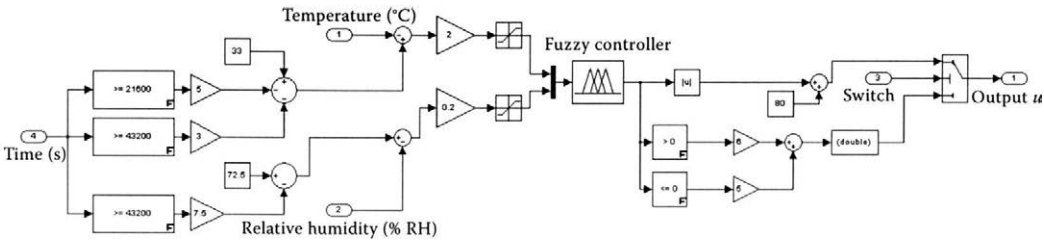

Fig. 5. Block diagram of control algorithm with the fuzzy controller

Fig. 7 describes the ability of the fuzzy controller to provide optimal temperature and humidity conditions for poultry breeding. In addition to stability, each control process must also meet the conditions of control quality in steady states. Selected indicators of descriptive statistics were used to evaluate the control quality in steady states. The data are shown in Table 2.

For internal temperature and humidity regulation, fuzzy control with 49 interference rules appears to be better. This is due to the fact that with increasing the number of interference rules (input fuzzy sets) of the fuzzy controller the control accuracy of physical parameters increases. When selecting the control algorithm, important is not only control quality but also energy consumption. The volt-ampere method was used for measuring the energy consumption during 10,000 s. Temperature was set to 28°C, and relative humidity was 72.5%. Fuzzy control with 49 interference rules is better not only for control quality but also for lower power consumption. Energy saving of the controller with 49 interference rules is 12.55% in comparison with the controller with 9 interference rules.

CONCLUSION

Using the fuzzy controller for microclimate control combines advantages of lower power consumption and higher control quality as compared to conventional controllers (PSD, PID, etc.). These parameters are improved with an increasing number of interference rules. The difference in energy consumption between the controller with 49 rules and with 9 rules is 12.55%. The accuracy of temperature and humidity regulation is higher by a decade. Another advantage is the possibility to implement the fuzzy controller into an existing system without modification and with a minimal investment.

The disadvantage is in increasing complexity and time consumption of setting the controller. Therefore, it is necessary to consider the cost-effectiveness of its setting with respect to saved funds from lower energy consumption. For large objects such as poultry breeding areas the investment return is short.

Fuzzy control provides a wide application in agricultural production where multiple variables are needed to be controlled simultaneously. Such applications are, for example microclimate control in

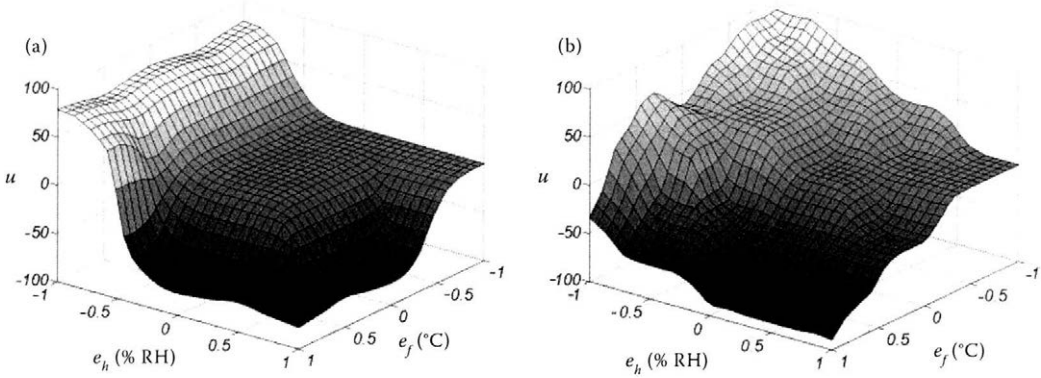

Fig. 6. Regulation area of the fuzzy controller of temperature and humidity: (a) with 9 interference rules, (b) with 49 interference rules

e_h – humidity control deviation; u – actuating variable; e_f – temperature control deviation

Table 2. Statistical indicators of control criteria in steady states for fuzzy control of internal temperature and relative humidity with 9 and 49 interference rules

Statistical indicator	Internal temperature		Internal relative humidity	
	9 rules	49 rules	9 rules	49 rules
Variance	0.046°C	0.0039°C	3.45% RH	1.82% RH
Standard deviation	0.216°C	0.062°C	1.858% RH	1.348% RH
Coefficient of variation	0.774%	0.225%	2.543%	1.86%
Average deviation	0.175°C	0.051°C	1.57% RH	1.069% RH

RH – relative humidity

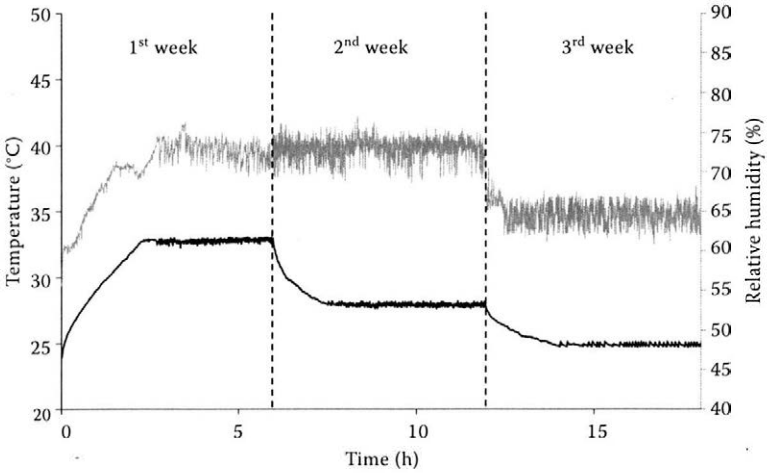

Fig. 7. Time waveform of temperature and humidity regulated by the fuzzy controller in closed breeding areas with 49 interference rules

greenhouses, drying of agricultural products and farm machinery steering.

References

GÁLIK R., 2004. Analýza mikroklimatických podmienok v hale na rozmnožovací chov nosníc. [Analysis of microclimatic conditions in a hall for production breeding of laying hens.] Acta Technologica Agriculturae, 3: 60–64.

MODRLÁK O., 2004. Fuzzy řízení a regulace. [Fuzzy control and regulation.] Available at http://www.kirp.chtf.stuba.sk/~bakosova/wwwRTP/tar2fuz.pdf (accessed January 15, 2013)

SKŘIVAN M., TŮMOVÁ E., VONDRKA K., DOUSEK J., LANCOVÁ B., OUŘEDNÍK J., OPLT J., 2000. Drúbežníctví. [Poultry Science.] Prague, Agrospoj, 2000.

Received for publication April 15, 2013
Accepted after corrections July 29, 2013

Corresponding author:

Ing. MARTIN OLEJÁR, PhD., Slovak University of Agriculture in Nitra, Faculty of Engineering, Department of Electrical Engineering, Automation and Informatics, Tr. A. Hlinku 2, 949 76 Nitra, Slovak Republic
phone: +421 376 415 783, e-mail: martin.olejar@uniag.sk

Performance parameters monitoring of the hydraulic system with bio-oil

I. Janoško, T. Polonec, S. Lindák

Department of Transport and Handling, Faculty of Engineering, Slovak University of Agriculture in Nitra, Nitra, Slovak Republic

Abstract

Janoško I., Polonec T., Lindák S., 2014. **Performance parameters monitoring of the hydraulic system with bio-oil**. Res. Agr. Eng., *60* (Special Issue): S37–S43.

In environmental terms, hydraulic fluids used in the hydraulic system of municipal vehicles represent problems related to a potential leakage from the system into the environment and the subsequent contamination of groundwater and soil. More environment-friendly way is to use green hydraulic fluids that are biodegradable in accidents. This paper aims to investigate the possibilities of biodegradable oil application and its adaptation in the hydraulic systems of municipal vehicles by monitoring the impact of the bio-oil Mobil EAL 46 ESSO on the performance parameters as flow, efficiency, durability, etc. Hydraulic pump revolutions were measured using a non-contact sensor based on the principle of magnetic induction change. Method of tightness monitoring was used to achieve results for functionality and wear of the hydraulic system. During 600 h of the test period no significant deterioration of performance parameters was detected. Results are useful for companies involved in waste collection.

Keywords: Variopress 518; bio-fluid; working hydraulics; power parameters

Developments in the area of municipal engineering hydraulic systems bring a number of benefits associated with facilitating the work during handling the solid municipal waste and, in addition to comfort and control, also the speed of individual working operations during the activity of hydraulic circuits of municipal vehicles.

With growing demands on the construction of hydraulic systems and improving their power parameters, the complexity of requirements for hydraulic fluids in terms of their biodegradability in the environment increases (Jablonický et al. 2012; Kosiba et al. 2012). It is a good reason because demands of an urban vehicle design increase the risk of disorders associated with hydraulic systems, and thus the risk of hydraulic fluid leakage into the environment increases (Janoško et al. 2004, 2008, 2010, 2012; Tkáč et al. 2008).

The hydraulic fluid Mobil EAL 46 ESSO is one of the fluids that are biodegradable and its content does not pollute the environment. It is a liquid that belongs to modern liquids with its appropriate additives improving the operational as well as functional and lubricating properties. It is therefore necessary to analyse the fluid, particularly in terms of its power parameters in the hydraulic system, but also its properties which the manufacturer states in its data sheet.

MATERIAL AND METHODS

Bio-hydraulic fluid Mobil EAL 46 ESSO. The selected hydraulic fluid Mobil EAL 46 ESSO (Exxon Mobil, Port Jerome du Gravenchon, France) is a high-quality and high-power lubricant that is de-

Supported by the Scientific Grant Agency KEGA of the Ministry of Education of the Slovak Republic and Slovak Academy of Sciences, Grant No. 044SPU-4/2014.

Table 1. Characteristics of the hydraulic oil Mobil EAL 46 ESSO

Properties of Mobil EAL 46 ESSO	Benefits of Mobil EAL 46 ESSO
Readily biodegradable hydraulic oil, very low level of water hazard – NGW (not hazardous to water)	reduces the possibility of environmental damage; reduces the potential costs of remediation and cleaning the spillage or leakage; it is becoming an integral part of the ecological environment in the enterprise
High viscosity index and low pour point	wide range of operating temperature
Excellent water separability	prevents formation of deposits and filter plugging, thereby increasing reliability machine devices
Exceptional corrosion protection and compatibility with many metals	limited corrosion of components and actuator systems within the hydraulic system, responding to steel and copper alloys
Excellent wear resistance properties and high-pressure properties	protects hydraulic groups and subgroups from wear and abrasion, extending the life of the hydraulic system
Quick air release properties	optimum efficiency of circulation and suitability for systems with small scoops of dirt
Good compatibility with sealing materials and communications	works equally well with elastomers which are used for petroleum oils

signed to meet requirements of environmentally friendly hydraulic fluids. The hydraulic fluid used in the hydraulic system Variopress 518 (FAUN Umwelttechnik GmbH & Co KG, Osterholz, Germany) is based on synthetic esters that are easily degradable. A high-performance complex of carefully selected ingredients enables this type of oil an excellent wear resistance, excellent high-pressure properties, thermal stability and also protection from corrosive agents.

Of course, a high oxidation resistance helps to protect the oil from increasing density and from the formation of sediments under high temperatures. Due to the high viscosity index of the base oil and low pour point, this type of oil can be used in a very broad range of operating temperatures. Unlike oils based on vegetable oils (HETG), environmentally friendly hydraulic oils based on synthetic esters (HESS), as this class of hydraulic oils is, can increase the overall performance of the hydraulic system Variopress 518 also during operation at higher temperatures, and they can offer improved thermal and oxidative stability. Table 1 presents the basic characteristics of the selected experimental oil.

Hydraulic system Variopress 518. Municipal vehicles have been selected for the experimental measurement of hydraulic system power parameters. In our case, we chose the hydraulic system Variopress 518 constructed on the platform of a Mercedes Benz chassis. Power parameters were established on the basis of the applied experimental methods, with monitoring the following variables: hydraulic fluid pressure, hydraulic pump revolutions, hydraulic fluid temperature, hydraulic arm lifting time and especially hydraulic pump power and the flow of hydraulic fluid. Fig. 1 shows the hydraulic system Variopress 518, which consists of two main hydraulic circuits. The front section of the circuit controls the peak discharge in the process of emptying of municipal solid waste, and the back section, which is the subject of the experimental measurement, is divided into two hydraulic circuits, of which one controls the container´s lifting hydraulics, and

Table 2. Measurement of hydraulic system tightness after 600 operating hours

Experiment No.	HGP state	Temperature (°C)	Ejection of piston rod (mm)		
			at the beginning	after 10 min	difference
1	ON	48.4	245	257.5	12.5
	OFF	48.6	245	258.3	13.3
2	ON	48.9	245	257.9	12.9
	OFF	49.5	245	258.7	13.7
3	ON	49.7	245	258.8	13.8
	OFF	49.8	245	259.8	14.8
4	ON	49.9	245	260.3	15.3
	OFF	50.0	245	261.2	16.2

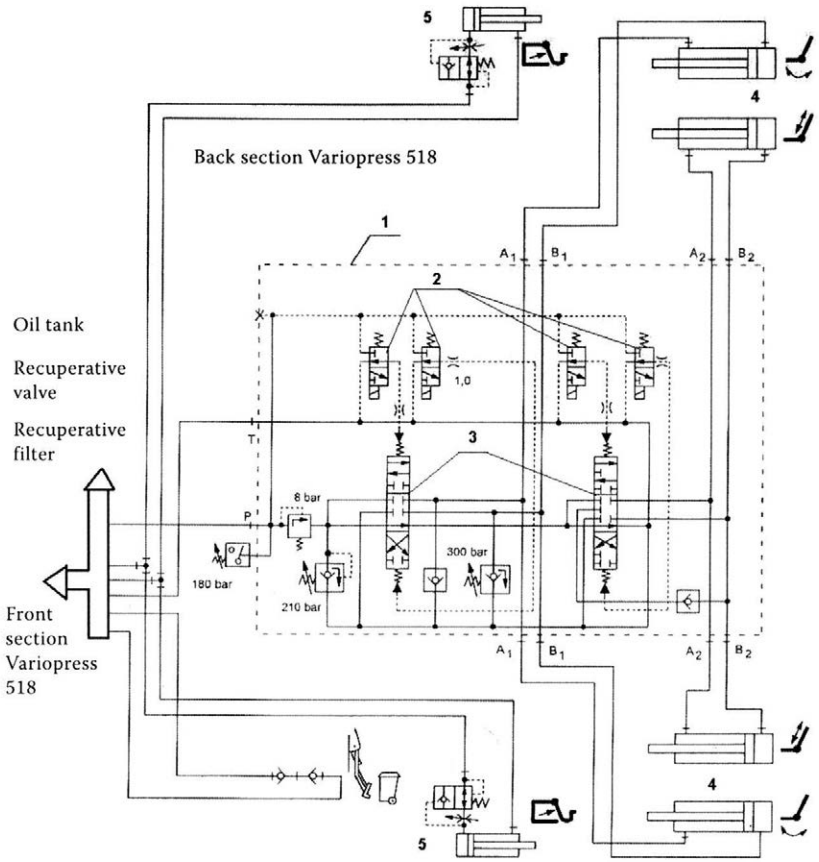

Fig. 1. Partial hydraulic system Variopress 518
1 – hydraulic distributors of pressing system; 2 – control hydraulic distributors; 3 – power hydraulic distributors; 4 – linear motor of hydraulic pressing plates; 5 – lifting mechanism containers; A1, A2, B1, B2 – inlet/outlet of linear power motors; P – main oil supply, T – return pipe in the tank

the second circuit provides partial processing of municipal solid waste by pressing and sliding board.

In the hydraulic system of the municipal vehicle, a hydraulic gear pump was used. We needed to know what the theoretic flow Q_{gt} of this system is. The theoretic flow supplied with the hydraulic pump which has two wheels is given by the size and count of gear gaps and revolutions:

$$Q_{gt} = V_{01} \times n \quad (1)$$

where:
Q_{gt} – theoretic flow (m³/s)
V_{01} – geometric capacity (m³)
n – revolutions (s⁻¹)

The geometric capacity can be calculated only approximately. For gearing without correction with an angle of meshing 20°, it is given by the following relation:

$$V_{01} = 2\pi \times D_t \times m \times b \quad (2)$$

where:
V_{01} – geometric capacity (m³)
D_t – thread effective diameter (m)
m – module (m)
b – wheπel width (m)

Due to the effect of flow efficiency, the real flow is lower and is given by the following relation:

$$Q_v = V_{01} \times n \times \eta_{vg} \quad (3)$$

where:
Q_v – real volume flow (m³/s)
V_{01} – geometric capacity (m³)

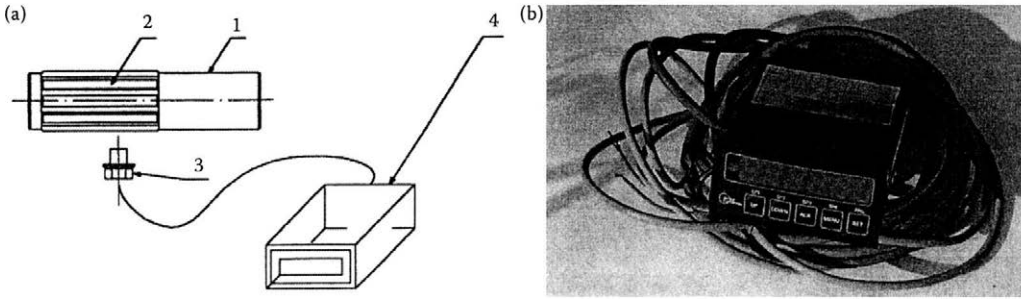

Fig. 2. Measured principle of hydraulic pump revolutions (a) and real view on display of Orbit Controls DC 7111 (b)
1 – mortise shaft; 2 – teeth; 3 – inductive sensor of revolutions; 4 – display Orbit Controls DC 7111

n – revolutions (1/s)
η_{vg} – flow rate recovery (–)

Gear pumps are made for flows from 1 dm^3/min to 400 dm^3/min. Working pressures normally and permanently reach the value of 12, at the top of 14–16 MPa. The flow rate recovery for the hydraulic gear pump is given by the following relationship:

$$\eta_G = \eta_{vg} \times \eta_{mg} \quad (4)$$

where:
η_G – total rate recovery (–)
η_{vg} – flow rate recovery (–)
η_{mg} – mechanic-hydraulic recovery (–)

For the flow of researched fluid, we need to know the flow of the hydraulic pump, which can be seen in Fig. 2:

$$Q_G = V_G \times n_G \times \eta_{vg} \quad (5)$$

where:
Q_G – flow rate of hydraulic pump (m^3/s)
V_G – capacity of hydraulic pump (m^3)
n_G – revolutions (1/s)
η_{vg} – flow rate efficiency of hydraulic pump (–)

There is a hydraulic motor that can be seen in Fig. 2, the role of which is the transmission of energy in the hydraulic system. So there is a need to know relations given for the flow of the hydraulic motor. Therefore, the flow of the hydraulic motor is given by the relation:

$$Q_M = V_M \times n_M \times \frac{1}{\eta_{vM}} \quad (6)$$

where:
Q_M – flow rate of direct motor (m^3/s)
V_M – capacity of direct motor (m^3)
n_M – revolutions (s^{-1})
η_{vM} – flow rate efficiency of motor (–)

Measuring methods. Under experimental methodology for obtaining objective information on the condition of the municipal vehicle with Variopress 518 in practice, we have designed and completed the required technical equipment which is necessary for assessing the power measurement of the hydraulic system.

Monitoring of hydraulic gear pump revolutions. For the measurement of hydraulic pump revolutions, we used a non-contact sensor (type of induction; SUA, own production, Nitra, Slovak Republic) based on the principle of magnetic induction change (Fig. 2). On the circumference of the hydraulic pump's shaft, two magnets are attached. The sensor was attached above the rotating magnets. The sensor responds to the movement of magnets and after hydraulic pump's rotation from the magnetic field influence, the sensor brought an output induced electrical signal to the electronic circuitry reader of a device Orbit Controls DC 7111 (Orbit Controls, Prague, Czech Republic), where the signal was further amplified and shaped

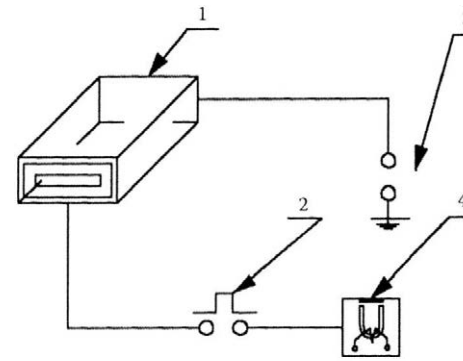

Fig. 3. Recording device of working time
1 – display; 2 – switch; 3 – power supply; 4 – electromagnet of hydraulic pump's shaft

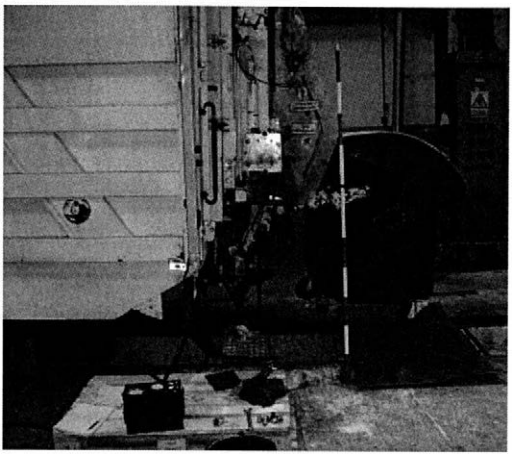

Fig. 4. Measurement of arms decrease

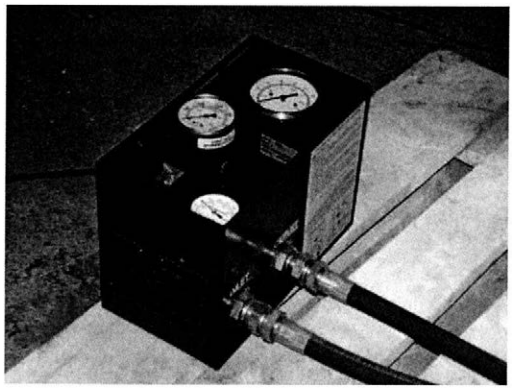

Fig. 5. Measurement of oil temperature and pressure in the system, (in-line hydraulic tester HT50A model C; SPX Corporation, Owantona, USA)

to the desired level of TTL (Compatible signal Transistor-Transistor Logic must have a minimum pulse width, an output voltage and current specification for any given hardware).

Measurement of hydraulic system operating time. The actually working time of the municipal vehicle hydraulic system was determined by a device that we was designed and produced at the Department of Transport and Handling (SUA in Nitra, Slovak Republic). The device is used for monitoring the operating time of the municipal vehicle hydraulic system with the hydraulic extension Variopress 518, continuously without any operator's intervention during one year.

Measurement of hydraulic system tightness. To assess the functionality and wear of the hydraulic system in view of the hydraulic fluid 46 ESSO Mobil EAL, a method of tightness monitoring used with load (540 kg) was applied. The load acted as resistance to the hydraulic system during working operations (Figs 4 and 5).

The aim of this method was to monitor the tightness elements (pressure valves, distributors) of the system in the given time after applying the experimental oil into the hydraulic system. Measurements were performed with the mentioned strain, though the exact position of the arms was exactly stabilized in a horizontal position, and after 10 min, a decrease of arms from their horizontal position and the length of the extended piston rod were recorded. The tightness assessment of the hydraulic system had a significant impact on the overall assessment and recommendation of the type of bio-oil for its use in the municipal vehicle hydraulic system.

RESULTS AND DISCUSSION

Evaluation of hydraulic system power parameters

The said performance indicators were assessed after 200, 400 and 600 operating hours of the municipal vehicle hydraulic system. Firstly, a default measurement of the hydraulic system was performed, and then the hydraulic system was examined periodically after 200 h of operation (Fig. 6).

According to the methodology of measurement, based on the measured values of power P in relation to flow Q, and after completing 200, 400 and 600 operating hours in the hydraulic system, we can note that the hydraulic fluid used in the hydraulic system has no influence on the reduction, modification or loss of hydraulic system performance. In the hydraulic system, there was no wear during the experimental measurements of the hydraulic pump, switchgear, and valves due to hydraulic fluid flowing in the system, which then would be reflected in a significant decline in the power of the system.

Tightness evaluation of the hydraulic system Variopress 518

The assessment of hydraulic system tightness was performed at each test measurement. Table 2 shows the measured values of arm's fall, or back section's ejected piston rod of the hydraulic system after 600 h of operation.

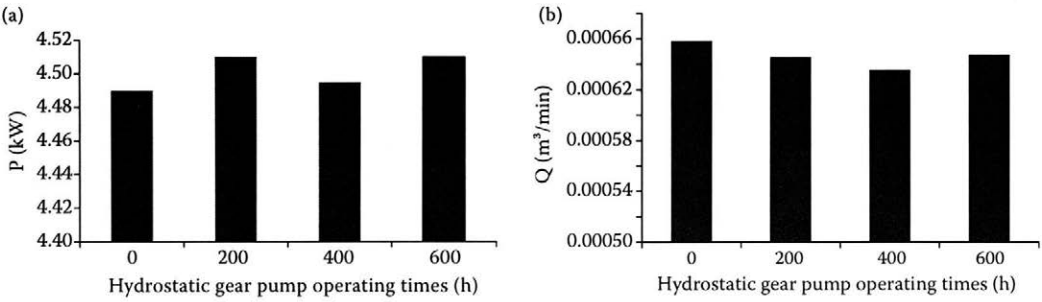

Fig. 6. Graphic view of measured (a) power data and (b) flow data
P – power of hydraulic gear pump; Q – flow of hydraulic gear pump at tested pressure

According to the methodology, it can be concluded that the resulting leakage did not show a significant effect of experimental hydraulic fluid on tightness elements of the system.

Standard analysis of hydraulic oil properties

The hydraulic oil was subjected to physical and chemical analysis such as kinematic viscosity, acid number of oil, the percentage content of water and polluting elements, Fe content and other. After initial measurement and subsequently after 200, 400 and 600 operating hours, the monitored parameters of bio-oil in the hydraulic system Vario-ress 518 were analysed. Final results were recorded in Table 3.

On the basis of experimentally observed properties of the hydraulic fluid ESSO Mobil EAL 46, it can be concluded that the hydraulic oil does not affect the hydraulic system components significantly with its properties. On the basis of findings, in terms of the pollutant content of elements in the hydraulic fluid, its application in a new hydraulic system may be advisable. The hydraulic fluid contains additives that improve the functional properties of the hydraulic system (antifoam ingredients, additives to improve corrosion properties), phosphoric acid contained in hydraulic fluid, but on the other hand, these agents are not suitable for certain types of sealants. Finally, it can be concluded that impurities contained elements moving within the prescribed tolerance limits.

CONCLUSION

This paper presents the results of monitoring the impact of the bio-oil Mobil EAL 46 ESSO on performance parameters of the municipal vehicle hydraulic system. The results are useful for transport companies involved in waste collection and farms operating similar hydraulic system.

The experimental organic liquid Mobil EAL 46 ESSO used in the hydraulic system of municipal vehicles based on esters and together with other additives is preferred to petroleum products that are biologically decomposed in the environment. The objective of the experiment was to investigate the possibility of biodegradable oil application and its adaptation to the hydraulic system of municipal vehicles. After an overall assessment of the results, it can be concluded that the experimental hydraulic fluid ESSO Mobil EAL 46 is suitable for use in hydraulic systems of municipal vehicles. Based on the findings, it can be stated that the hydraulic fluid maintains its properties without adversely affecting the performance parameters of the hydraulic system.

Table 3. Chosen parameters of the hydraulic bio-oil Mobil EAL 46 ESSO

Operating time (h)	Kinematic viscosity (mm^2/s)	Acid number (mg/g)	Mechanical impurities (% wt.)	Flashpoint (°C)	Water content (% wt.)	Iron content AAS (mg/kg)
0	39.61	0.69	0.012	300	< 0.025	7.25
200	42.12	0.63	0.012	300	0.025	7.25
400	45.32	0.62	0.014	240	0.035	7.45
600	53.31	0.67	0.015	220	0.050	8.00

References

JABLONICKÝ J., TKÁČ Z., MAJDAN R., MÜLLEROVÁ D., HUJO Ľ., VOZÁROVÁ V., 2012. Hodnotenie vlastností biopalív a biomazív. [Evaluation of Biofuels and Biolubricants.] Nitra, SUA in Nitra: 143.

JANOŠKO I., SEMETKO J., PETROVIČ A., 2004. The degradable bio oils in municipal engineering. Czasopismo Techniczne 6-M/2004,*45*: 297–302.

JANOŠKO I., ŠIMOR R., ČÉRI M., 2008. Advisement of the effect of bio-oil on the parameters of municipal vehicle hydraulic system. In: Advances in Automotive Engineering. VUT Brno, Czech Republic, Vol. 2: 130–135.

JANOŠKO I., ŠIMOR R., CHRASTINA J., 2010. The bio-oil used in the hydraulic system of the vehicle for waste collection. Acta Techologica Agriculturae, *13*: 103–108.

JANOŠKO I., MOJŽIŠ M., CHRASTINA J., POLONEC T., 2012. Testovanie výkonových parametrov hydraulickej sústavy komunalného vozidla s bioolejom. [Testing the performance parameters of the hydraulic system of municipal vehicle with bio-oil.] In: XXXVIII. Mezinárodní konference kateder dopravních, manipulačních, stavebních a země dělských strojů. Plzeň, Czech Republic: 41–46.

KOSIBA J., TKÁČ Z., MAJDAN R., HUJO Ľ., 2012. The test of tractor hydrostatic pump by application of synthetic oil in the hydraulic circuit of tractor. In: SED 2012 – Science and higher education in function of sustainable development. Uzice, High Business-Technical School of Uzice: 1–7.

TKÁČ Z., KROČKO V., MAJDAN R., MIKUŠ R., 2008. The laboratory testing device dedicated to evaluation of technical durability of hydrostatic pumps. In: Visnik Lvivskogo nacionalnogo agrarnogo universitetu: agroinžinerni doslidženja No. 12. 2. Lvov, Lvivskij nacionaľnij agrarnij universitet: 747–753.

Received for publication April 15, 2013
Accepted after corrections October 14, 2013

Corresponding author:

Doc. Ing. IVAN JANOŠKO, CSc., Slovak University of Agriculture in Nitra, Technical Faculty, Department of Transport and Handling, Tr. A. Hlinku 2, 949 76 Nitra, Slovak Republic
phone: + 421 37 641 4114, e-mail: ivan.janosko@uniag.sk

Determining the management zones with hierarchic and non-hierarchic clustering methods

J. Galambošová[1], V. Rataj[1], R. Prokeinová[2], J. Prešinská[1]

[1]*Department of Machines and Production Systems, Faculty of Engineering, Slovak University of Agriculture in Nitra, Nitra, Slovak Republic*
[2]*Department of Statistics and Operation Research, Faculty of Economics and Management, Slovak University of Agriculture in Nitra, Nitra, Slovak Republic*

Abstract

Galambošová J., Rataj V., Prokeinová R., Prešinská J., 2014. **Determining the management zones with hierarchic and non-hierarchic clustering methods**. Res. Agr. Eng., *60* (Special Issue): S44–S51.

Delineation of the management zones of a field is commonly used in precision agriculture technology. There are many techniques used to identify management zones. The most used technique is *k*-means clustering, where the number of clusters is managed by the user. The paper deals with clustering the yield data and electromagnetic data of a 17 ha field using the Ward's method followed by the *k*-means clustering method. The cubic clustering criterion was used to determine the number of clusters. Based on results, it can be concluded that it is beneficial to combine the *k*-means clustering method with the hierarchic method (Ward's method).

Keywords: Ward's method; k-means clustering; CCC; yield data; EMI

Precision farming technology is based on a site-specific approach to field treatments. Before implementation of this technology, the variability of the field has to be assessed in the first step. Operations can be conducted variably, or the site-specific approach can be used. For the latter one, management zones should be determined, and the field operation can be conducted based on them. Mostly, fertiliser application or soil tillage operation is carried out. However, other application such as e.g. variable irrigation (Chiericati et al. 2007) is possible.

Based on Khosla et al. (2010), there are numerous techniques for delineating management zones. Some of them are based on single soil or crop property or a combination of several that are known to affect crop productivity and yield. As Ortega and Santibanez (2007) reviewed, there are several approximations for the development of site-specific management zones. The authors reported that the first approach is based on soil and/or relief information, including topographic maps, direct soil sampling, non-invasive soil sampling by electrical conductivity equipment, and soil organic matter or organic estimated by remote sensing. The second approach is based on yield maps, combining data from several seasons, while the third is the integration of the two previous approaches and considers soil and/or relief information plus the use of yield maps. Zhang et al. (2009) developed a ZoneMAP web application, which designs the management zones based on satellite imagery, which the authors suggested as a preliminary basis when a yield map is not available. Delin and Berglund (2005) suggested to create management zones based on risk levels for drought and waterlogging, to be used in site-specific N application (based on information on soil electrical conductivity and elevation). Fleming and Westfall (2000) concluded that

Supported by the European Union within the frame of the Project No. ITMS 26220220014.

farmer-developed management zones appear to be effective in identifying different management zones; however, ground verification is needed to develop accurate Variable rate technology (VRT) maps from the zones. The need for confirmation of specific soil characteristics was reported also by KING et al. (2005) when they evaluated the analysis of yield map sequences and electromagnetic induction (EMI) soil sensing as potentially cost-effective methods for identifying and mapping "management zones" (MZ) within fields. RATAJ and GALAMBOŠOVÁ (2006) proposed to use the cluster analyses for identifying high- and low-profitability zones.

GUASTAFERRO (2010) compared the techniques for identification of MZs: (1) the ISODATA method, (2) the fuzzy *c*-means algorithm and (3) a non-parametric density algorithm. They concluded that all the methods have advantages and disadvantages. However, they suggest to manage the variation within one year, and to combine the use of MZs with crop-based in-season remote sensing when using them in that particular conditions. The hierarchic as well as non-hierarchic clustering procedures can be used for management zones determination (RUS, KRUSE 2011; TIWARI, MISRA 2011). The most common is the use of a cluster procedure using the k-means or fuzzy *k*-mean method (MINASNY, MCBRATNEY 2002; ORTEGA, SANTIBÁÑES 2007).

However, the estimation of a number of clusters is needed in advance. Statistical determination of the number of clusters or practical field-management considerations can be used as proposed by TAYLOR et al. (2003). LI et al. (2008) used fuzzy performance index (FPI) and normalized classification entropy (NCE) to determine the optimal cluster numbers. FRIDGEN (2000) reported that the measures of cluster performance indicated no advantage of dividing fields into more than four or five management zones. Moreover, year-to-year differences in an appropriate number of management zones were attributed to weather and crop type.

Based on the literature review, the most used technique in precision agriculture is *k*-means clustering (non-hierarchical method), which requires the estimation of the number of clusters based on previous knowledge of the farmer (expert knowledge) or management considerations are included.

The aim of this paper is to point out to the possibility of the hierarchic method as complementary to the non-hierarchic clustering method in order to (a) estimate a statistically significant number of management zones of a given field which can be used as an input for the non-hierarchical method and (b) to interpret the results of clustering process with the support of statistics.

MATERIAL AND METHODS

At the first stage, the cubic clustering criterion (CCC) will be used to estimate the statistically significant number of clusters. The CCC criterion can be used to estimate the number of clusters using Ward's method and the k-means method (SAS Institute Inc. 1983). The values of CCC greater than 2 or 3 indicate good clusters; values between 0 and 2 indicate potential clusters, but they should be considered with caution. Very negative values of the CCC, such as –30, may be due to outliers (SAS Institute Inc. 1983). The clustering analyses will be conducted using two procedures. In the first step, the Ward's method (hierarchic method) will be used followed by the non-hierarchic method (*k*-means clustering).

Ward's method. This method involves an agglomerative clustering algorithm. It starts out with *n* clusters of size 1 and continues until all the observations are included into one cluster. This method attempts to minimize the Sum of Squares (SS) of any two (hypothetical) clusters that can be formed at each step. The ESS is considered as a measure of homogeneity of the cluster. This method is regarded as very efficient; however, it tends to create clusters of small size. At the first step, when each object represents its own cluster, the distances between those objects are defined by the chosen distance measure (The Pennsylvania State University 2004).

Error Sum of Squares:

$$\mathrm{ESS} = \sum_i \sum_j \sum_k |X_{ijk} - \bar{x}^2_{i.k}| \quad (1)$$

where:

X_{ijk} – value for variable k in observation j belonging to cluster i

R-Square – proportion of variation explained by a particular clustering of the observations

$$r^2 = \frac{\mathrm{TSS} - \mathrm{ESS}}{\mathrm{TSS}} \quad (2)$$

where: TSS is Total Sum of Squares

$$\mathrm{TSS} = \sum_i \sum_j \sum_k |X_{ijk} - \bar{x}^2_{..k}| \quad (3)$$

As a result, a dendrogram is plotted. Here, each stage of clustering processed is displayed and the R-Square is plotted at *y* axis.

Table 1. Basic statistics of the input data

Parameter/unit	No. of samples	Average	Minimum	Maximum	Standard deviation
EMI (mS/m)	31	49.51	39.42	56.64	4.74
Yield in 2009 /(t/ha)	31	6.93	2.52	9.8	0.82
Yield in 2010 (t/ha)	31	1.99	0.11	3.08	0.37
Yield in 2011 (t/ha)	31	7.73	5.67	10.46	0.78

EMI – electromagnetic induction

***k*-Means method**. Based on McQueen (1967), the procedure follows a simple and easy way to classify a given data set through a certain number of clusters (assume k clusters) fixed a priori. The main idea is to define k centroids, one for each cluster. These centroids should be placed in a cunning way because different location causes different result. So, the better choice is to place them as much far away from each other as possible. The next step is to take each point belonging to a given data set and associate it to the nearest centroid. When no point is pending, the first step is completed and an early groupage is done. At this point we need to re-calculate k new centroids as barycentres of the clusters resulting from the previous step. After we have these k new centroids, a new binding has to be done between the same data set points and the nearest new centroid. A loop has been generated. As a result of this loop we may notice that the k centroids change their location step by step until no more changes are done. In other words centroids do not move any more. Finally, this algorithm aims at minimizing an objective function, in this case a squared error function. The objective function is

$$J = \sum_{j=1}^{k} \sum_{i=1}^{n} ||x_i^{(j)} - c_j||^2 \quad (4)$$

where: $||x_i^{(j)} - c_j||^2$ – chosen distance measure between a data point $x_i^{(j)}$ and the cluster centre c_j is an indicator of the distance of the n data points from their respective cluster centres (A Tutorial on Clustering Algorithms).

For clustering procedure, Ward's method conducted in SAS (version 4.3, SAS Institute Inc., Cary, USA) as well as the k-means clustering method conducted in Statistica (Statistica CZ 10; StatSoft, Tulsa, USA) was used.

Data used. The above-described methods were applied to data obtained from yield monitoring during three seasons (2009 – spring barley; 2010 – oilseed rape; 2011 – winter wheat) at a 17 ha experimental field. The information on field variability was extended by data on electromagnetic induction (EMI) measured by Geonics EM38 (Geonics Limited, Mississauga, Ontario, Canada). In order to estimate the management zones within the given field, 31 monitoring points were designed across the field and data from all datasets were allocated

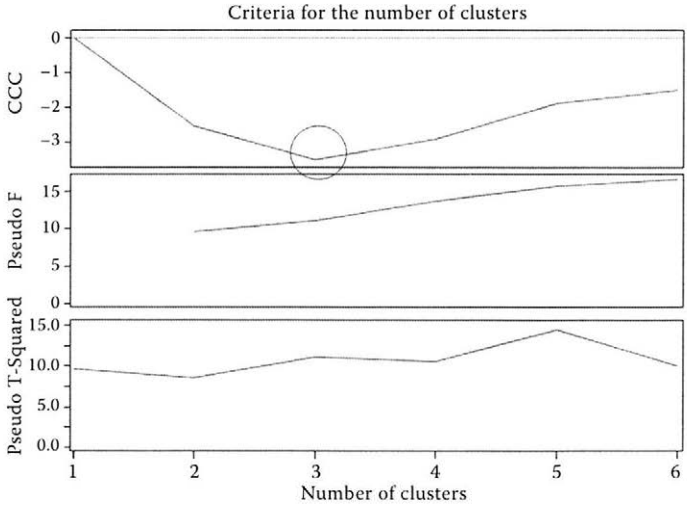

Fig. 1. Estimation of the number of clusters
CCC – cubic clustering criterion; pseudo T-Squared; pseudo F – output statistics

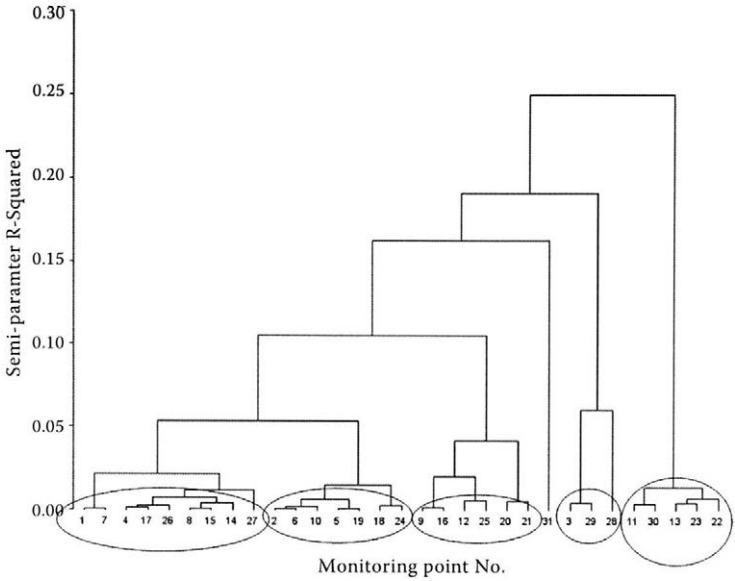

Fig. 2. Output of Ward's method – dendrogram

to these points. This means the values of yield and EMI for these 31 monitoring places were an input dataset for the analyses.

In order to be able to process the yield data from different seasons and of different crops, the preprocessing of these data was conducted and standardized normal values were calculated based on the following formula:

$$SNV = \frac{(x - \bar{x})}{SD} \times 100\ \% \quad (5)$$

where:

SNV – standardized normal values

x – actual value of parameter

$\bar{x}$ – arithmetic mean

SD – standard deviation

The results of cluster analyses have to be interpreted from the spatial aspect. Only the members of a cluster (in our case the monitoring point) lying in a near distance and creating one area can be used for creating management zones. Therefore, the data were displayed with support of the geographical information system (GIS) ArcGIS 10.1. (ESRI, Redlands, USA) and the results were interpreted.

RESULTS AND DISCUSSION

The experimental field is represented by 31 monitoring points, which were designed across the field. All the data from yield maps and EMI maps were subtracted for these points. The data were preprocessed, and the SNV value (standardized normal value) was calculated (Table 1). First of all, the CCC was calculated, and the appropriate number of clusters was selected. The results are given in Fig. 1. According to CCC criterion, the number of statistically significant clusters was estimated for 3. As it was proposed in the methodology, the hierarchical method (Ward's method) was applied at first

Table 2. Results of cluster analyses – cluster members and Euclidean distances

Cluster 1	Member	11	12	13	22	23	30				
	Euclidean distance	49.20	40.94	27.03	50.95	36.12	44.62				
Cluster 2	Member	2	4	5	6	8	9	10	14	15	16
	Euclidean distance	47.13	27.43	39.20	36.63	8.11	63.16	31.05	45.55	20.12	83.07
Cluster 2	Member	17	18	19	21	24	25	26	27	31	
	Euclidean distance	45.61	76.75	30.98	118.97	64.16	50.67	44.74	73.96	192.48	
Cluster 3	Member	1	3	7	28	29					
	Euclidean distance	40.67	53.49	50.13	106.14	56.35					

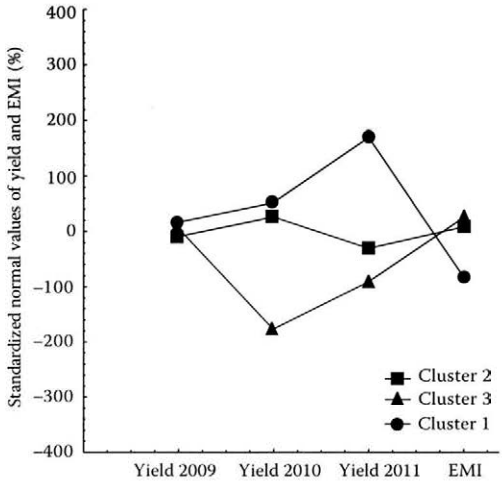

Fig. 3. The means of each cluster
EMI – electromagnetic induction

in order to explore the data. The principle of this method is to cluster the data based on homogeneity. Based on the dendrogram (Fig. 2), it is obvious that in the first stage of the clustering process, the monitoring point number 31 was not assigned to any cluster, which means that the yield performance during the years was not similar to any of the other places. Ward's method allowed identifying the most homogenous places (represented by monitoring points) and also outliers.

In the second step, the *k*-means clustering method was applied to the data. The principle of this method is to create clusters which are as heterogeneous as possible. As it is the non-hierarchical

Table 3. Standardized normal values (SNV) for yield and electromagnetic induction for the areas of cluster No. 3

Monitoring point	SNV (%)			EMI
	2009	2010	2011	
1	31.52	−102.75	−98.03	−0.36
3	−83.78	−161.36	−52.91	64.80
7	17.29	−84.33	−88.43	−14.03
28	167.78	−315.43	−83.63	34.60
29	−89.02	−211.60	−122.98	53.51

EMI – electromagnetic induction

method, the number of required clusters has to be set up at the beginning. As explained above, the number of clusters was selected based on CCC criterion. The results are shown in Fig. 3, where the means of each cluster are defined, and in Table 2, where the members of each cluster are defined. The data were plotted in GIS, and their spatial localisation was considered. Based on Fig. 4, it can be concluded that two clusters create compact areas of the field and one of them not. The clusters can be interpreted as follows:

(a) The cluster No. 1 comprises areas where yield was above the average of the field in all the three seasons. This area could be considered as a high-yielding zone of the field. The results were compared with the digital terrain model, and it was shown that this zone lays in terrain depreciation with better water availability, which is confirmed also by the EMI map (Fig. 5). The values of EMI displayed in light colour reached values from 23.1 to 51.12 mS/m, the dark colour goes for values from 51.12 to 79.11 mS/m.

Fig. 4. The spatial display of cluster and its comparison with digital terrain model

Silty loam soil is typical for the entire field; therefore the change of EMI values is expected to be due to the change of the moisture content.

Monitoring point 31 lays at the same area; however, due to waterlogging problems, the yield in 2009 and 2011 was extremely low and so this location was assigned to a different management zone.

(b) Average-yielding zone – cluster No. 2 – almost all the rest of the field.

(c) Low-yielding areas – cluster No. 3 – the performance of these monitoring points is given in Table 3. The cluster No. 3 comprises only 5 monitoring points, which are not located next to each other.

When further analysing the results and looking at the dendrogram (Fig. 2), the monitoring points of cluster 2 can be described as follows:

Monitoring points 1 and 7 are characterized by good performance in 2009, but low yield in 2010 and 2011 as well as similar values of conductivity. Monitoring points 3 and 29 are characterised by an extremely low yield in all the three years; the cause is soil compaction at the headlands of the field. The monitoring point number 28 was not clustered in the first stage of the analyses with any point and is characterised by an extremely high yield in 2009 and an extremely low yield in 2010 and 2011. The

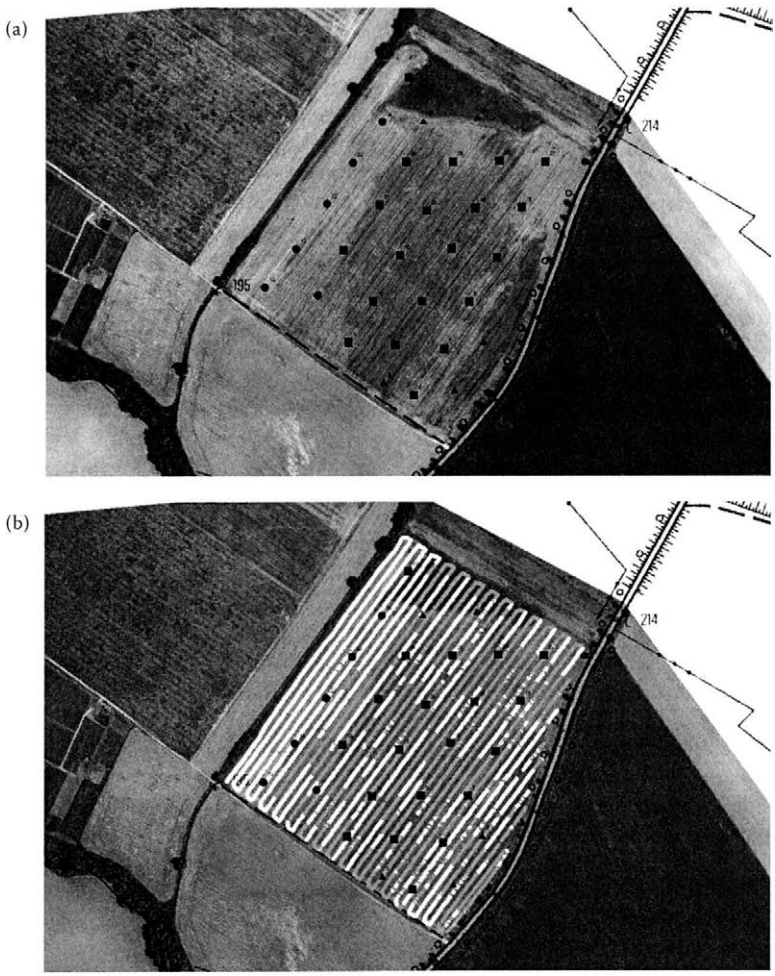

Fig. 5. Location of waterlogged area which caused the yield problems in (a) 2010 and 2011, and (b) electromagnetic induction data of the field

● cluster 1; ■cluster 2; ▲ cluster 3

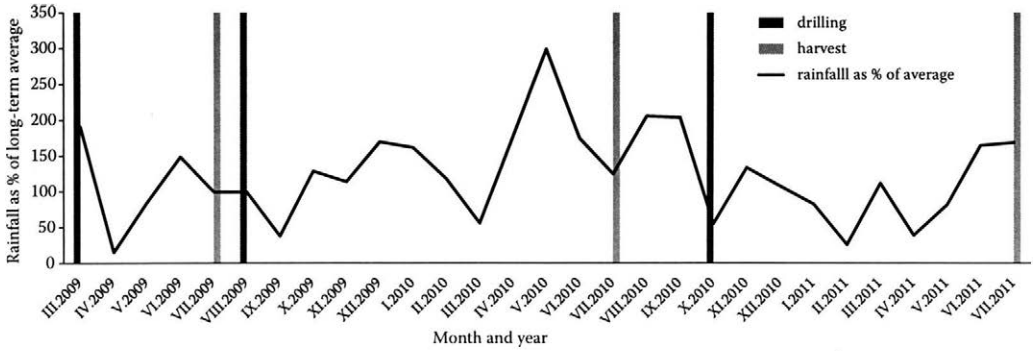

Fig. 6. Rainfall and timing of drilling and harvest operation

extremely low yields at these areas were caused by waterlogging problems in 2010 (Fig. 5) caused by extreme rainfall in 2010 (in May 2010 there was 300% rainfall compared to average), followed by problems with crop establishment in 2011 as the areas were waterlogged. The average rainfall as well as the dates of drilling and harvesting operations are given in Fig. 6.

Therefore, it can be concluded that the different performance of these areas (represented by the monitoring points) was caused by waterlogging and compaction. When an appropriate management operation would be conducted (drainage and sub-soiling), the areas would be included in the management zones No. 1 and No. 2.

Furthermore, monitoring point No. 31 was assigned to the cluster No. 2, which is characterised by an average-yielding performance along years. However, this is not characteristic for this monitoring point. The yield in 2009 and 2011 reached extremely low values at this area. Only in 2010 the yield reached values above the average. Looking at the results of analyses (Table 2), the Euclidean distance of this point within the cluster reaches the value of 192.48 so this point is the most distant point from the cluster centre. Therefore, it can be stated that there was a problem at this area. Again, waterlogging problems caused the differences, and this monitoring point should be included in management zone (cluster) 1 after an appropriate management operation is conducted at this area.

CONCLUSION

The results of these analyses showed that it is beneficial to use both the hierarchical and non-hierarchical clustering methods when determining the management zones from yield maps. The hierarchical method allows determining the statistically significant number of clusters as well as to help to interpret the data.

Also, Ward's method can be used as input information before conducting the k-means clustering method.

Further testing over a broader scope of fields and crop production systems is needed to confirm these results.

References

A tutorial on clustering algorithms. Available at http://home.dei.polimi.it/matteucc/Clustering/tutorial_html/kmeans.html

Chiericati M., Morari F., Sartori L., Ortiz B., Perry C., Vellidis G., 2007. Delineating management zones to apply site-specific irrigation in the Venice lagoon watershed. In: Stafford J.V. (ed.), Proceedings from 6th European Conference on Precision Agriculture 07 (6ECPA). Skiathos, Greece: 599–605.

Delin S., Berglund K., 2005. Management zones classified with respect to drought and waterlogging. Precision Agriculture, *6*: 321–340.

Flemming K.L., Westfall D.G., Wiens D.W., Brodahl M.C., 2000. Evaluating farmer defined management zone maps for variable rate fertilizer application. Precision Agriculture, *2*: 201–215.

Fridgen J.J., 2000. Delineation and analysis of site-specific management zones. In: Conference on Geospatial Information in Agriculture and Forestry, Lake Buena Vista, Florida, 10–12 January, 2000.

Guastaferro F., Castrignano A., De Benedetto D., Sollitto D., Troccoli A., Cafarelli B., 2010. A comparison of different algorithms for the delineation of management zones. Precision Agriculture, *11*: 600–620.

KHOSLA R., WESTFALL D.G., REICH R.M., MAHAL J.S., GANGLOFF W.J., 2010. Spatial variation and site-specific management zones. In: OLIVER M., 2010. Geostatistical Applications for Precision Agriculture. London, Springer.

KING J.A., DAMPLNEY P.M.R., LARK R.M., WHEELER H.C., BRADLEY R.I., MAYR T.R., 2005. Mapping potential crop management zones within fields: Use of yield-map series and patterns of soil physical properties identified by electromagnetic induction sensing. Precision Agriculture, *6*: 167–181.

MCQUEEN B.,1967. Some methods for classification and analysis of multivariate observations. In: Proceedings of 5th Berkeley Symposium on Mathematical Statistics and Probability. Berkeley, University of California Press, *1*: 281–297

MINASNY B., MCBRATNEY A.B., 2002. FuzME Version 3.0. Sydney, Australian Centre for Precision Agriculture. The University of Sydney.

LI Y., SHI Z., WU CH., LI H., LI F., 2008. Determination of potential management zones from soil electrical conductivity, yield and crop data. Journal of Zhejiang University Science B, 9: 68–76

ORTEGA R.A., SANTIBÁÑEZ O.A., 2007. Determination of management zones in corn (*Zea mays* L.) based on soil fertility. Computers and Electronics in Agriculture, *58*: 49–59.

RATAJ V., GALAMBOŠOVÁ J., 2006. Farm production planning based on 4-years site-specific information. In: Agricultural Engineering for a Better World: XVI CIGR World Congress, September 3–7, 2006. Bonn, Düsseldorf, VDI Verlag GmbH: 375–376.

RUSS G., KRUSE R., 2011. Exploratory hierarchical clustering for management zone delineation in precision agriculture. Advances in Data Mining. Applications and Theoretical Aspects Lecture Notes in Computer Science, *6870*: 161–173.

SAS Institute Inc., 1983. SAS Technical Report A-108, Cubic Clustering Criterion. SAS Institute, Carry.

TAYLOR J.C., WOOD G.A., EARL R., GODWIN R.J., 2003. Soil factors and their influence on within-field crop variability II: Spatial analysis and determination of management zones. Biosystems Engineering, *84*: 441–453.

The Pennsylvania State University, 2004. Ward's method. Available at http://sites.stat.psu.edu/~ajw13/stat505/fa06/19_cluster/09_cluster_wards.html

TIWARI M., MISRA B., 2011. Application of cluster analysis in agriculture – A review article. International Journal of Computer Applications, *36*: 43–47.

ZHANG X., Shi L., Jia X., Seielstad G., Helgason C., 2010. Zone mapping application for precision-farming: A decision support tool for variable rate application. Precision Agriculture, *11*: 103–114.

Received for publication April 15, 2013
Accepted after corrections July 29, 2014

Corresponding author:

Ing. JANA GALAMBOŠOVÁ, PhD., Slovak University of Agriculture in Nitra, Faculty of Engineering, Department of Machines and Production Systems, Tr. Andreja Hlinku 2, 949 76 Nitra, Slovak Republic
phone: +421 37 6414 344, e-mail: jana.galambosova@uniag.sk

Sorption isotherms of agricultural products

I. Vitázek, J. Havelka

Department of Transport and Handling, Faculty of Engineering, Slovak University of Agriculture in Nitra, Nitra, Slovak Republic

Abstract

Vitázek I, Havelka J., 2014. **Sorption isotherms of agricultural products**. Res. Agr. Eng., *60* (Special Issue): S52–S56.

The aim of the paper is to expand the theory of sorption and equilibrium moisture contents as well as to present the methodology of developing two types of sorption isotherms – I and II. The attention is also paid to the importance of the isotherms in the thermodynamics of drying and in the process of storage of agricultural products. Presented methodology of obtaining the isotherms is based on selected equations of the theory of adsorption and on the results of experimental measurements of equilibrium moisture content. Definition of the new isotherm II is introduced as dependence of equilibrium moisture content dry basis on time at constant temperature, constant relative moisture of the ambient air and stable biological properties (e.g. germination). The results show following graphic dependences: isothermal distort plane; sorption isotherm I of maize grains at various temperatures; moisture loss rate in dependence on time and sorption isotherm II. These theoretical dependences supported by experimental measurements broaden the scope of the theory of sorption and may be successfully applied in long-term storage of maize grains.

Keywords: equilibrium moisture; drying; thermodynamics; organic materials; drying curve

Agricultural products are characterised by high moisture content, which makes their long-term storage impossible. Therefore, post-harvest processing ends with a drying process with removal of free moisture and one part of bound moisture. Residual moisture content enables long-term storage without a decrease in quality. This value is of significant importance. Therefore, it is prescribed in technical standards that determine the max. volume and min. volume of moisture content. These values are in the range of equilibrium moisture content of a given material with the ambient atmosphere. Equilibrium moisture content is therefore an important parameter which is used in the thermodynamics of drying and also in the thermodynamics of storage.

For their research the authors studied excellent seminal works of drying theory, Czech from Valchař et al. (1967), Polish from Pabis (1982), Hungarian from Imre (1974) and German, in Slovak translation, from Maltry and Pötke (1966). Remarkable publications about equilibrium moisture in agricultural products include those from Henderson (1952) and Štencl (2000a,b).

As a result, equilibrium moisture content was measured and relevant relationships were studied in the research. The paper presents complex theory of sorption isotherms with the intention to introduce this theoretical contribution to the experts in thermodynamics and to pass this knowledge to the workers in drying, especially to those who deal with long-term storage of agricultural products.

MATERIAL AND METHODS

Complex theory. In the theory of thermodynamics of organic materials, only the prescribed standard parameter for moisture content – moisture content dry basis with the relation, were used:

$$u = M_w/M_{db} \quad (1)$$

where:
u – moisture content dry basis
M_w – moisture mass in the given material (kg)
M_{db} – mass of dry basis in the given material (kg)

The equilibrium moisture of the given material is moisture content dry basis relevant to the state of thermal equilibrium of the given material and ambient gas atmosphere.

Moisture in the material is free moisture on its surface and bound moisture inside this material, without moisture in chemical structures.

Adsorbed moisture is moisture on the surface of the material kept with molecular forces.

The curve of sorption isotherm is a graphic presentation of equilibrium moisture content in dependence on the relative moisture of ambient gas atmosphere φ at constant temperature T.

The equilibrium moisture of the given material is to be described with a universal relation (HAVELKA 1978):

$$u_e \cong F(T, \varphi, \tau, bio) \quad (2)$$

where:
u_e – equilibrium moisture dry basis
F – function
T – temperature of the material and ambient atmosphere (K)
φ – relative moisture of the ambient atmosphere
τ – time from the end of drying process (days)
bio – parameter of biologic quality of this material

Post-harvest processing is performed in the way that this bio-parameter remains constant with the highest value in the whole process and also during storage.

The relation of $F(T, \varphi, \tau, bio)$ cannot be provided in an analytical form. In research works, sorption isotherm values are obtained from laboratory measurements of samples. The relation F gives a graphic description of an isothermal distort plane with T = const., *bio* = const. The scheme of this is shown in the coordinates u, φ, τ in Fig. 1.

Sorption isotherms. For the analysis of Eq. (2), a total differential of the following equation was used:

$$du_e = (\delta F/\delta T)dT + (\delta F/\delta\varphi)d\varphi + (\delta F/\delta\tau)d\tau + (\delta F/\delta bio)dbio \quad (3)$$

In practice, only processes with *bio* = const are performed.

Two types of sorption isotherms were studied by the means of this relation of total differential and isothermal distort plane (Fig. 1).

Sorption isotherm I. This sorption isotherm is described with differential Eq. (4) and graphically presented as a section of isothermal distort plane with the level of given time τ scheme (Fig. 1).

The differential equation for this sorption isotherm is:

$$du_e = (\delta F/\delta\varphi)d\varphi;\ T = \text{const.},\ \varphi = \text{const.},\ bio = \text{const.} \quad (4)$$

The analytic relation is:

$$u_e = F_1(\varphi);\ T = \text{const.},\ \varphi = \text{const.},\ bio = \text{const.} \quad (5)$$

This isotherm is used in the thermodynamics of drying. The course of this u_e (Eq. (5)) is to be stated only with laboratory measurements on a material sample.

The relation from HENDERSON (1952) was used:

$$1 - \varphi = e^{-k \times T \times u^n} \quad (6)$$

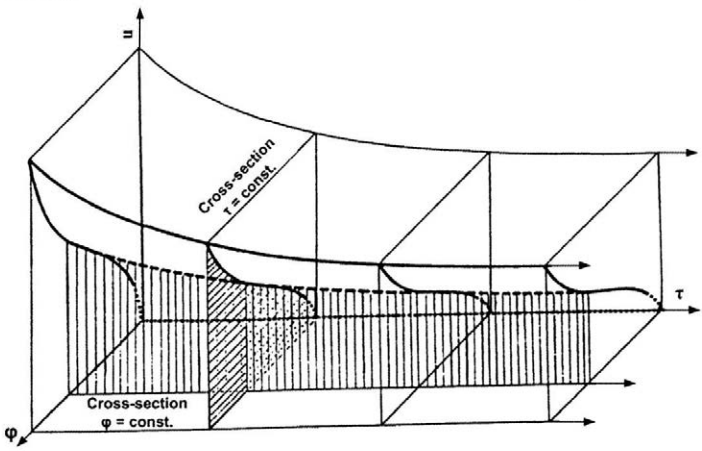

Fig. 1. Isothermal distort plane
τ – time; T – temperature; u – moisture content dry basis; φ – relative moisture of the ambient atmosphere

where:
e – base of natural logarithm
k, n – coefficients of the Henderson's relation
T – temperature of ambient air (K)
u – moisture content dry basis

For the derivation of sorption isotherm on another temperature, the following relation by means of the Henderson's equation was obtained:

$$u_e = u_{el} \times (T_1/T)^{1/n} \quad (7)$$

Sorption isotherm II

Sorption isotherm II is a curve produced with the section of isothermal distort plane with the plane of φ = const. (scheme in Fig. 1).

The differential equation of this sorption isotherm is:

$$du_e = (\delta F/\delta\tau)d\tau;\ T = \text{const.}, \varphi = \text{const.}, bio = \text{const.} \quad (8)$$

The analytic relation of this is:

$$u_e = F_2(\tau);\ T = \text{const.}, \varphi = \text{const.}, bio = \text{const.} \quad (9)$$

The actual course from the laboratory measurement of samples of the given material was gained.

The analytic relation of u_e (Eq. (9)) as a curve of natural fall of moisture loss rate N^x was developed:

$$N^x = du_e/d\tau = -a \times (u_e - u_{e\infty}) \quad (10)$$

where:
N^x – moisture loss rate
du_e – differential of equilibrium moisture dry basis
$d\tau$ – differential of time
a – time constant of the given material
u_e – equilibrium moisture dry basis
$u_{e\infty}$ – equilibrium moisture dry basis at infinite time

With its integration, the relation for u_e was gained:

$$u_e = u_{e\infty} + (u_{e0} - u_{e\infty}) \times \exp(-a \times \tau) \quad (11)$$

Where:
u_e – equilibrium moisture dry basis
$u_{e\infty}$ – equilibrium moisture dry basis at infinite time
u_{e0} – equilibrium moisture dry basis at the beginning
a – time constant of the given material
τ – time

Isotherm II demonstrates the long-term course of equilibrium moisture at storage or at cooling. It enables to calculate the mass of moisture produced in this process.

RESULTS AND DISCUSSION

Sorption isotherm I for maize

From laboratory measurements, the values of equilibrium moisture contents of maize grains at the temperature of 40°C were obtained. This isotherm is shown in Fig. 2. From these values, the values of constant k and n in the Henderson's equation with non-linear regression were calculated.

Henderson's equation:

$$\varphi = 1 - e^{-0.116393 \times T \times u^{2.092267}} \quad (12)$$

where:
φ – relative moisture of the ambient atmosphere
e – base of natural logarithm
T – temperature of ambient air
u – moisture content dry basis

With Eq. (7), the values for the temperatures of 10°C were calculated and presented in Fig. 2.

Sorption isotherm II for maize grains

The samples of maize from the previous section were used for the laboratory measurement of moisture losses in long-term storage. The value of u_e (equilibrium moisture dry basis) was obtained by exploratory calculations. From this the analytic relation for moisture loss rate was gained (Fig. 3):

$$N^x = -0.01546 \times e^{-(\tau/36.2)} \quad (13)$$

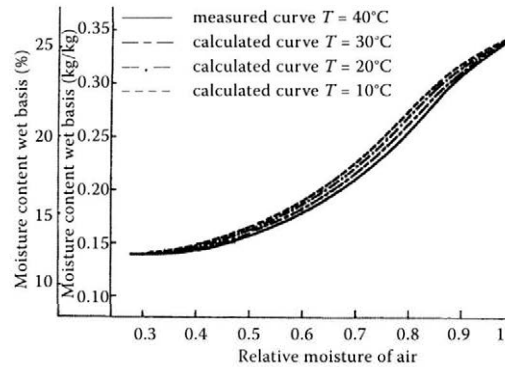

Fig. 2. Sorption isotherms of maize grains

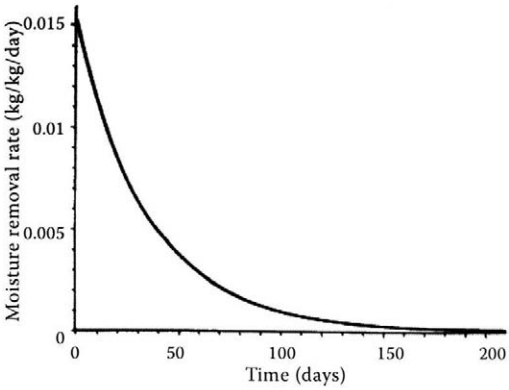

Fig. 3. Moisture loss rate of maize grains

where:

N^{τ} – moisture loss rate

e – base of natural logarithm

τ – time

The analytic relation of equilibrium moisture content:

$$u_e = 0.1 + 0.56 \times e^{-(\tau/36.2)} \quad (14)$$

Graphic demonstration is presented in Fig. 4. The value of $u_{e\infty}$ is only an analytic calculating value.

In the course of long-term storage of agricultural products, one part of moisture content is released due to the biological activity of this material. This moisture must be removed to prevent deterioration of this material. This moisture is removed with cold airing. The flow of unsaturated air removes this moisture in continual or cyclic manner.

Similar situation is at cooling of agricultural products. With the knowledge of sorption isotherm I and sorption isotherm II, a considerably higher amount of moisture is to be removed than in the case of cold airing. The knowledge of these two sorption isotherms allows to calculate with the thermodynamics of wet air the course of this process and to propose an optimal technical solution of the storage equipment (Vitázek 2011).

The theory of sorption isotherm I is very objectively presented in the work of Nikitina (1963). Any similar method was not found in any relevant source. This method may be considered as an important improvement in the theory of sorption of humidity in the long-term processes in agriculture.

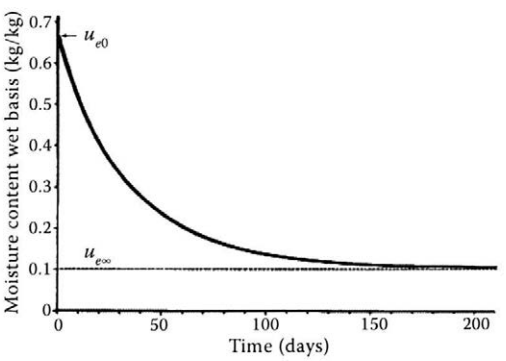

Fig. 4. Sorption isotherm II of maize grains

u_{e0} – equilibrium moisture dry basis at the beginning; $u_{e\infty}$ – equilibrium moisture dry basis at infinite time

CONCLUSION

The drying of harvested grain and other agricultural products is carried out on the principle of drying curve and isotherm I. A long-term conservation of such materials is theoretically solved by means of isotherm II for the whole period of conservation.

Isotherm II enables to determine and analyse the conditions of the conservation process. Moreover, it deals with the disposal of spontaneous release of moisture by ambient air.

Process managers in dryers and storages of agricultural products use the knowledge of complex isothermal sorption in their practice. These basic principles considerably improve the process of drying and storage.

Conducted experiments and derived theory indicate a significant importance of further research into the thermodynamics of long-term conservation of all agricultural crops stored in great amounts.

References

Havelka J., 1978. Termodynamika dlhodobej konzervácie poľnohospodárskych produktov. [Thermodynamics of long-time conservation of agricultural products.] Acta Technologica Agriculturae: 189–197.

Henderson S.M., 1952. A Basic Concept of Equilibrium Moisture. In: Agricultural Engineering for January 1952: 29–32.

Imre I., 1974. Száritási közikönyv. [Manual of Drying.] Budapest, Müszaki Könyvkiado: 1122.

Maltry W., Pötke E., 1966. Technika poľnohospodárskeho sušiarenstva. [Technics of Drying in Agriculture.] Bratislava, SVPL: 490.

Nikitina L.M., 1963. Tablicy ravnovesnogo udelnogo vlagosoderžanija I energii svjazi vlagi s materialama. [Ta-

bles of Equilibrium Moisture Contents and Binding Energy of Moisture with Material.] Moscow, Gosenergoizdat: 174.

Pabis S., 1982. Teoria kon wekcionogo suszenia produktov rolniczych. [Theory of Heat Conduction Drying of Agricultural Products.] Warszawa, PWRiL: 229.

Štencl J., 2000a. Equilibrium moisture content of *Festuca pratensis* in near ambient air drying conditions. Acta Technologica Agriculturae, 3: 21–26.

Štencl J., 2000b. Equilibrium moisture content as a control parameter for a meadow grass drying process in a barn. Acta Technologica Agriculturae, 3: 27–31.

Valchař J. et al., 1967. Základy sušení. [Basic Concepts of Drying.] Prague, ČVUT/SNTL: 396.

Vitázek I., 2011. Technika sušenia v teórii a v praxi – Obilniny. [Drying Technics in Theory and Practice – Cereals.] Nitra, SUA in Nitra: 102.

Received for publication April 15, 2013
Accepted after corrections October 14, 2013

Corresponding author:

Doc. Ing. Ivan Vitázek, CSc., Slovak University of Agriculture in Nitra, Faculty of Engineering, Department of Transport and Handling, Trieda A. Hlinku 2, 949 76 Nitra, Slovak Republic
phone: +421 37 6414 756, e-mail: ivan.vitazek@uniag.sk

Monitoring of conditions of agricultural machines' parts in operation

P. Polák, R. Mikuš, V. Kročko

Department of Quality and Engineering Technologies, Faculty of Engineering, Slovak University of Agriculture in Nitra, Nitra, Slovak Republic

Abstract

Polák P., Mikuš R., Kročko V., 2014. **Monitoring of conditions of agricultural machines' parts in operation.** Res. Agr. Eng., *60* (Special Issue): S57–S65.

This contribution focuses on problems of monitoring the runout of tractor diesel motor parts used in agricultural operation. Crankshafts from the agricultural tractors of type Zetor 6911 are used as samples for measuring the runout and circularity. The first sample of the crankshaft is loaded in the tractor used in livestock production, and the second one is used in vegetable production. Measured values of the runout and circularity of both samples are evaluated by tables and polar diagrams. Results of the experiment show the amount of runout and the following wear of agricultural machine parts in different operating conditions of agricultural production.

Keywords: crankshaft; deviation, circularity; runout measurement; wear

The importance of usage of agricultural equipment is in elimination of any hard work (Líška 2008; Poničan, Korenko 2008). The wear of several parts and a decrement of machine operability occur during the usage of agricultural equipment in the manufacturing process (Páltik 2007). The lifetime of agricultural machines has to be dealt with when economic effectiveness is the topic. Depreciation charge, return on investment and operation expenditures ratio put into machinery and technico-economic evaluation of used and new machines and technologies along with their appropriate reproduction could not be done without knowing the lifetime. Agricultural machinery lifetime knowledge is essential for manufacturer production amount and selection of machines and spare parts (Kročko et al. 2007). Lifetime optimisation rules are valid generally, in the present economical environment too. The machinery should be replaced after an optimum operation time, in the moment of the lowest unit operation costs (Drlička, Mikuš 2007).

An example can be the crankshaft of the agricultural tractor. This contribution deals with problems of monitoring the runout of tractor diesel motors parts that are used in agricultural operation. Measurements of runout and circularity are accomplished on the crankshafts of the agricultural tractors of type Zetor 6911 (Zetor Brno, Czech Republic). Measured values of runout and circularity are evaluated by tables and polar diagrams in the experiment. The results allow comparing the amount of runout and the following wear of individual machine parts in different agricultural operations.

Turbocharged diesel engine is currently the most preferred for medium-sized drives in drive units (tractors, trucks, marine drives). In addition, continually increasing share in the highly competitive automotive market due to its reliability, combines with very low fuel consumption. During the past decade, mathematical modeling has paved the way for an in-depth study of diesel engines. However, most research has focused on thermodynamics,

which has a direct effect on heat release and subsequent performance and pollutant emissions to the environment. On the other hand, questions about engine dynamics, e.g. complex movement of the connecting rod, crank linkage mechanism, crank and its deformation, torsional vibration, etc., are often ignored (GIAKOUMIS at al. 2007).

The optimization of individual operations in the parts manufacturing is a role of engineering technology, which consists in determination of the optimal, the most economic or the most productive conditons for the performance of the defined operation. Economic conditions or conditions of the maximum productivity are studied within optimizing the cutting conditions for machines. The optimal cutting material and tool and the optimal combination of cutting conditions (cutting speed, feed and depth of cut) are defined by the conditions mentioned above (KOTUS et al. 2002). An effective balanced solution between external stress and the resistance of parts in the cross-section and surface is certainly a choice of an economical system: basic material – surface layer. Heat treatments, chemical-heat treatments of surfaces and metal coatings are considered as appropriate technologies of creating wear-resistant layers from an economic point of view. These technologies increase the wear resistance of materials significantly but not as much as, for example techniques of diffusional saturation or material surfacing (KOVÁČ et al. 2005).

MATERIAL AND METHODS

Crank mechanism. The crank mechanism is the basic part of the internal combustion piston engine that converts the linear reciprocating movement of the piston into the rotary movement of the crankshaft. The function of the engine is not possible without this mechanism.

Forces that affect the crank mechanism. Gas pressure causes a force impact on surfaces in the combustion chamber. So forces of gas pressure are considered in the calculation of forces in the engine mechanism (force on the piston), of forced oscillation of a valvular train (force on a valvular disk), and of solidity of a cylinder, crankshaft and other parts. The force of gas pressure affecting the piston surface is a very interesting information in terms of forces acting in the engine mechanism:

$$F_{pl} = S \times p_{(\alpha)} \quad (1)$$

where:

F_{pl} – power by gas pressure acting on the piston surface

S – projection of the piston surface area perpendicular to the axis of the piston

$p_{(\alpha)}$ – pressure change in the cylinder depending on the angle of rotation of the crank α

Inertia forces. Inertia forces are created at uneven linear movements, and even or uneven rotative motion (centrifugal forces) in internal combustion engines. All inertia forces have a periodic character in engine operation, which causes engine vibration. This fact urges designers of engines to minimize the inertia force by balancing. Piston engines, in which also linear movements exist besides the rotative motion, are engines that can be balanced only partially. In addition to negative impacts, inertia linear forces have also a positive effect on reducing the load of the crank mechanism because of substraction from the force caused by gas pressure on the piston (especially during the expansion stroke).

Calculation of inertia forces of rotating parts F_{zr} in the crank mechanism:

$$F_{zr} = m_r \times r \times \omega^2 \quad (2)$$

where:

m_r – total weight of rotating parts (kg)

r – radius (mm)

ω – rotation speed of the crankshaft (rotations/min)

Calculation of inertia forces of linear parts F_{zr} in the crank mechanism:

$$F_{zp} = m_p \times a \quad (3)$$

$$m_p = m_{piston} + m_{piston\ pin} + m_{piston\ ring} + m_{op} \quad (4)$$

where:

m_p – total weight of linear sliding parts (piston, piston pin, piston rings and linear sliding part of the piston rod m_{op}; Fig. 1)

a – distance from the axis of the crank pin

Studied object. Crankshafts produce elastic vibrations which stress them to bending, torsion, tension, and sag of the shaft can also occur. Therefore, the function of the crankshaft is changing. Main pins placed into slide bearings are crucial parts with wear and deformation. Therefore, the object of using optical measurements is to measure the runout of crankshafts in the agricultural tractor after its load in operation. The measurement was located in the major places of pins. The measurement of roundness of major pins is related closely.

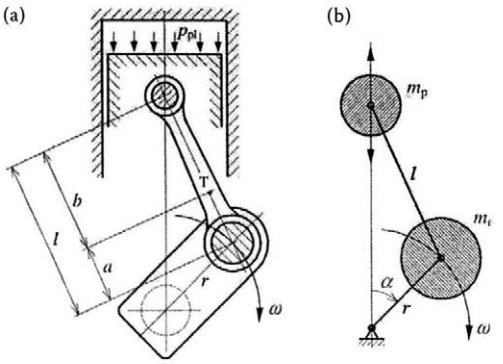

Fig. 1. Crank mechanism (a) and scheme drive crank mechanism (b) (HLAVŇA et al. 2000)

p_{pl} – pressure on the piston surface; m_p – torque on tap piston; m_r – torque rod; ω – torque crank; l – length of the rod; α – angle of rotation of the crankshaft; r – space between the connecting rod pivot; α – the axis of rotation of the crankshaft; b – distance from the pivot axis song does gravity rod; a – space between the connecting rod piston pin axis of the connecting rod; T – center rod

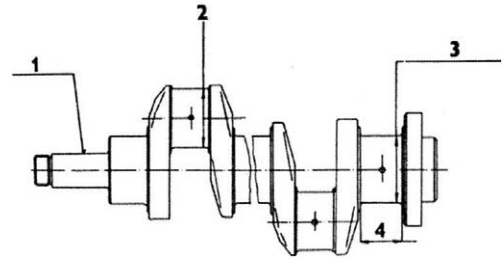

Fig. 2. Crankshaft of the tractor Zetor 6911 (Zetor Brno 1978)
1 – crankshaft; 2 – rod pins; 3 – main pins; 4 – width of the main pin

Methodology. Based on the defined objectives of this work, the basic methodology was chosen for the solution: selection of a specific type of crankshaft, determination of measured parts of the crankshaft, measured quantities depending on the measuring device, and analysis and evaluation of the obtained results.

Characteristic of the monitored crankshaft. Measurements were carried out for two crankshafts (Fig. 2) which were demounted from agricultural machines Zetor 6911 and were in operation for 20,000 Mh. The crankshaft No. 1 is from the tractor in livestock production, and the crankshaft No. 2 is from the tractor in plant production. It is a four-cylinder diesel engine crankshaft with an angular position of bends of the crankshaft (180°). The crankshaft has five main and four rod pins; the main pins are of a larger diameter and width than the rod pins. Each bend of the crankshaft is balanced by a counterweight that balances the uneven run of the crank mechanism and thereby reduces the stress onto the bearings in which the shaft is located. The counterweight is attached to the first, fourth, fifth and the last arm of the crankshaft. The crankshaft is made of grey cast iron by casting; working surfaces of the shaft are finished by grinding, lapping, and superfinishing.

Optical apical device. In order to eliminate the laborious counting, we recommend an adjustment of the zero starting point as follows: to rotate a setting wheel until the bottom window shows 0'0" and it coincides with the index line; to loose a clamp and a grooved spiral and to tilt a crank to the upper position; to turn a gross adjuster until the top win-

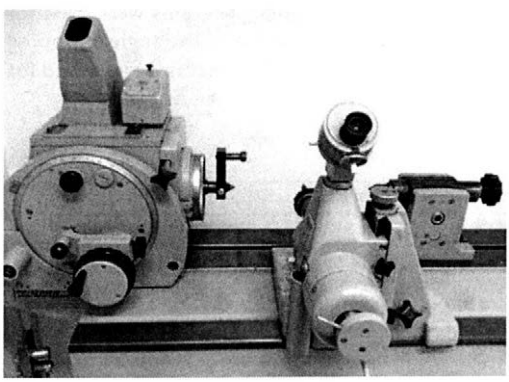

Fig. 3. Optical head with a tailstock and an additive device on a basic board 1,600 mm

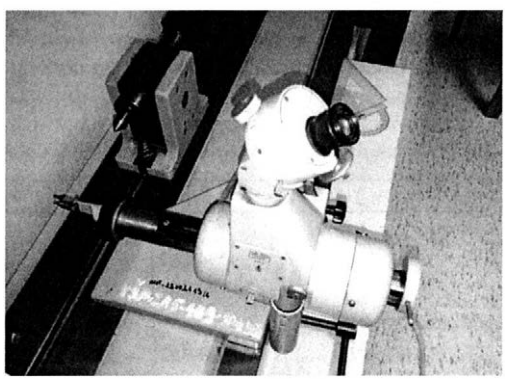

Fig. 4. Device for measurements of axial distances

dow shows 0°; to tighten the grooved spiral; to move an adjuster until the measuring spiral is not located between marked double grooves 00; to set an approximate scale to zero that can be turned by a hand and cannot be fasten. After the clamp and the grooved spiral are tightened, we can start to work. The clamps have to be lost for setting the next steps. Each minute a second steps can be done by the setting wheel during the operation. Degrees are set to tens of minutes after work. The approximate scale is used to a gross angular adjustment (KORENKO et al. 2010).

Measurement of circular radial runout (Figs 3 and 4). After reconstitution device to access the procedure for setting up the horse head. Then we can proceed to the actual display of parts, namely the crankshaft between the centers of the optical device and tailstock. Firstly, the crankshaft was thread through the clamping heart and placed on the tip of the optical head. The tip was slided out the tip of the tailstock by turning a screw until it clicks into the centring hole of the crankshaft. The emphasize was put on a force of screw tightening so it could not cause a bend of the shaft – buckling. A dial indicator and a holder provided together with a device marked 24-151-1 were placed on a clean grinded surface of the basic board. The arms of the holder were directed to achieve the horizontal orientation of a sliding measuring rod of the dial indicator. The measurement of runout were performed on points of the main crankshaft's pins. The dial indicator was gently pressed against the shaft so the pointer made one revolution around its axis. Tipping a lever (10) and turning a wheel (9) clockwise showed deflection of the pointer of the dial indicator. The max. value of deflection and the angle of deflection of the shaft were detected within deflection and were subtracted them from the optical head P3. If necessary, a correction and offset the tailstock on a desired value (in accordance with paragraph 3.2.3c (Zetor Brno 1978) was made, and it was necessary to repeat the measurement of eccentricity. The actual measurement proceeded at the exact shoulder of the crankshaft. Tipping the lever and setting the wheel served for setting the display of the optical head P3 to angle 0°. The measurement was be carried out at angular intervals of 60° and repeated up to angle 360°. The dial indicator (marked as 24-151-1) helped to read a measured value at each interval shifted by 60° from the scale. The entire measurement was repeated at the same angular values for each main pin of the other crankshaft. Deviations from circular radial runout were calculated and graphical relationships are demonstrated. The main pins are on the x-axis, and the amount of deviation in millimeters is on the y-axis. The greatest deviation of the crankshaft points could be defined from a curve. Further, the values of the average deviation of runout on both shafts were calculated and compared.

Measurement of roudness. The same installation of the crankshaft as in the case of runout measurement was used. The optical dividing head P3 was used for angular tipping. It was used to set the angle that we will move in the range from 10° to 360°. An additional device for measuring the axial distance – radius was used to measure the radius of the main crankshaft's pins. The device on the basic board in front of the measured pin was moved. The tip for the axial distance of the measuring adittional device was set on the axis of the crankshaft perpendicularly. The cylinder with the tip was pressed against the surface of the pin but not too intensively. Lighting allowed to project the actual value of axial radial distance (r) into ocular from which the values could be read. Graphic relationships in the form of polar diagrams were used for measured values, which reflect the angle of tipping and the radius of pin. Polar diagrams were used for presenting the results of roundness deviations.

Table 1. Circularity deviations (Min; mm) for the main pins of the crankshaft No. 1

r (mm)	Pin 1	Min	Pin 2	Min	Pin 3	Min	Pin 4	Min	Pin 5	Min
Crankshaft No. 1										
r_{max}	34.655	0.05	34.652	0.047	34.663	0.066	34.686	0.095	34.649	0.052
r_{min}	34.605		34.605		34.597		34.591		34.597	
Crankshaft No. 2										
r_{max}	34.767	0.053	34.782	0.086	34.788	0.081	34.781	0.075	34.768	0.053
r_{min}	34.714		34.696		34.707		34.706		34.715	

r – axial distance radius; r_{max} – largest radius measured profile; r_{min} – smallest radius measured profile

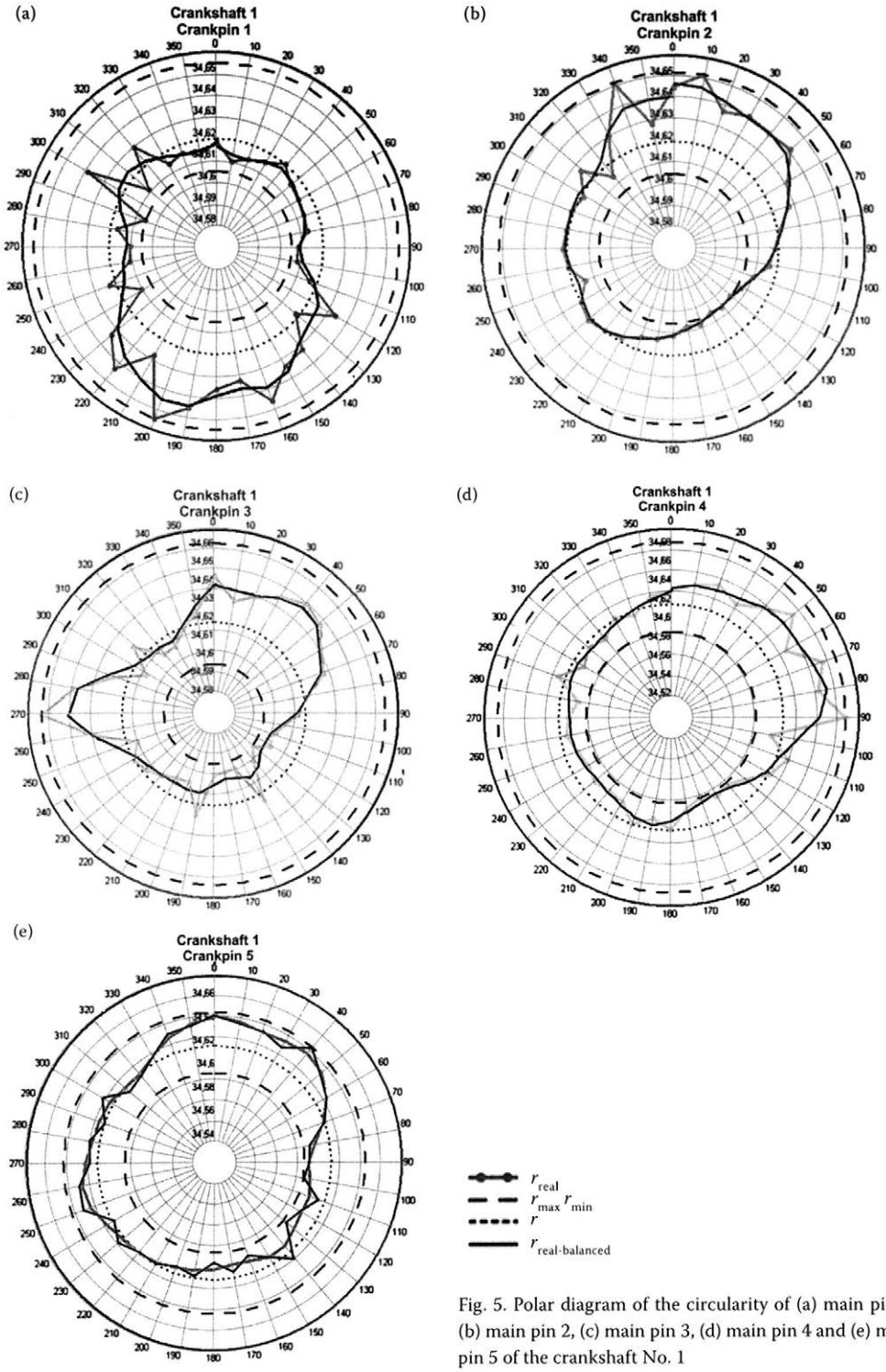

Fig. 5. Polar diagram of the circularity of (a) main pin 1, (b) main pin 2, (c) main pin 3, (d) main pin 4 and (e) main pin 5 of the crankshaft No. 1

RESULTS AND DISCUSSION

Results of circularity measurements and their graphical demonstration

Measurement of circularity of the crankshaft No. 1 (Fig. 5)

The first main pin of the crankshaft No. 1 is characterised by r_{max} = 34.655 at angle 200° and r_{min} = 34.605 at angle 290°. The difference forms the width of the anuloid with values 0.005 mm = 5 mm. Calculations were repeated for all the main pins of both crankshafts.

Table 1 shows r_{max} and r_{min} according to the relation $r_{max} - r_{min} = min$, calculated min. width of anuloids – deviations of circularity min.

Measurement of circularity of the crankshaft No. 2 (Fig. 6)

Table 1 shows r_{max} and r_{min} according to the relation $r_{max} - r_{min} = min$, calculated min. width of anuloids – deviations of circularity *min*.

Results of circular radial runout and its graphical representation (Fig. 6)

The circular radial runout of the circumferential surface's component was determined at the shaft rotation of 360° by the max. value of deviaton v_{max} and minimal value of deviation v_{min}, which were measured by using the dial indicator. The difference between these values was referred to the deviation of circular radial runout ρ_H. It was calculated for the first and the other main pins:

$$\rho_H = v_{max} - v_{min} = 0.307 - 0.3 = 0.007 \text{ mm} \quad (5)$$

where:

v_{max} – max. measured deviation from axial rotation (mm)
v_{min} – min. measured deviation from axial rotation (mm)

Average runout of the main pins of the crankshaft No. 1 (Table 2):

$$\bar{x}_1 = \frac{1}{N}\sum_{i=1}^{N} x_i = (0.007 + 0.012 + 0.012 + 0.016 + 0.013)/5 = 0.0138 \text{ mm}$$

Average runout of the main pins of the crankshaft No. 2 (Table 2):

$$\bar{x}_2 = \frac{1}{N}\sum_{i=1}^{N} x_i = (0.027 + 0.036 + 0.45 + 0.037 + 0.024)/5 = 0.0338 \text{ mm}$$

Difference of runout:

$$\bar{x} = \bar{x}_1 - \bar{x}_2 = 0.0338 - 0.0138 = 0.02 \text{ mm}$$

Demands on material attributes grow concurrently with a continuous increase in performance. Development is directed to materials with improved resistance and lifetime, with improved mechanical attributes, less weight and lower cost especially. The crank mechanism also requires its care for a reliable function. The use of appropriate materials and their subsequent chemical-heat

Tab. 2. Deviation v (mm) of runout of the crankshafts No. 1 and No. 2 (Fig. 7)

Angle (°)	Pin 1	Pin 2	Pin 3	Pin 4	Pin 5
Crankshaft No. 1					
60	0.301	0.298	0.303	0.3	0.304
120	0.3	0.302	0.299	0.305	0.299
180	0.302	0.306	0.305	0.308	0.305
240	0.305	0.31	0.314	0.314	0.31
300	0.307	0.308	0.32	0.316	0.312
360	0.306	0.303	0.313	0.308	0.309
ρ_H	0.007	0.012	0.021	0.016	0.013
Crankshaft No. 2					
60	0.528	0.531	0.535	0.520	0.529
120	0.521	0.520	0.519	0.519	0.522
180	0.529	0.527	0.532	0.538	0.530
240	0.540	0.544	0.548	0.554	0.538
300	0.548	0.556	0.564	0.557	0.546
360	0.537	0.545	0.550	0.541	0.534
ρ_H	0.027	0.036	0.045	0.037	0.024

v – measured deviation from the axis of rotation in this section; ρ_H – circular radial run-surface components

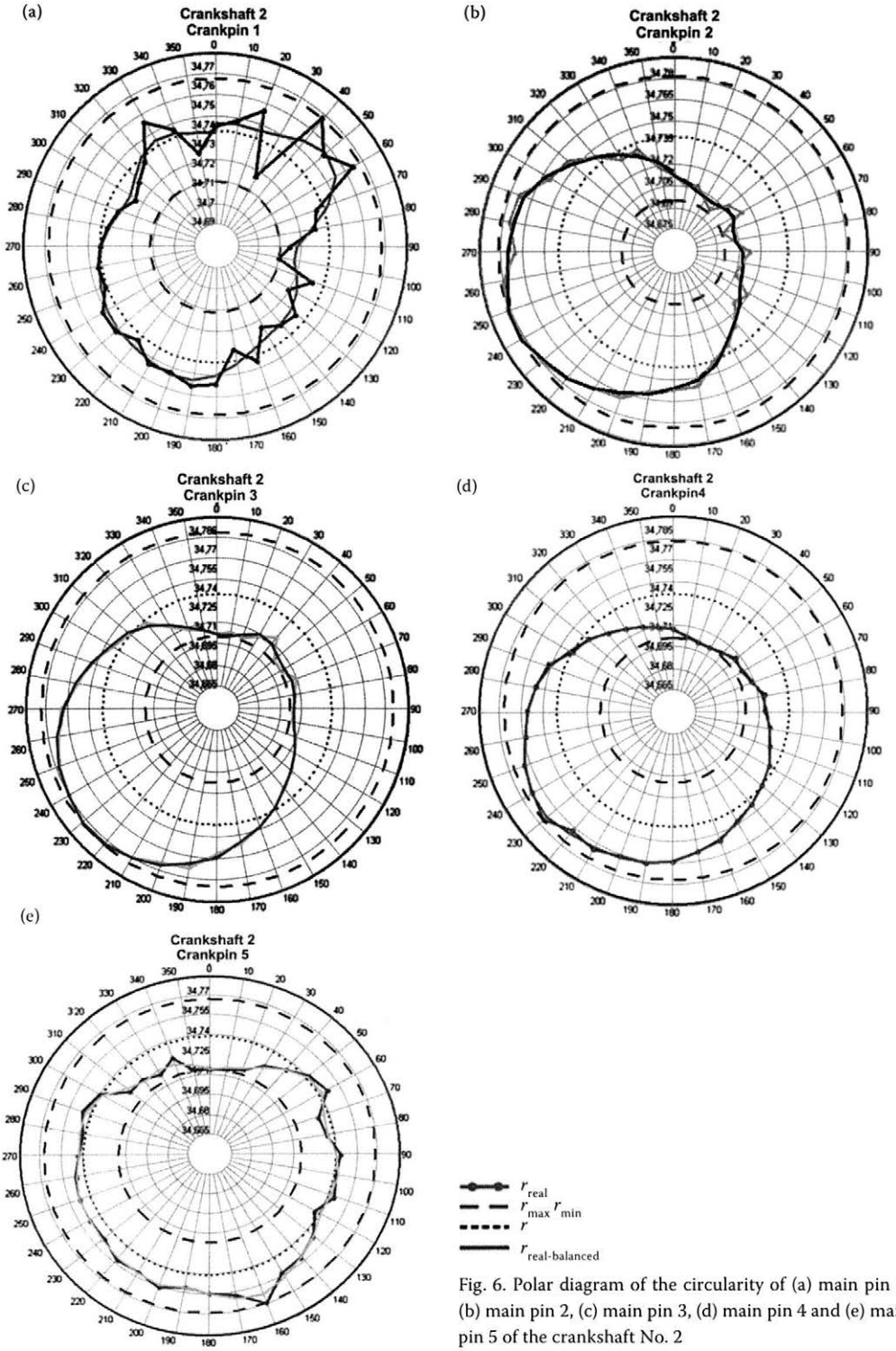

Fig. 6. Polar diagram of the circularity of (a) main pin 1, (b) main pin 2, (c) main pin 3, (d) main pin 4 and (e) main pin 5 of the crankshaft No. 2

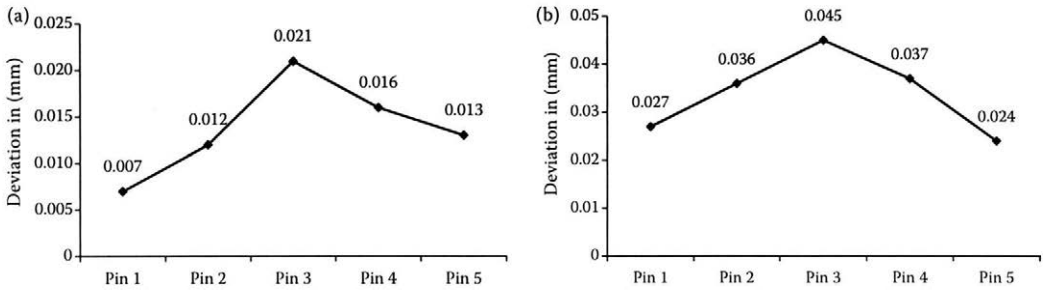

Fig. 7. Relationship between the deviation of runout and the constituent main pin of the (a) crankshaft No. 1 and (b) crankshaft No. 2.

treatment leads to ensuring the lifetime and reliability of the crank mechanism. Important is the quality of lubrication and lubricants. Temperature in the combustion chamber of diesel engines is changing up to 1,000–1,200°C. Pressure can reach values up to 25 MPa in diesel engines. The operating speed of some components must be also taken into account. The piston, valves, crankshaft, etc. are exposed to changes in conditions of nearly 17 times/s at 1,000 rpm. It is up to 50 times/s at 3,000 rpm. Also, a great tribological degradation due to fitting interaction of engine parts must be taken into the account.

According to GIAKOUMIS et al. (2007), in the analysis of the turbodiesel engine under load the following results were obtained:

Moment of inertia affects the crankshaft deformation mainly in surface portion, but it applies only to the total engine with relatively low-speed rotations. It means the max. deformation during one cycle cylinder engine. Significant levels can be expected during transient operation, depending on the intended increase of the load. Instantaneous max. deformation can be up to 50% higher compared with the corresponding mean, as in intermediate cycles. Minor variations in the load, as well as stiffer crankshaft design are key parameters for the reduction of crankshaft torsional deformations.

A significantly degraded factor of crankshafts is also pitting, which usually becomes a deposit of fatigue crack. Therefore, the last two of named steels are usually carburized, nitrided or carbon-nitrided. The crankshaft is a component in the engine that bears the greatest mechanical load. Terms of the crankshaft´s load are static and dynamic. The pressure exerted by an explosion of fuel is transferred through the piston and connecting rods, the inertia force of pistons and connecting rods, vibration, etc. Earlier, nodular cast iron served for crankshafts. Modern engines are equipped with crankshafts of forged steel or cast iron. Micro-alloyed steel Fe-0.5C-0.8Mn-0.25s-0.1V was proved as a suitable alternative and becomes more widespread due to lower cost and excellent mechanical attributes (does not require an additional hardening). Hot forging with cooling in air is sufficient for the creation of carbides and nitrides of vanadium in a structure (GIRMAN 2011).

CONCLUSION

The measurements show that the difference of runout between the shaft No. 1 used within livestock production and the shaft No. 2 used within vegetable production was 0.02 mm. The shafts were in operation for 20,000 Mh. The shaft loaded in vegetable production had the average runout of the main pins of 0.0338 mm while the shaft in livestock production had 0.0138 mm. A greater stress and forces affect the crankshaft from vegetable production in comparison with livestock production.

References

DRLIČKA R., MIKUŠ R., 2007. Vývoj ekonomiky opráv poľnohospodárskych strojov/Trend in agricultural machines repair costs. In: 12th International Scientific Conference accompanying event of International Machinery Fair 2008. Nitra, SUA in Nitra, 197–201. Available at http://www.slpk.sk/eldo/2007/025_07/46.pdf

GIAKOUMIS E.G., RAKOPOULOS C.D., DIMARATOS M., 2007. Study of crankshaft torsional deformation under steady-state and transient operation of turbocharged diesel engines. Journal of Multi-Body Dynamics, 222: 17–30.

GIRMAN V., 2011. Kovové materiály automobilových konštrukcií – I. Motor a jeho súčasti. [Met-

al materials of automobile constructions – I. Engine and its components.] In: Materials Engineer/ Materiálový inžinier. Available at http://www.materialing.com/materialy_motorov_castI

HAJDÁK H., 2008. Opotrebenie vačkových mechanizmov. [Wear of Cam Mechanisms.] Nitra, SUA in Nitra: 67.

HLAVŇA V., KUKUČA P., ISTENÍK R., LABUDA R., LIŠČÁK Š., 2000. Dopravný prostriedok – jeho motor. [Vehicle – its Engine.] 1st Ed. Žilina, University of Žilina: 442.

KOTUS M., ŽITŇANSKÝ J., PETRÍK M., 2002. Optimalizácia technologického postupu výroby strojovej súčiastky. [Optimization of technological procedure of machine part production.] In: Kvalita a spoľahlivosť strojov. [The Quality and Reliability of the Machines.] Nitra, SUA in Nitra: 122–124.

KOVÁČ I., ŽARNOVSKÝ J., ŽITŇANSKÝ J., 2005. Vrstvy odolné proti opotrebeniu. [Wear-resistant layers.] In: New Trends in Technology System Operation, 20–21 October 2005. Košice, Technical University: 160–161.

KROČKO V., MIKUŠ R., DRLIČKA R., 2007. Trends of agricultural machinery in Slovakia. In: Proceedings of the 5th Research and Development Conference of Central and Eastern European Institutes of Agricultural Engineering, June 20–24, 2007. Kiev, National Agricultural University of Ukrajine: 61–67.

KORENKO M., ŽITŇANSKÝ J., DRLIČKA R., KOVÁČ I., 2010. Základy strojárskych technológií. [Basics of Engineering Technologies.], 1st Ed. Nitra, SUA in Nitra: 118.

LÍŠKA E.. BAJLA J., CANDRÁKOVÁ E., FRANČÁK J., HRUBÝ. D., ÍLLEŠ L., KORENKO M., NOZDROVICKÝ L., POSPÍŠIL R.,. ŠPÁNIK F., ŽEMBERY J., 2008. Všeobecná rastlinná výroba. [General Crop Production.] 1st Ed. Nitra, SUA in Nitra: 421.

PONIČAN J., KORENKO M., 2008. Stroje pre rastlinnú výrobu: stroje na zber krmovín, zrnín, ľanu, zemiakov, zeleniny a ovocia. [Machines for Crop Production: Machines for Harvesting Forage Crops, Grains, Flax, Potatoes, Vegetables and Fruits.] 1st Ed.. Nitra, SUA in Nitra: 248.

PÁLTIK J., FINDURA P., POLC M., 2007. Poľnohospodárske stroje: skúšanie, konštrukcia, použitie. I. časť. [Agricultural Machines: Testing, Construction, Usage. Part 1.] 1st Ed. Nitra, SUA in Nitra: 190.

Zetor Brno, 1978. Dílenská příručka traktorů Zetor 6911. [Service Manual of Tractors Zetor 6911.] 1st Ed. Brno, Zetor: 200.

Received for publication April 16, 2013
Accepted after corrections October 14, 2013

Corresponding author:

Ing. PAVEL POLÁK, PhD., Slovak University of Agriculture in Nitra, Faculty of Engineering, Department of Quality and Engineering Technologies, 949 76 Nitra, Slovak Republic
phone: + 421 37 641 4104, e-mail: pavel.polak@uniag.sk

Determination of mechanical properties of soil under laboratory conditions

V. Malý, M. Kučera

Department of Machine Design, Faculty of Engineering, Slovak University of Agriculture in Nitra, Nitra, Slovak Republic

Abstract

Malý V., Kučera M., 2014. **Determination of mechanical properties of soil under laboratory conditions**. Res. Agr. Eng., *60* (Special Issue): S66–S69.

This paper presents the mechanical properties of soil. In order to determine the properties of soil under laboratory conditions, a special measuring device was constructed, viz. a bevameter. Two types of soil with different levels of moisture were examined and their mechanical properties were determined. Measurements were taken of non-compressed soil. A measuring network was set up, consisting of measuring and recording devices. In the course of measuring, the force and penetration depth of the pressing plate were recorded simultaneously. Three different diameters of pressing plate were used, namely 38, 50 and 70 mm. The pressure on the contact area was calculated after completion of the measurements, and the relationships between pressure and penetration depth were presented graphically.

Keywords: pressure; penetration depth; bevameter; soil moisture

The use of mobile machines in agriculture causes undesirable soil compaction, resulting in changes in soil properties. The degree of soil compaction can be determined by measuring the physico-mechanical properties of the soil. Once this has been achieved, adequate steps may be implemented to improve soil conditions, e.g. by applying protective technologies of soil cultivation. There is a real need for the determination of soil properties, under laboratory conditions as well as under real-life operating conditions.

Under laboratory conditions more exact and objectively comparable results can be obtained. The scientific importance of the study of these results lies in the field of terramechanics. At present, several methods are known for determining the physico-mechanical properties of soil, and a number of appropriate measuring devices and measuring tools is used. From a historical and factual point of view, the valuable theoretical and practical work carried out by Bekker (1961, 1969) and his disciple Wong (1980, 1989) should be noted. Based on extensive experiments and theoretical analyses, Bekker (1961) described in mathematical terms the physical reactions taking place in the contact zone between wheel and soil. From this he derived the basic relationships for vertical and horizontal force effects (penetration and rolling-resistance) resulting from the movement of the wheel over the soil. All his mathematical derivations are based on the experimental data obtained through the use of measuring devices and measuring equipment. The measurements were carried out in laboratory conditions, each penetration test being performed at least twice. Round plates of various diameters were used, whereby the penetration depth of the plates was recorded together with the pressure exerted. Bekker (1961) made use of a measuring device called a "bevameter", which serves experimentally to determine:

– penetration depth in relation to pressure exerted,
– shear stress related to soil movement.

Supported by the Scientific Grant Agency VEGA of the Ministry of Education of the Slovak Republic and the Slovak Academy of Sciences, Grant No. 1/1064/11.

Table 1. Granularity of soil samples

Soil sample	Soil particles according to size (%)				
	> 0.25 mm	0.25–0.05 mm	0.05–0.01 mm	0.01–0.001 mm	< 0.001 mm
Z1	6.16	5.57	53.8	17.92	16.55
Z2	40.49	13.52	25.67	10.61	9.71

In Slovakia, BAJLA (1998) has spent considerable time studying the mechanical properties of soil. He performed extensive experimental measurements using a vertical and horizontal penetrometer of his own construction. Also, VARGA (2010) has performed extensive measurements of the mechanical properties of soil, with a view to determining the effect of soil resistance in the case of a uniform plowing depth through the use of a three-point hitch tool pulled by a tractor. The deformation characteristics of soil at compressive load under laboratory conditions were reported by ABRAHÁM (2005).

MATERIAL AND METHODS

For determination of mechanical properties of soil at simple load by pressure under laboratory conditions a measuring device specially designed at the Department of Machine Design, Faculty of Engineering, Slovak University of Agriculture in Nitra, Slovakia was used. This measurement device with accessories (Fig. 1) consists of a single-phase asynchronous motor Klimac KT1 type (ZPA, Prešov, Slovak Republic). The motor is equipped with limit switches and an overload protection (OP KT1; ZPA, Prešov, Slovak Republic), which is adjustable with a spring preload of the torque clutch. The shaft of the motor is connected to the gear box (Klimac KT 1; ZPA, Prešov, Slovak Republic) by input-shaft. This gear box drives the spindle nut, which is attached to the double-wing propeller of the optoelectronic revolution sensor (RS; DMD SUA, Nitra, Slovak Republic). The optoelectronic force sensor (SS 1000N; DMD SUA, Nitra, Slovak Republic) is mounted between the sliding bar of the spindle and the pressing plate. A soil sample is placed in a metal container. Based on the number of spindle nut revolutions and the thread pitch s = 6 mm, the penetration depth of the pressing plate can be set. The pressure value depends on the force and surface area of the pressing plate. The data measured are continuously processed by computer, displayed on a monitor and recorded on a recording device (PC-IBM; IBM, New York, USA).

The laboratory measurements of the mechanical soil properties at simple pressure load were performed under following conditions. The soil was moistened to the desired moisture before the experiment and then placed in a container with dimensions 640 × 440 × 400 mm up to a height of 370 mm.

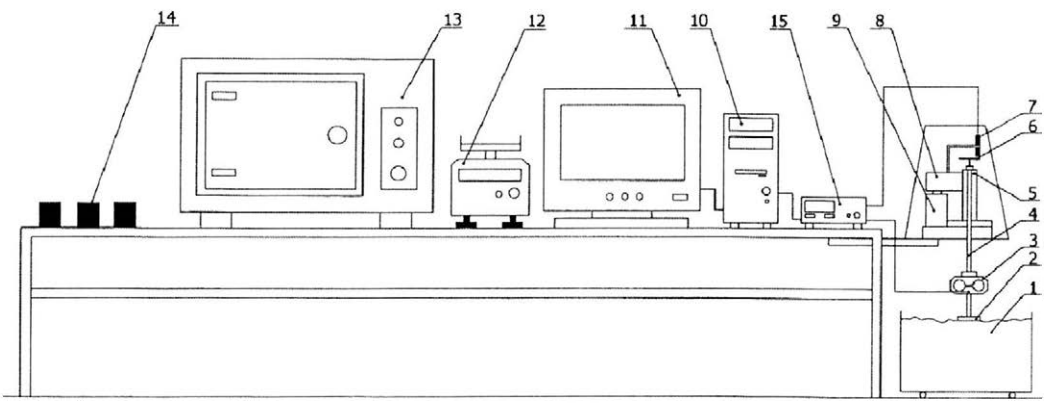

Fig. 1. Measuring network for measurement and evaluation of the bevametric test

1 – metal bin with soil; 2 – pressure plate; 3 – force sensor; 4 – displacement rod of servomotor; 5 – arbor nut; 6 – two wing propeller; 7 – rpm sensor; 8 – gearbox; 9 – single phase asynchronous electric motor; 10 – computer; 11 – monitor, 12 – weight; 13 – drier; 14 – sample; 15 – recorder

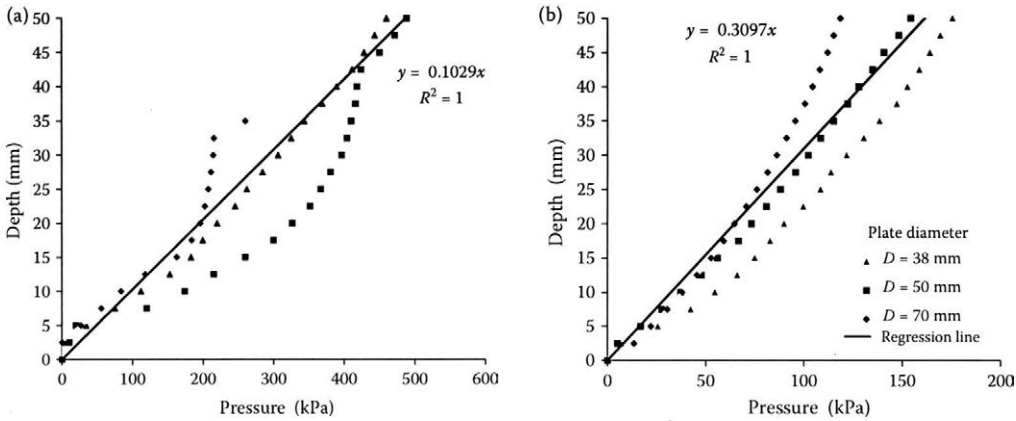

Fig. 2. Relationship between pressure and depth for soil moisture (a) 4.8%, (b) 16.03% and granularity Z1

For the laboratory measurements, following soil samples were used:

– soil moisture 4.81% and 16.03%, granularity Z1,
– soil moisture 5.7% and 17.03%, granularity Z2.

The soil moisture mentioned above is expressed in weight percentage. The granularity of soil samples is presented in Table 1.

RESULTS AND DISCUSSION

The results obtained from the experimental measurements of soil compaction using a bevameter, with soil moisture w = 4.81% and granularity Z1 confirm that penetration depth h increases linearly in relation to pressure p (Fig. 2a). It can be further observed that plate diameter has an effect on the penetration depth for the same value of pressure. In this case the relationship between pressure and penetration depth may be expressed by regression line $y = 0.1029x$ with correlation coefficient $R^2 = 1$, as shown Fig. 2. For example for a pressure p = 400 kPa and plate diameter D = 50 mm the penetration depth is 40 mm.

Different results were obtained for soil moisture w = 16.03% and the same granularity Z1 (Fig. 2b). Fig. 2b shows that for pressure p = 100 kPa the penetration depth is approximately 30 mm. Similar results were obtained for granularity Z2 and analogous values of soil moisture, as compared in Fig. 3. Ultimately, the summary diagram shown in Fig. 4 graphically illustrates the results obtained from the experimental measurements of soil compaction for various soil moisture and granularity levels.

Based on the obtained results mentioned above it can be concluded that dry soil with a moisture level about 5% does not change expressively its mechanical properties, not even after compression and regardless of granularity. However, at a level of soil

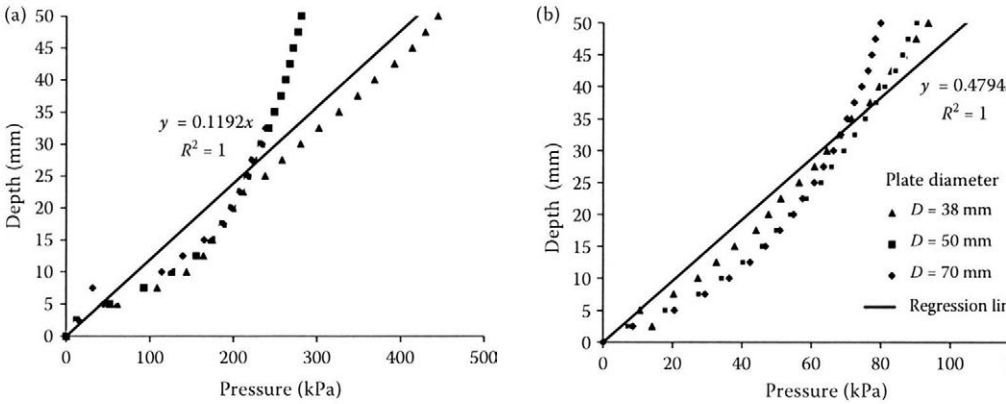

Fig. 3. Relationship between pressure and depth for soil moisture (a) 5.7%, (b) 17.03% and granularity Z2

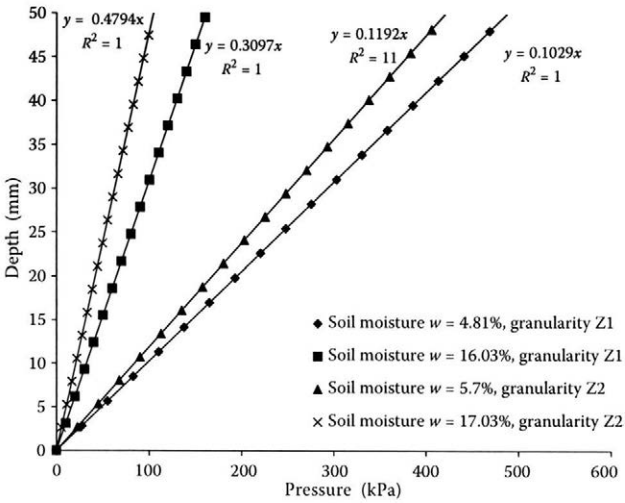

Fig. 4. Relationship between pressure and depth after regression analysis for various soil moisture and granularity levels

moisture of 16–17% the change in mechanical soil properties after compression is the highest of all, up to 4-fold.

So, in view of the fact that the most favourable moisture level for standard types of soil for cultivation is within 15–17% range, it is recommended to use all available means (dual tyres, caterpillar tractors, soil protection technologies) to reduce soil compaction caused by mobile agricultural machines.

CONCLUSION

The laboratory experiments and measurements identified a number of new relationships which have, up to now, never been presented in this way, and which need to be further theoretically analysed. In the first place, there is an interesting fact that reduction in plate diameter, and thus in the surface area of the pressing plate, will generally little decrease the pressure for the same value of penetration depth; it may be considered as anomaly or paradox. This paradox may be explained by the fact that by pressing the plate into the soil, the soil is compressed on area equal to the surface area of the plate, while at the same time soil is cut and pushed away at the circumference of the plate. However, in calculating the pressure values, the shear stress at the circumference of the plate is not taken into consideration. As a result, the pressure values are to some extent distorted.

References

Abrhám R., 2005. Interakcia pôdy a pojazdového ústrojenstva. [Interaction of soil and driving mechanism.] [Ph.D. Thesis.] Nitra, SUA in Nitra: 161.

Bajla J., 1998. Penetrometrické merania pôdnych vlastností. [Penetrometrical Measurements of the Soil Properties.] Nitra, SUA in Nitra: 112.

Bekker M.G., 1961. Theory of Land Locomotion, The Mechanics of Vehicle Mobility. Ann Arbor, University of Michigan Press: 522.

Bekker M.G., 1969. Introduction of Terrain Vehicle Systems. Ann Arbor, University of Michigan Press: 846.

Varga F., 2010. Odpor pôdy a jeho vplyv na reguláciu trojbodového závesu traktorov. [Soil resistance and its influence on the control of three point hitch of tractors.] [Ph.D. Thesis.]. Nitra, SUA in Nitra: 151.

Wong J.Y., 1980. Data processing methodology in the characterization of the mechanical properties of terrain. Journal of Terramechanics, *1*: 13–41.

Wong J.Y., 1989. Terramechanics and Off-Road Vehicles. Amsterdam-Oxford-NewYork-Tokyo, Elsevier: 251.

Received for publication April 16, 2013
Accepted after corrections November 26, 2014

Corresponding Author:

Ing. Vlastimil Malý, PhD., Slovak University of Agriculture in Nitra, Faculty of Engineering, Department of Machine Design, Tr. A. Hlinku 2, 949 76 Nitra, Slovak Republic
phone: + 421 37 641 4109, e-mail: vlastimil.maly@uniag.sk

Machinability improvement using high-pressure cooling in turning

R. Drlička, V. Kročko, M. Matúš

Department of Quality and Engineering Technologies, Faculty of Engineering, Slovak University of Agriculture in Nitra, Nitra, Slovak Republic

Abstract

Drlička R., Kročko V., Matúš M., 2014. **Machinability improvement using high-pressure cooling in turning.** Res. Agr. Eng., *60* (Special Issue): S70–S76.

Process fluids are used primarily for their cooling and lubricating effect in machining. Many ways to improve their performance have been proposed; the analysis of some of them is provided in the paper. The effect of high pressure cooling has been investigated with regard to chip formation and tool life. Standard and for high pressure application particularly designed indexable cutting inserts were used with fluid pressure 1.5 and 7.5 MPa. The pressure effect on tool life at different feed rates was observed as well. Not each cooling pressure value or machined material showed favourable chip formation. Tool life though has improved significantly while machining with a lower feed rate.

Keywords: tool; indexable insert; high pressure cutting fluid application; cutting parameters; tool life

Management methods for managing the manufacturing processes and for quality improvement of product should be a part of every production organization (Korenko, Kaplík 2011). Not only in times of economic crisis but also in times of growth and prosperity of economy, manufacturing organizations must strive in order to the outputs of their production processes are most effective and achieve the best results. That way you can ensure the company's prosperity, growth and position in the market (Korenko et al. 2010).

The term machinability is understood as a complex of machined material properties, fulfilled by particular criteria such as cutting tool life, a simple achieving of shape and dimension accuracy, machining performance, low system load – low cutting resistance, and chip generation. Technological properties of cutting/cooling fluids used in machining influence the machining process quality (Kročko et al. 2012).

Chip generation is important for fully automated lines to prevent possible downtime occurrence due to cough and reeled up chips in the working space or chip conveyor. The chip reeled on the cutting edge can damage the finished surface on the machined part, cutting tool, or shorten the cutting tool life. Long bulky chips handling can introduce hazard/risk of operator's injury. This is why the shape and size of chip has to be under control.

The turning process is mainly a continuous cut with a high probability of long chip creation. The proper cutting parameters selection, such as cutting speed (v_c), the depth of cut (a_p) and feed per revolution (f_n) along with cutting tool micro- and macro-geometry and coating, can affect the chip shape and size (Žitňanský et al. 2012). On the contrary, the machined part material, specifically its chemical composition (effect of C, Cr, Ni, Mn and S content), thermal treatment and mechanical properties (tensile strength, yield strength, ductility) cannot be affected usually.

Cooling strategies could be divided as follows:
– high volume rate of cooling fluid,

– high pressure cooling,
– dry machining,
– cooling medium constitution change,
– minimum quantity lubrication (MQL),
– oil mist lubrication.

Machining with using no or min. amount of cutting fluid has become a global trend. This cannot be used for specific material groups and machining operations because of unfavourable chip formation, machined surface quality and allowances and machining performance. A standard cooling system is used in many machines, i.e. cooling fluid flow through a big diameter nozzle. This system function is more rinse, with a removal of chips, temperature decrease in machining workspace and cutting system elements preservation.

Standard cooling is not sufficient because of quite high temperature generation in the cutting zone in machining. Cutting fluid cannot reach the zone of the highest temperature in case of the standard cooling system because the fluid evaporates, and then vapours generated do not allow the cutting fluid to access the cutting edge, resulting usually in thermal cracks on it. That is why dry cutting was preferred using no cooling fluids.

Introducing a new approach to the cooling process – high-pressure cooling involves cooling fluid application using a high-pressure nozzle. A lamellar flow of the fluid is achieved, causing the contact area of the removing chip and cutting tool on the rake is reduced. The high cutting flow velocity is not so much influenced by water vapours. The cooling and lubricating effect is increased, and chip forming and breaking is improved. A jet of fluid pressure blast at the back of the chip and into the nip between the chip and the rake face provides cooling and an efficient and non-wearing chip-breaking action (Byers et al. 2006).

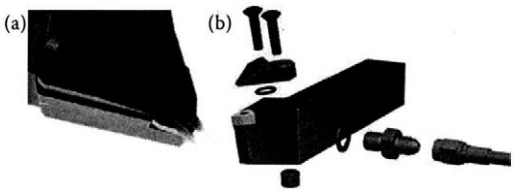

Fig. 1. Jet Stream system, Seco (a) type of cooling, (b) assembly of Jet Stream

High pressure cooling results in few advantages, including higher cutting parameters use, cutting edge life extension (from 20% up to 70%), and a better chip control and removal. Some disadvantages include higher initial costs, higher power consumption, higher system maintenance costs, higher demands on cooling emulsion, and working space exhausting.

MATERIAL AND METHODS

Analysis of selected tool manufacturer's solutions. Standard tools cannot be used, although they are equipped with cooling fluid channels through the tool. The cooling channel is of a too large diameter, and it is not directed to the cutting zone properly. Several manufacturers offer own tooling systems for high-pressure cooling in various concepts.

The company Seco (Fagersta Stainless AB, Fagersta, Sweden) offers a Jet Stream system (Fig. 1). The advantage of this system is a rigid clamping of the indexable cutting insert (ICI), but two channels for cooling fluid application are not pointed to the ICI tip when machining with a small depth of cut. Moreover, cooling channels finish is not ideal, so swirl flow instead of lamellar one can occur at lower pressures.

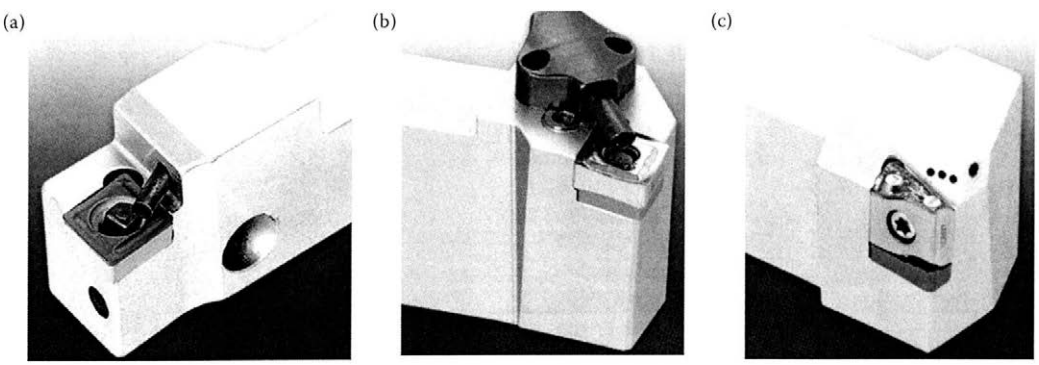

Fig. 2. Iscar HP-HELI TURN (a) fixed cooling channels, (b) with housing and (c) the nozzle tube integrated in a holder

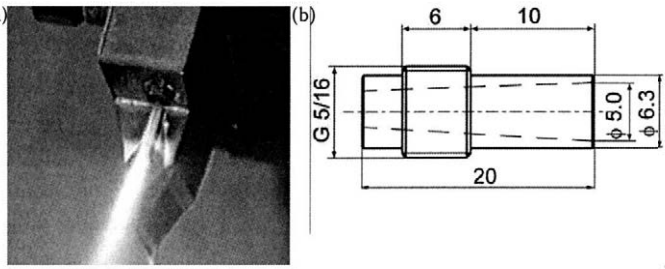

Fig. 3. Nozzle and cooling of ChipBlaster company (a) example of cooling and (b) shape of nozzle tube

The Iscar company (Tefen, Beit-Dagan, Israel) offers two systems: JET HP – HELI TURN (Fig. 2), with ICI clamped tangentially (designed for conceptual ICI) and then standard ISO ICI.

Holders HELI TURN for ISO ICI do not have designed the cooling pipe reliably. The pipe is inserted into the holder body and is pulled out by the pressure of cooling fluid running into. The pipe itself is not designed to concentrate the pressure to one spot and became a barrier for long chip running out of the cutting zone.

As the first company on the market, ChipBlaster offers a comprehensive solution of high-pressure cooling (Fig. 3). It was the first applying for the patent of the cooling pipe as a nozzle for laminar flow. Tool holders are designed for standard ICI, and it allows selecting the proper nozzle diameter with regard to the pump performance. The only disadvantage of this system is that it only contains one nozzle, limiting the disposable depth of cut.

Another company selected, offering tools for high-pressure cooling, is Sandvik Coromant AB (Sandviken, Sweden). It offers tool holders for ISO ICI with three cooling nozzles used (Fig. 4), exchangeable, similarly to the ChipBlaster solution, in accordance with flow rate generated by the pump type. ICI clamping is in some respect an obsolete solution, using a clamp, but no barrier is created for cutting fluid application to the cutting zone with an appropriate angle, forming an angle of 10° with rake.

The advantage of this system is the possibility of cutting fluid direction, according to the machined surface type, i.e. a cylinder or face surface. The cutting fluid stream can be pointed to the ICI tip in case of finishing operation (Fig. 5).

Used indexable cutting inserts. Standard ISO indexable cutting inserts can be used for high-pressure cutting tools, but they have to be equipped with a wider groove so that no mechanical barrier is present in front of the cutting edge to disturb the cooling fluid flow. To fulfil this requirement, a specific ICI with a special shape for high-pressure cooling is recommended by manufacturers (Fig. 6).

Seco has a specific ICI geometry, adjusted to SECO tool holders. These holders use two cooling channels completely modified to their ICI, with a wide opened groove (Fig. 7).

RESULTS AND DISCUSSION

The aim of laboratory sets was to compare chip generation and type in particular machining conditions. A standard geometry MM2025 was compared to an optimised geometry for high-pressure cooling MMC2025 (Fig. 8) in laboratory tests. Particular ICIs in a standard tool holder rigid clamp (RC)

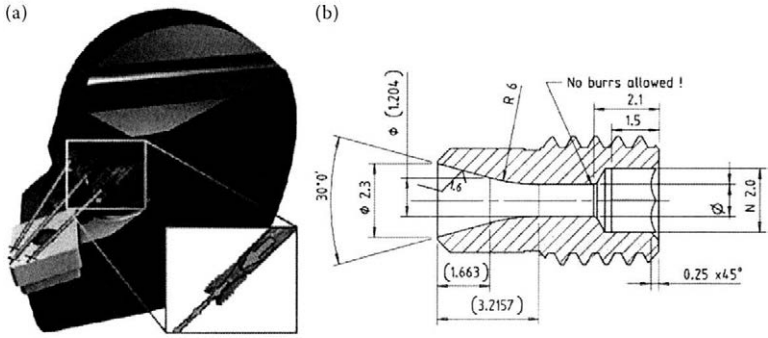

Fig. 4. Cooling system Sandvik Coromant (a) and a detail of cooling nozzle design (b)

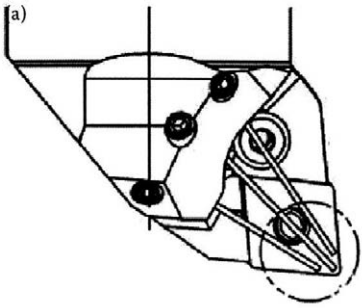

Fig. 5. Cooling fluid lines of flow distribution to the cutting zone (a) concentrated flow cooling in one place and (b) destination of the flow cooling on the inserts

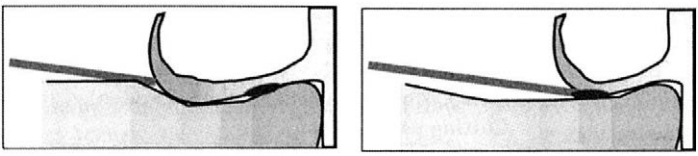

Fig. 6. Difference between geometry standard (a) and specific shape optimized for high pressure (b) of ICI and its application in high-pressure cooling tool holders

and special tool holder for high-pressure cooling at the cooling fluid pressures of 1.5 and 7.5 MPa on the Okuma machine (Okuma, Oguchi-cho, Japan) were compared. Workpiece material was austenitic stainless steel 1.4404 (ThyssenKrupp, Essen, Germany). Facing was used as a machining operation. Cutting parameters were used as follows:

cutting speed v_c = 200 m/min; depth of cut a_p = 1.0 mm; feed per revolution f_n = 0.12 mm and 0.2 mm. Used ICI type – CNMG120408.

Resulting chips are presented in Fig. 9:

(a) Tool holder effect: the use of RC clamp and standard cooling system does not improve chip generation either at higher cooling fluid pressure. In spite of that, the use of tool holder for high-pressure cooling improved chip generation even at lower pressure of cooling fluid (1.5 MPa), with a spiral chip going away easily. The chip generated at pressure 7.5 MPa was naturally broken, elemental.

(b) Feed effect: the common theory was confirmed that higher feed values improve chip generation with machined surface finish deteriorating (not measured in our tests).

(c) Indexable cutting inserts geometries did not influence chip generation so much, mainly thanks to the fact that both geometries were equipped with a wide groove, forming no barrier to cooling fluid.

To prove the fact that high-pressure cooling can be used at pressure 0.7 MPa, roughing operation was used with a demand of as most as possible material removal rate achievement. The following materials were used in machining:

- austenitic steel 1.4301, hardness 180 HB (ThyssenKrupp, Essen, Germany),
- deep-drawing sheet – low carbon steel C15, hardness 125 HB (ThyssenKrupp, Essen, Germany).

A long chip is generated when machining these materials at standard conditions, causing significant problems mentioned above.

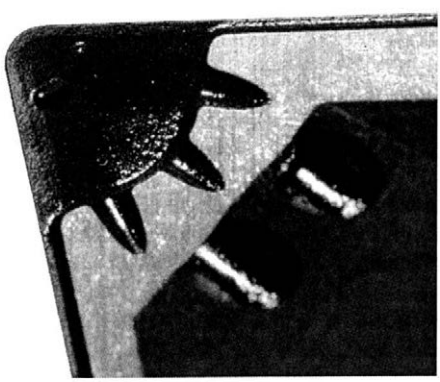

Fig. 7. Detail of SECO ICI for high-pressure cooling with position of cooling channels

Test No. 1

- machine tool Mori Seiki NL2500,
- material 1.4301, austenitic stainless steel,
- tool holder used: C5-PDJNL-35060-15HP (Sandvik Coromant AB, Sandviken, Sweden),
- indexable cutting insert used: DNMG150608-MMC 2025 (Sandvik Coromant AB, Sandviken, Sweden).

Cutting parameters:

- cutting speed v_c = 150 m/min,
- feed per revolution f_n = 0.25 mm,

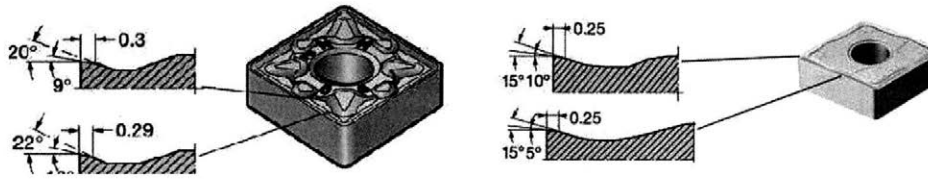

Fig. 8. Geometry of (a) MM – standard geometry (medium feed for stainless steel) and (b) MMC – optimized medium geometry for stainless steel for high pressure coolant

- depth of cut a_p = 2.0 mm,
- cooling fluid pressure p = 0.7 MPa.

Tool life was 8 machined pieces (cutting time 36 min). The original solution tool life was 6 machined pieces (cutting time 27 min) with the same parameters.

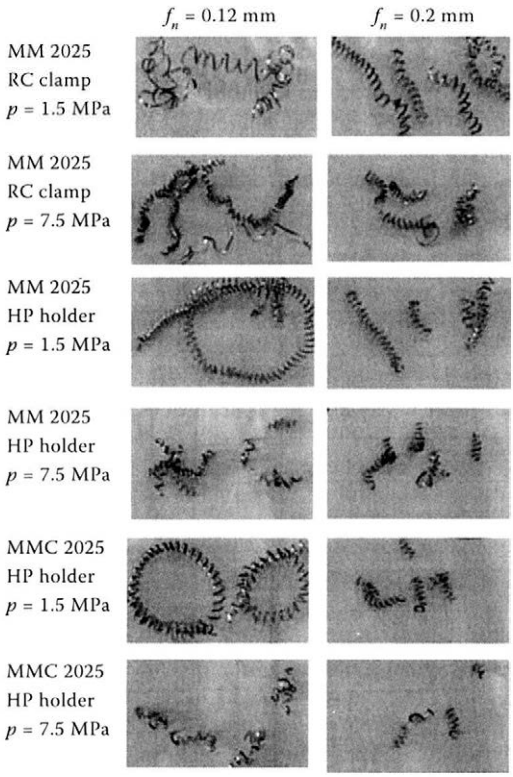

Fig. 9. Chip generated in machining using different geometries, clamping systems and cooling emulsions pressures at two different feeds

MM – standard geometry (medium feed for machining stainless steel); p – cooling pressure; f_n – feed rate; MMC – optimized medium geometry for stainless steel for high pressure coolant; HP – high pressure holder

Test No. 2

- machine tool Famar (Famar S.r.l., Avigliana, Italy),
- material C15 (ThyssenKrupp, Essen, Germany),
- ICI type used: CNMG120408-MMC 2025 (Sandvik Coromant AB, Sandviken, Sweden).

Cutting parameters:

- cutting speed v_c = 250 m/min,
- feed per revolution f_n = 0.4 mm,
- depth of cut a_p = 1.5 mm,
- cooling fluid pressure p = 0.7 MPa.

The tool life was 54 machined pieces (cutting time 77.4 min). The original solution tool life was 20 machined pieces (cutting time 28.6 minutes).

An example of resulting chips from this test is provided in Fig. 10.

High-pressure cooling success conditions:

- emulsion cleanness – filter devices cannot remove contamination with a size higher than 5 μm,
- emulsion concentration – 8–10%,
- proper nozzle diameter for an appropriate emulsion flow rate (pressure, volume) with pressure applicable area 0.7–7.0 MPa,

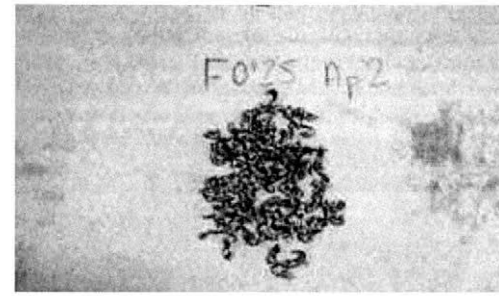

Fig. 10. Chips shape when machining using high-pressure cooling, f_n = 0.25 mm, a_p = 2 mm

Fig. 11. Cutting tool set used in machining tests

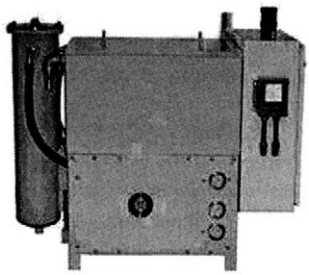

Fig. 12. High-pressure cooling device with filtration (Swiss Blaster SD30)

– multistep cutting tools use with an adjustable base unit only; otherwise, the risk of flow rate loss occurs.

The use of ICI geometry other than that designed for high-pressure cooling (Fig. 11) can result in a lower cutting edge life or proper function loss. Other ICI geometry can be used only in case of proper nozzle diameter combination.

The above-mentioned test was carried out at the CNC lathe (Famar S.r.l., Avigliana, Italy) with standard filtration up to 50 μm; approximately five min after test start, the nozzles got choked up with small chip particles. The machine tool has to be fitted with a filtering system for high-pressure cooling (Fig. 12). Filtering using paper filters or a hydrostatic filter system with high filter capacity should be used to prevent blockage of the holes, along with constant surface finish and longer tool and coolant life ensuring (STEPHENSON, AGAPIOU 2006).

The effect of feed rate on tool life with high-pressure cooling is depicted in Fig. 13. The material used in this test was steel grade 11523 of hardness 180HB, ICI CNMG120408-PMC 4224, cutting speed v_c = 335 m/min, and depth of cut a_p = 2.0 mm. Three different feed per revolution values were used: 0.2, 0.3 and 0.4 mm.

Sensibility of standard and special ICI geometry tool life on cooling fluid pressure

Another test was carried out to find out an influence of cooling fluid pressure on the tool life of standard ICI geometry and special high-pressure ICI geometry. The material used was steel grade 11523 of hardness 180HB (ThyssenKrupp, Essen, Germany).

The geometry of the cutting insert was CNMG120408-PMC and PM 4225. Cutting parameters: cutting speed v_c = 300 m/min, depth of cut a_p = 2.0 mm and feed per revolution f_n = 0.2 mm.

The tool life criterion was the wear area size of flank VB 0.2 mm. The result is shown in Fig. 14.

CONCLUSION

The first conclusion is that high-pressure cooling is not working properly with pressure value 0.7 MPa when machining the material with a continuous chip (deep-drawing sheet metal). It is no problem to obtain an elemental chip when machining materials giving natural broken chip (Test No. 1). Although the elemental chip (or favourably formed) was not obtained in both tests, high-pressure cooling proved a positive effect on cutting edge life.

When observing chip generation with different feed rates, we found useful using a lower feed rate in case of HPC geometry of indexable cutting insert. Machining with feed per revolution 0.2 mm produced a well-formed chip in the whole range of

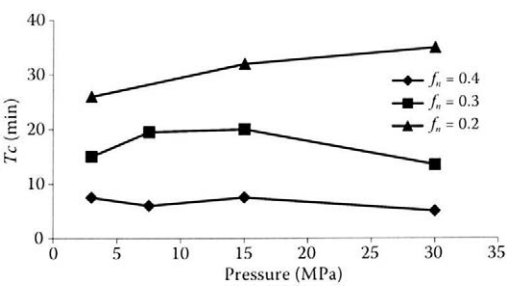

Fig. 13. Effect of feed rate at various cooling fluid pressures on tool life

Tc – tool life, *fn* – feed rate per revolution

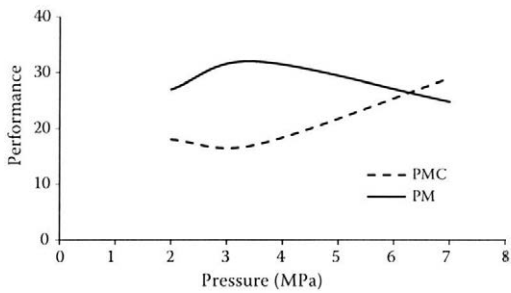

Fig. 14. Effect of cooling fluid pressure on standard (PM) and special high-pressure (PMC) ICI geometry tool life

cooling pressure used and tool wear occurred on the flank only.

At higher feed rates per revolution 0.3 and 0.4 mm, the chip was elemental, but the feed stressed (loaded) the cutting edge much more, resulting in groove wear on the rake.

After that, we can say it is better to use standard geometry in case of low cooling pressures device available, while optimised geometry is suitable only at high cooling pressure values (from 7.0 MPa).

References

Byers J.P., 2006. Metalworking Fluids. 2nd Ed. Boca Raton, CRC Press.

Korenko M., Kaplík P., 2011 Improvement of process performance and efficiency in a production organisation using a Six Sigma method. Acta Technologica Agriculturae. *14*: 105–109.

Korenko M., Kaplík P., Bulgakov V., 2010 Implementation of 5 S approach in the manufacturing organization. In: Naukovij visnik Nacionalnogo universitetu bioresursiv i prirodokoristuvanja Ukrajiny. Kijiv, Nacionaľnyj Univesitet bioresurstv prirodokoritsuvanja Ukrajiny: 59–64.

Kročko V., Žitňanksý J., Drlička R., Polák P., Korenko M., 2012. Environmental impact of cutting fluids to the quality of surface finish in turning. In: Proceedings from MendelTech, March 29–April 4, 2012. Brno, Mendel University in Brno.

Stephenson D.A., Agapiou J.S., 2006. Metal Cutting Theory and Practice. Boca Raton, CRC Press.

Žitňanský J., Žarnovský J., Kročko V., Mikuš R., 2012. The monitoring of machining inherent. In: Naučni trudove. Ruse, Bulgaria, Angel Kanchev University of Ruse: *51*: 196–200.

Received for publication April 16, 2013
Accepted after corrections October 10, 2013

Corresponding author:

Ing. Róbert Drlička, PhD., Slovak University of Agriculture in Nitra, Faculty of Engineering, Department of Quality and Engineering Technologies, Tr. A. Hlinku 2, 949 76 Nitra, Slovak Republic
phone: +421 37 641 4101, fax: +421 37 7417003, e-mail: robert.drlicka@uniag.sk

Design of active stability control system of agricultural off-road vehicles

J. Rédl, V. Váliková, J. Antl

Department of Machine Design, Faculty of Engineering, Slovak University of Agriculture in Nitra, Nitra, Slovak Republic

Abstract

Rédl J., Váliková V., Antl J., 2014. **Design of active stability control system of agricultural off-road vehicles**. Res. Agr. Eng., *60* (Special Issue): S77–S84.

Part of active stability control system design of an agricultural technological vehicle designated for working in mountain and foothill areas is described. The principle of active control of angular velocities of the centre of gravity has been used. During the manoeuvre, active tipping axes are identified by orientation of the weight vector. From experimental tests of a machine MT8-222 based on the Standard STN 47 0170, the real records of angular velocities were obtained. Tests were executed on the slope with an average slope of 32 degrees. From computation critical angular velocities were gained, by which the machine could get into the position of labile stability during the manoeuvre. The regulator was simulated in Matlab®, which controlled the actual value of angular velocity compared with the critical one. In case the boundary zone of critical angular velocity was reached, the regulator sends a signal to the fuel control system and then vehicle speed decreased. During experimental tests, the vehicle did not turn over. Therefore, the angular velocity was simulated by a generated function so that the functionality of the designed regulator was verified.

Keywords: vehicle dynamics; mathematical modelling; simulation

The influence of dynamic effects of the ride of an agricultural mechanism on a sloping terrain is the main cause of its rollover. Following the rollover of the machine, leakage of technical fluids, damage of the machine as well as injuries of the driver, frequently fatal, can occur. This is documented by records of the National Labour Inspectorate of the Slovak Republic, which registers 12,874 occupational injuries in agriculture from 2000, from which 66 cases were caused by agricultural mechanisms. Up to 13 accidents were caused by vehicle overturns. Safety at work and operational safety of agricultural mechanisms are monitored by the European Agency for Safety and Health at Work. The agency states that in the United Kingdom transport with agricultural vehicles was the main reason of fatal injuries of workers in agriculture during the years 1999 and 2009. The cases as being struck by a moving vehicle with a 25% share or trapped by something collapsing and overturning with a 7% share of all fatalities are registered (European Agency for Safety and Health at Work 2011). Because of this, the main priority of producers of agricultural machines nowadays is an implementation of intelligent stability control systems, mainly of those which work on a sloping terrain of more than 15 degrees.

A remarkable contribution in the research of stability of agricultural machines operation was achieved by Grečenko (1983, 1986) who inter alia presents that dynamic stability is part of the slope stability of agricultural vehicles. A significant con-

tribution in the research of static and dynamic stability of agricultural off-road vehicles was presented by Šesták et al. (1987), who dealt with the static stability and slope stability of machines working on the sloping terrain. Fundamental results of the dynamic stability research were published in the works of Šesták et al. (1989, 1993). The methodology of determining the slope stability of agricultural vehicles in Slovakia was presented by Šesták et al. (2000). Also, Spencer and Gilfillan (1976), Chisholm (1979a,b), and Swanghart (1987) markedly contributed with their works to the problem of vehicle dynamic stability and to the research of the dynamics of vehicle rollover on the slope. With the arrival of modern information technology begins an era of more intensive research and modification of existing methods and the specification of some terramechanics theories. Pacejka (2005) and Genta (2006) also contributed with notable works. The phase of increasing the operational safety of agricultural vehicles begins with implementation of intelligent systems into vehicle control systems, with connection to gyroscopic sensors and accelerometers. The utilization and suitability of use of accelerometers in vehicle dynamics is described by MacDonald (1990). Contemporary development is oriented mainly towards modelling and dynamic simulations in various CAD/CAM programs, which allow motion simulations of vehicles with more degrees of freedom. Input forcing functions appear as an appropriate supplement. For simulation of dynamics of the vehicle Fiat Arborio et al. (2000) use the stability analysis in Matlab and Adams Car. Strassberger and Guldner (2004) describe the "Active Stabilizer Bar System" developed by BMW and called dynamic drive. Dynamic drive significantly reduces roll angle during cornering. Zolotas et al. (2006) discussed various issues related to creating models for controllers design, which can be applied to complex dynamic systems. The prediction of vehicle dynamics on soft soil in the Adams system is published also by Fassbender et al. (2007). A complex system of active stability control ADAS (Advanced Driver Assistance Systems) is described by McNair (2007), where the system directly communicates via satellite connection. Pro/Engineer is used for vehicle dynamics simulation by Bradley et al. (2009). Mikleš et al. (2011) dealt with constructional parameters of forest machines, which directly influence the centre of gravity of the machine, and with the determination of static and dynamic stability of forest machines. At modern machines there are used modern active technologies such as Electronic stability control (ESC). ESC is safety feature that detects and prevents (or recovers from) skids. It can help keep the driver from losing control of the car in a panic swerve or when driving on slippery roads (Gold 2013). Mitsubishi Motors Corporation (2013) uses Active Stability Control (ASC) which helps drivers maintain in adverse weather conditions and during emergency manoeuvres. In BMW vehicles is Dynamic Stability Control (DSC) used. DSC adds safety to facilitating vehicle control even in adverse driving conditions or on tough surfaces. It ensures the highest possible levels of stability when driving and it maximizes traction of all wheels when setting off or accelerating (BMW 2013).

MATERIAL AND METHODS

Spatial identification of vehicle. The mathematical model of the vehicle was created with six degrees of freedom, whereby the mass of the whole machine is represented by a single point, namely

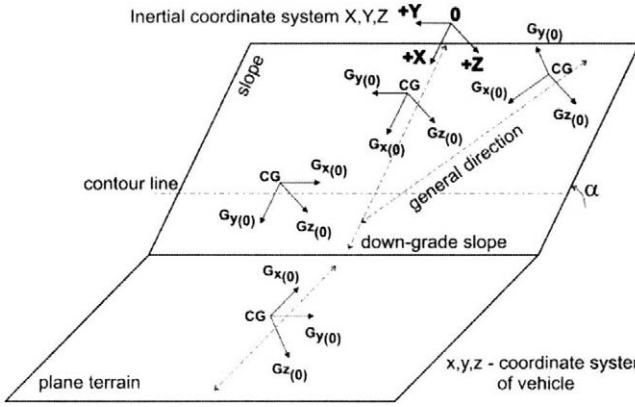

Fig. 1. Spatial identification of the vehicle

α – angle of slope; CG – centre of gravity; Gx,Gy,Gz – components of weight vector

the centre of gravity. We followed the Standard SAE J670_200801 (2008) in terms of the terminology of vehicle dynamics. In Fig. 1, there is depicted a model of the slope with a defined inertial coordinate system (X, Y, Z). The vehicle and its moving on the slope is represented by the motion of the centre of gravity, in which the coordinate system of the vehicle (x, y, z) is oriented. Particular orientations of the weight vector as well as its components are defined according to Fig. 1.

In terms of spatial identification of the vehicle and transformations in the inertial system and in the coordinate system of the vehicle, there were chosen Euler's parameters. A symbolic matrix notation is:

$$[\Lambda'] = \frac{1}{2}[\Omega] \times [\Lambda] \quad (1)$$

where :

$[\Lambda']$ – matrix of parameters derivation

$[\Omega]$ – matrix of angular velocities

$[\Lambda]$ – matrix of parameters

By solution of this system of differential equations, we obtain direction cosines of the transformation matrix between vectors determined in the coordinate system fixed to the vehicle and inertial space. These are:

$$\begin{aligned} &a_{11} = \lambda_0^2 + \lambda_1^2 - \lambda_2^2 - \lambda_3^2, a_{12} = 2(\lambda_1 \times \lambda_2 + \lambda_0 \times \lambda_3) \\ &a_{13} = 2(\lambda_1 \times \lambda_3 - \lambda_0 \times \lambda_2), a_{21} = 2(\lambda_1 \times \lambda_2 - \lambda_0 \times \lambda_3) \\ &a_{22} = \lambda_0^2 + \lambda_2^2 - \lambda_3^2 - \lambda_1^2, a_{23} = 2(\lambda_2 \times \lambda_3 + \lambda_0 \times \lambda_1) \\ &a_{31} = 2(\lambda_3 \times \lambda_1 + \lambda_0 \times \lambda_2), a_{32} = 2(\lambda_2 \times \lambda_3 - \lambda_0 \times \lambda_1) \\ &a_{33} = \lambda_0^2 + \lambda_3^2 - \lambda_1^2 - \lambda_2^2 \end{aligned} \quad (2)$$

From parameters (Eq. 2), we obtain the transformation matrix as follows:

$$[M_T] = \prod_{i=1,2,3,\ldots}^{n} \begin{bmatrix} a_{11} & a_{12} & a_{13} \\ a_{21} & a_{22} & a_{23} \\ a_{31} & a_{32} & a_{33} \end{bmatrix}^{-1} \quad (3)$$

Components of the angular velocity vector of the centre of gravity in the inertial system are determined as follows:

$$[\Omega_{Ts}] = [M_T] \times [\Omega_T] \quad (4)$$

where:

$[\Omega_{Ts}]$ – matrix of angular velocities of the centre of with respect to the inertial coordinate system,

$[\Omega_T]$ – matrix of angular velocities of the centre of gravity with respect to the coordinate system of the vehicle

The dynamic analysis of automotive vehicle stability involves also determining the components of the vehicle weight in the initial position and also during the ride.

Components of the vehicle weight in the initial position (vehicle does not move) are determined as follows:

$$[G_0] = [T_x] \times [T_y] \times [T_z] \quad (5)$$

where:

$[G_0]$ – matrix of vehicle weights in the initial position on the slope,

$[T_x]$, $[T_y]$, $[T_z]$ – matrices of rotations with respect to the x, y, z axes

$[G]$ – matrix expressing the total weight of the machine at rest on a flat ground

$$[T_x] = \begin{bmatrix} 1 & 0 & 0 \\ 0 & \cos\alpha & \sin\alpha \\ 0 & -\sin\alpha & \cos\alpha \end{bmatrix}$$

$$\begin{bmatrix} G_{X(0)} \\ G_{Y(0)} \\ G_{Z(0)} \end{bmatrix} = \begin{bmatrix} \cos\beta & 0 & -\sin\beta \\ 0 & 1 & 0 \\ \sin\beta & 0 & \cos\beta \end{bmatrix} \times \begin{bmatrix} \cos\gamma & \sin\gamma & 0 \\ -\sin\gamma & \cos\gamma & 0 \\ 0 & 0 & 1 \end{bmatrix} \times \begin{bmatrix} 0 \\ 0 \\ G \end{bmatrix} \quad (6)$$

The following transformation is used for computing the weight components during the ride:

$$[G_i] = [M_{T(i)}] \times [G_0] \quad (7)$$

where: $[G_i] = \begin{bmatrix} G_{x(i)} \\ G_{y(i)} \\ G_{z(i)} \end{bmatrix}$ – matrix of the components of vehicle weights during the ride in the i-th instant of time

Stability criterion. In the process of dynamic stability determination, it is important to identify tipping axes, which are dependent on the construction of the given machine (rigid vehicle, vehicle divided by axial or vertical pin).

The vehicle is in an unstable position when the value of kinetic energy determined with respect to the chosen tipping axis is greater than the value of potencial energy spent on the centre of gravity displacement into a limiting static position. Stability vanishes at the moment when the vehicle begins to turn over about some of the tipping axes. The loss of control occurs when the vehicle does not conform to driver's interventions. Vehicle control is fully influenced by the properties of the base and radial force or the vertical load of the wheels. In a real description of the dynamic stability criterion, we followed the work of Šešták et al. (1993), where determination of the dynamic stability criterion, obtained from vehicle operation, involves changes in the direction of the weight vector with respect

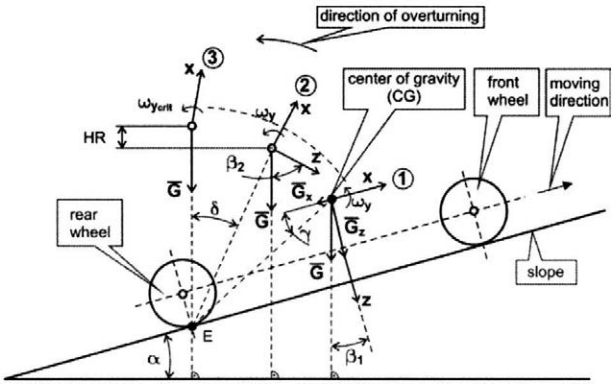

Fig. 2. Overturning dynamics
ω_y – angular velocity; $\omega_{y\text{-}crit}$ –critical angular velocity; HR – vertical difference; α – angle of slope; β, γ, δ – instantaneous angles of rotations of the automotive vehicle; E-point – rear tipping axis in the plane; $\bar{G}$ – weight vector; $\bar{G}_z$, $\bar{G}_y$ – components of weight vector; x, z – coordinates of the vehicle

to the determining tipping axis and inertial effects. Weight components of the vehicle in the initial position on the slope can be defined according to Fig. 2. The real phase of overturn begins with the angular rotation of the front (rear) part of the vehicle, with respect to the rear (front) part, about the internal tipping axis. Tipping axes are represented by the joining lines of points, which are the contact points of the tyre with the base. In Fig. 2, the rear tipping axis in the plane is represented by the point *E*. In the mathematical description of stability criterions, there are considered external tipping axes because the loss of contact of the only wheel with the base is not the condition of total stability loss of the machine. The real description of stability criterions, obtained from the operation of the automotive vehicle, then involves changes in the direction of the weight vector and inertial effects. According to instantaneous angles of rotations of the automotive vehicle, components of the weight vector are obtained by transforming the weight vector components from the initial start position, as introduced in Eq. (7). Relations describing the stability with respect to the rear tipping axis are for the known weight vector *G* determined according to Fig. 2. The value of the resultant of the vehicle weight in the plane *TXZ* of the coordinate system fixed to the vehicle is:

$$G = \sqrt{G_X^2 + G_Z^2} \tag{8}$$

The instantaneous direction of the resultant, oriented from the *Z* axis of the coordinate system fixed to the vehicle, will be:

$$SH = \frac{\frac{\pi}{2} - \arctan\frac{CG_z}{X_r}}{\beta_1} \tag{9}$$

Then, we can define a conventionally used stability coefficient with the relation:

$$\beta_1 = \arctan\frac{G_X}{G_Z} \tag{10}$$

where:
CG_z, X_r – dimensions found on the machine

If $SH = 1$, the machine is at the limit of static stability; if $SH < 1$, the total loss of stability occurs. In this procedure, the coefficient *SH* then informs the researcher about the backup of real stability in regard to the limit static value in each instant of time of realisation. Stability criterions are further derived in terms of Fig. 2. The radius of rotation of the centre of gravity towards the point *E* is determined as follows:

$$\overline{ECG} = \sqrt{CG_z^2 + X_r^2} \tag{11}$$

By the influence of dynamic effects which turn the machine about the tipping axis represented by the point *E*, the position of the centre of gravity is changed from position 1 to position 2 by vertical difference *HR*, which can be expressed as:

$$HR = \overline{ECG}\left(\cos\delta - \cos\left(\frac{\pi}{2} - \beta_1 - \gamma\right)\right) \tag{12}$$

Seeing that the kinetic energy of the vehicle which performs general plane motion is given by the sum of kinetic energy concentrated in the centre of gravity and kinetic energy of rotational motion about the centre of gravity, and the rotational motion is related to the space which is moved with the centre of gravity, we can determine the kinetic energy in point 1. The required angular velocity is determined from the experiment, and it must hold that $\omega_y > 0$. Kinetic energy is then expressed by the relation:

$$KH = \frac{1}{2}J_y \times \omega_y + \frac{1}{2}\omega_y^2 \times \overline{ECG}^2 \times m \tag{13}$$

If we set $g = 10$ m/s^2, then after modification we obtain:

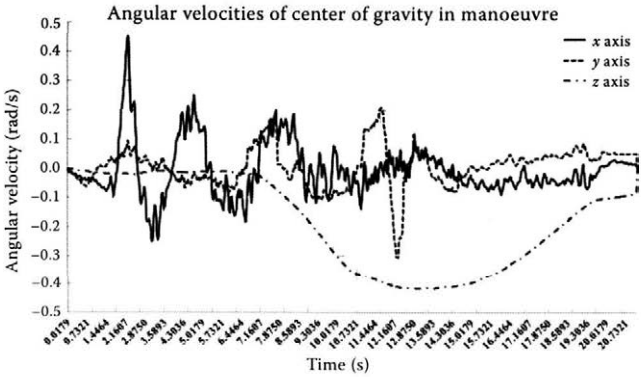

Fig. 3. Angular velocities of the centre of gravity during the manoeuvre

$$KH = \frac{1}{2}\omega_y^2 \times \left(J_y + 0.1G \times \overline{ECG}^2\right) \quad (14)$$

It is obvious that this kinetic energy is consumed during the process of the centre of gravity turning from position 1 to position 2 and this leads to $KH = HR \times G$.

In case the vehicle deflects from the slope, dynamic stability criterion DH can be set as follows. According to Fig. 2, we determine angle δ:

$$\delta_R = \arccos\left(\frac{KH}{G \times \overline{ECG}} + \cos\left(\frac{\pi}{2} - \beta_1 - \gamma_R\right)\right) \quad (15)$$

Next, we determine angle β_2:

$$\beta_2 = \frac{\pi}{2} - \delta - \gamma \quad (16)$$

After that, dynamic stability coefficient DH yields to:

$$DH = \frac{\frac{\pi}{2} - \gamma}{\beta_2} \quad (17)$$

If the position of the centre of gravity CG is in the limiting static position, it means that the straight line $\overline{ECG}$ is perpendicular to the horizontal plane of the slope and the point CG lies above the tipping axis (represented by the point E), then the point CG earns the potential energy PH, which is:

$$PH = m \times g \times \Delta h \quad (18)$$

where: $\Delta h = \overline{ECG} - \overline{ECG} \times \sin(\beta_1 + \gamma)$

and after modification:

$$PH = G \times \overline{ECG}\,(1 - \sin(\beta_1 + \gamma)) \quad (19)$$

Dynamic stability is violated if the angular velocity ω_y is so high that the kinetic energy causes the satisfaction of the condition $KH \geq PH$. From the introduced equations we can discover the limiting angular velocity ω_{HRA} at which the mentioned phenomenon could occur. Critical angular velocity is in the form:

$$\omega_{y_{crit}} = \sqrt{\frac{2G \times \overline{ECG} \times (1 - \sin(\beta_1 + \gamma))}{J_y + 0.1G \times \overline{ECG}^2}} \quad (20)$$

The condition of stability violation is $\omega_y \geq \omega_{y_{crit}}$. The mathematical formula for the other tipping axes is analogical.

Conditions of experiment. The listed angular velocities (Fig. 3) were obtained from the real experimental measurement. Driving manoeuvre was

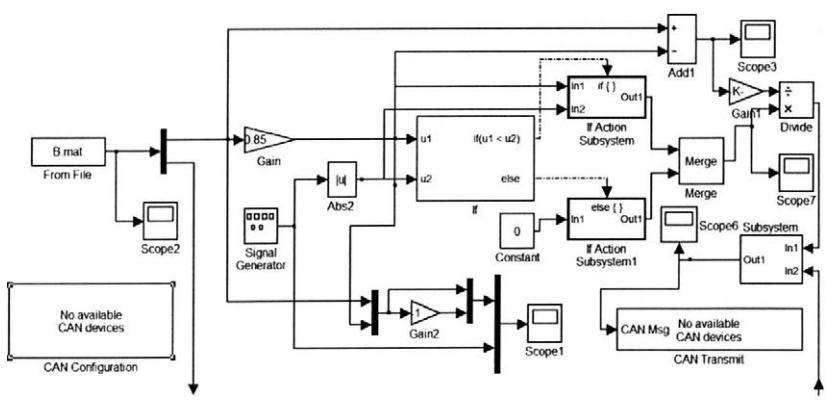

Fig. 4. Scheme of stability control zone

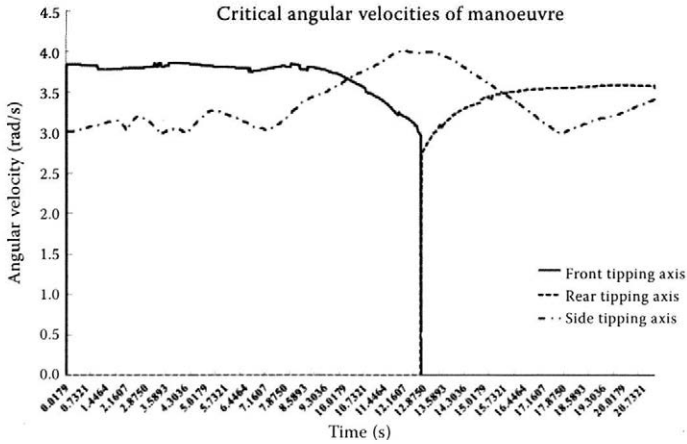

Fig. 5. Critical angular velocities during the manoeuvre

the ride on the slope along the down-grade slope with turning to the down-grade slope. The experimental test was performed following the Standard STN 47 0170. Priority was mainly given to the composition and humidity of the terrain on which the test was performed. The botanical composition of the terrain consisted of plants like *Festuca pratensis* Huds. 15%, *Poa pratensis* L. 30%, *Dactylis glomerata* L. 30%, *Arrhenatherum elativ* 5%, *Alopecurus pratensis* L. 5%, clovers 5%, and other plants 10%. The humidity of the terrain was determined according to the methodology of Jobbágy and Simoník (2006). The share of humidity was lower than 50%, which means that the surface of the terrain was specified as dry.

RESULTS AND DISCUSSION

In Fig. 4, there is depicted the scheme of stability zone control of the agricultural off-road vehicle. It is possible to describe the control principle as a verification of the measured angular velocity from accelerometers or from the gyroscopic sensor placed in the centre of gravity. Verification is in comparing with the critical angular velocity (Fig. 5) at which an unstable position occurs. The output of control is the limitation of engine power and also the velocity if the measured angular velocity comes near to the critical one. The zone of power control is determined in this way, as it is seen in Fig. 6.

This verification is involved in the part of the block scheme *If, If Action Subsystems*, where the real angular velocity is compared with the critical one. If the real angular velocity reaches 60% of the critical angular velocity, the regulation starts to work, and if it is not reached, then the system is not intervened. In order that the operating personnel still has the control of the vehicle, 15% of the engine power is taken away, which stabilizes the vehicle that in a minor extent reacts on the steep-

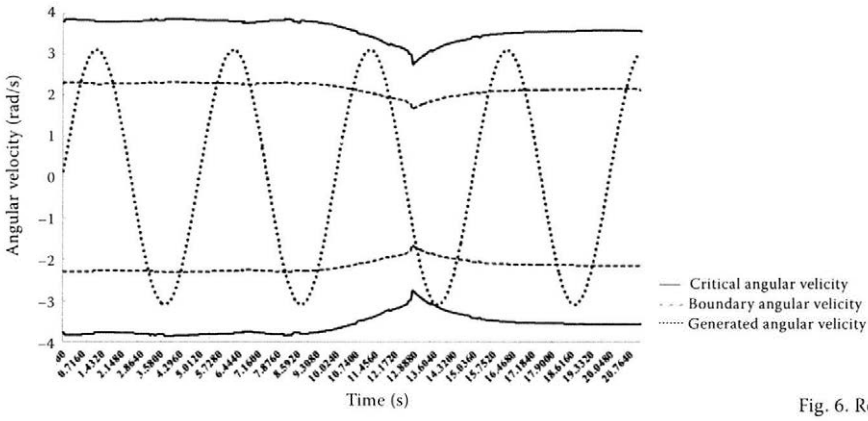

Fig. 6. Regulation of system

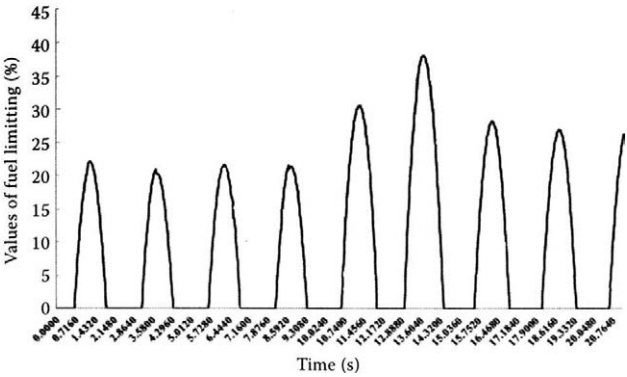

Fig. 7. Response signal of regulator

ness of the amplitude of excitement from the base. However, it is necessary to realise the control for two tipping axes of the machine so that the general stability is inherent. Connecting and validation is in charge of the block *Subsystem*, in which the signals of the control for particular axes of tilt are connected. At present, interconnection and limitation of engine power is possible to be solved via a control unit, which communicates through a *CAN* bus. In older mechanical systems, control would require an independent device, which would restrict the injection of the fuel into the engine. AP regulator is used for control. This type of regulator was chosen because of the absence of knowledge of the dynamical and operating parameters of the specific controlled machine.

Seeing that during the experimental tests the vehicle did not turn over, we simulated the angular velocity by the generated function $\sin(\omega \times t + j)$ to verify the functionality of designed regulator. The response is depicted in Fig. 7.

CONCLUSION

In this contribution, the part of the active stability control system of the agricultural off-road vehicle was presented. It is designated for operation in mountain and foothill areas, where the risk of overturn is very high. This is proven also by analyses of national institutions of occupational safety in the EU. The methodology of acquiring the angular velocities is based on the Standard STN 47 0170. The testing manoeuvres were realised on the machine MT8-222 Synona according to the performed agro-technical operation for the given machine. In the specified way, we obtained the critical angular velocities from experimental measurements. We projected a control system in Matlab, the functionality of which was verified by the generated function as no vehicle rollover occurred during the experiment. By verification we obtained the control signal, the intensity of which is expressed in percentage of the taken engine power of the machine. It is possible to connect the designed system with the control units of the fuel control system (e.g. EDC for Common Rail) through the CAN port. Proposed solution developed at our department can be used also for older machines, which do not include modern active stability control systems.

References

Arborio N., Munaretto P., Velardocchia M., Riva N., Suraci E., 2000. Vehicle Dynamics and Stability Analysis with Matlab and Adams Car. Available at http://web.mscsoftware.com/support/library/conf/adams/euro/2000/Fiat_Poli_Vehicle_Dynamics.pdf

Bradley J., Tansley G.D., Dominy J., 2009. A modeling strategy for vehicle dynamics using Pro/ENGINEER. International Sports Engineering Association, *11*: 119–129.

BMW, 2013. Dynamic Stability Control (DSC). Available at http://www.bmw.com/com/en/insights/technology/technology_guide/articles/mm_dynamic_stability_control.html (accessed October 16, 2013).

Chisholm C.J., 1979a. A Mathematical model of tractor overturning and impact behaviour. Journal of Agricultural Engineering Research, *24*: 375–394.

Chisholm C.J., 1979b. Experimental validation of a tractor overturning simulation. Journal of Agricultural Engineering Research, *24*: 395–415.

European Agency for Safety and Health at Work, 2011. Maintance in Agriculture – A Safety and Health Guide. Luxembourg, Publication Office of the European Union: 57.

Fassbender F.R., Fervers C.W., Harnisch C., 2007. Approaches to predict the vehicle dynamics on soft soil. Vehicle System Dynamics Supplement, *27*: 173–188.

GENTA G., 2006. Motor Vehicle Dynamics – Modeling and Simulation. Singapore, World Scientific Publishing Co. Pte. Ltd.: 537.

GOLD A., 2013. Electronic stability control (ESC). Available at http://cars.about.com/od/thingsyouneedtoknow/a/ESC.htm (accessed October 16, 2013).

GREČENKO A., 1983. Dynamická stabilita jako součást svahové dostupnosti zemědelských strojů. [Dynamic stability as part of side slope stability of agricultural machinery.] Zemědelská technika, *29*: 643–658.

GREČENKO A., 1986. Metoda určování svahové dostupnosti zemědelských vozidel. [Method of determination of side slope stability of agricultural vehicles.] Zemědelská technika, *32*: 577–598.

JOBBÁGY J., SIMONÍK J., 2006. Porovnanie dvoch metód stanovenia vlhkosti pôdy. [Comparison of two methods of soil moisture determination.] Acta Horticulturae et Regiotecturae, *8*: 213–217.

MACDONALD G.A., 1990. A review of low cost accelerometers for vehicle dynamics. Sensors and Actuators A: Physical, *21*: 303–307.

MCNAIR K.M., 2007. MEMS sensor fusion for vehicle dynamic control. In: Vehicle Dynamic Expo 2007, May 8–10, 2007, Stuttgart: 1–18.

MIKLEŠ M., TKÁČ Z., JABLONICKÝ J., HUJO Ľ., KRILEK J., 2011. Lesnícke stroje a zariadenia. [Forestry Machines and Mechanisms.] Zvolen, Technická univerzita vo Zvolene: 294.

Mitsubishi Motors Corporation, 2013. ASC (Active Stability Control). Available at http://www.mitsubishi-motors.com/en/spirit/technology/library/asc.html (accessed October 16, 2013).

PACEJKA H.B., 2005. Tire and Vehicle Dynamics, 2nd Ed. SAE International: 642.

SAE J670_200801. Vehicle Dynamics Terminology. Warrendale, SAE International.

SCHWANGHART H., 1987. Kipp-umsturzverhalten eines schleppers. Landtechnik, *11*: 489–490.

SPENCER H.B., GILFILLAN G., 1976. An Approach to the assessment of tractor stability on rough sloping ground. Journal of Agricultural Engineering Research, *21*: 169–176.

STRASSBERGER M., GULDNER J., 2004. BMW's dynamic drive: an active stabilizer bar system. IEEE Control Systems Magazine, *24*: 28–29, 107.

STN 47 0170, 2001. Poľnohospodárske stroje a traktory. Stanovenie svahovej dostupnosti. Bezpečnosť práce. [Agricultural tractors and machinery. Gradeability test methods. Safety of work.]

ŠESTÁK J., SKLENKA P., ŠKULAVÍK J., MARKOVIČ M., 1987. Statická stabilita a svahová dostupnosť horskej kosačky MT8-046-SP2-212 a samojazdného zberacieho voza MT6-063, ASN-055. [Static stability and side slope stability of mountain mower-machine MT8-046-SP2-212 and of self-driven collecting vehicle MT6-063, ASN-05.] Zemědělská technika, *33*: 105–122.

ŠESTÁK J., SKLENKA P., ŠKULAVÍK J., MARKOVIČ M., 1989. Dynamická stabilita univerzálnej horskej hnacej jednotky MT8-046. [Dynamic stability of universal mountain driving unit MT8-046.] Zemědelská technika, *35*: 579–596.

ŠESTÁK J., SKLENKA P., ŠKULAVÍK L., 1993. Matematické modely terénnych vozidiel určené na popis ich správania pri práci na svahu. [Mathematical models of terrain vehicles determined to describe their behaviour while working on the slope.] Nitra, SUA in Nitra: 91.

ŠESTÁK J., RÉDL J., MARKOVIČ M., 2000. Stanovenie svahovej dostupnosti poľnohospodárskych vozidiel. [Assessment of side slope stability of agricultural vehicles.] Research of Agricultural Engineering, *46*: 53–58.

ZOLOTAS A.C., PEARSON J.T., GOODALL R.M., 2006. Modelling requirements for the design of active stability control strategies for a high speed bogie. Multibody System Dynamics, *15*: 51–66.

Received for publication April 17, 2013
Accepted after corrections December 3, 2013

Corresponding author:

Doc. Ing. JOZEF RÉDL, PhD., Slovak University of Agriculture in Nitra, Faculty of Engineering, Department of Machine Design, Tr. A. Hlinku 2, 949 76 Nitra, Slovak Republic
phone: +421 37 641 5669, e-mail: redl@is.uniag.sk

The effect of evaporative cooling on climatic parameters in a stable for sows

Ľ. Botto[1], J. Lendelová[2], A. Strmeňová[1], T. Reichstädterová[2]

[1]*Institute for Breeding Systems and Animal Welfare, Animal Production Research Centre Nitra, Nitra, Slovak Republic*
[2]*Faculty of Engineering, Slovak University of Agriculture in Nitra, Nitra, Slovak Republic*

Abstract

Botto Ľ., Lendelová J., Strmeňová A., Reichstädterová T., 2014. **The effect of evaporative cooling on climatic parameters in a stable for sows**. Res. Agr. Eng., *60* (Special Issue): S85–S91.

The aim of this study was to find out the effect of indirect evaporative cooling on microclimatic parameters in a stable for sows. A high-pressure system was used for cooling, the nozzles sprayed water into the outside air before its entering into the building. Temperature-humidity index during cooling was higher by 0.9 than in the section without cooling ($P < 0.001$). Due to low indoor air flow velocity (below 0.18 m/s), a change in apparent temperature by the Comprehensive Climate Index (CCI) was only 1.94°C. It would be possible to provide markedly better cooling effectiveness by increasing the air velocity up to 2 m/s, which may improve the CCI by 19.8% and thus to achieve better environmental conditions for housed sows. The efficiency of evaluated evaporative cooling system was moderate because the nozzles were placed outdoors and only part of humidified and cooled air was drawn into the building through inlet openings, and also because the indoor air-flow velocity was low.

Keywords: cooling system; water evaporation; summer period; pigs

Current modern types of pigs are demanding as to conditions of stable environment. Pigs are relatively sensitive to high environmental temperatures when compared to other species of farm animals. A lot of research has been done on the factors affecting heat production in pigs (Brown-Brandl et al. 2001). Air temperature as cardinal environmental factor is influenced by relative humidity and air flow velocity. Optimum parameters of temperatures, relative humidity and air velocity for pigs in Slovakia were presented by Botto et al. (1995). Recommended optimum of the air temperature for pregnant sows is 12–20°C at relative humidity 50–75%. Max. air flow velocity at optimum temperature is 0.3 m/s and at temperature higher than optimum it is 2.0 m/s.

Heat waves during summer cause large losses in productivity in animal husbandry. Sows are exposed to heat stress when temperature exceeds the upper critical temperature of the thermoneutral zone of the sow (Black et al. 1993). Thermoneutral zone is the range of environmental temperatures within which the metabolic rate is minimum and independent of temperature. The temperatures that bound this zone are known as upper and lower critical temperatures (Webster 1991). Above the upper critical temperature of this zone the animal will reduce both production and reproduction to control body temperature. Sows begin to feel the negative effects of heat stress at a temperature of 20°C, and temperatures of 26°C and higher are

Supported by the European Regional Development Fund, Operational Programme Research and Development, Project CEGEZ No. 26220120042 and by the Scientific Grant Agency VEGA of the Ministry of Education of the Slovak Republic and the Slovak Academy of Sciences, Grant No. 1/0609/12.

considered a critical for pigs (CHRISTIANSON et al. 1982; QUINIOU et al. 2001). Heat stress is one of the major concerns in pork production during summer period because pigs do not have functional sweat glands like other livestock species to assist them in efficiently removing body heat (SOUZA 2009). Above the upper limit of the thermal neutral, feed consumption is reduced to limit the metabolic heat production (LE DIVIDICH et al. 1998). Heat stress in pigs impairs the animals' welfare and environment (HUYNH 2005; MIHINA et al. 2011) and economics of pig industry (ST-PIERRE et al. 2003). The pigs would rid themselves of excess body heat by panting or surface wetting in water or their own excreta under the high ambient temperature and humidity (AARNINK et al. 1996; HUYNH et al. 2006). High ambient temperatures cause heat stress and contribute to an increase in sow nonproductive days (ST-PIERRE et al. 2003). The more heat an animal produces internally by its metabolism, the smaller is its capacity for tolerating external heat (BROUČEK et al. 2009; ZHANG et al. 2011). Environmental hot and humid weather conditions have a great impact on the performance, genetic components and hygienic conditions in pigs (DONG et al. 2001; ZUMBACH et al. 2008; POGRAN et al. 2011). Exposing of sows to heat stress before mating and during early pregnancy may cause reduction in the conception rate and increase in the embryo mortality (RENAUDEAU et al. 2003), therefore negatively affecting subsequent reproductive performance (SURIYASOMBOON et al. 2006). Response to heat stress begins with increased respiration rate, continues with decreased feed intake, and leads to increased rectal temperature (HUYNH 2005). Decreased feed intake and increased rectal temperature are good indicators of decreased performance of heat-stressed pigs (HUYNH et al. 2005).

Utilization of enhanced air flow is one possible method of cooling during high ambient temperatures. In this system the sensational effect of temperature perception is applied. It means that at equal ambient temperature but higher air flow the ambient temperature is sensationally decreased. The cooling effect of air movement is typically expressed by effective temperature, the temperature that animals actually feel (XIN, MCFADDEN 1995).

BARBARI and CONTI (2009) found out that the high velocity air stream combined with wet floor was preferred by sows during the hottest period. Floor cooling could increase the lying behaviour and improve the production together with reproductive performance of swine (SILVA et al. 2006).

Evaporative cooling such as water dripping, showering system and evaporative pads are common and effective way in practice (BULL et al. 1997), but often limited to high relative humidity conditions with inducing additional water vapour into the animal occupied zone (LUCAS et al. 2000). Water evaporation cause air-cooling in the building but at the same time, it causes an increase in humidity. This is usually acceptable in regions with hot-dry climates but in wet regions, in order to limit the adverse effects on indoor humidity, special attention must be paid to the accurate control of fogging and ventilation (HAEUSSERMANN et al. 2007).

One way how to eliminate heat stress of sows is indirect evaporative cooling, method that uses outside air humidification before its inlet into the building. Outdoor air cooled by evaporation of cold water from sprayed space under the roof at an angle of 45° to the outdoor environment is led to animals, while improving the quality of the indoor environment. This reduces the air temperature, it does not increase critically the relative humidity and temperature-humidity index (THI) (NOAA 1976; HAHN 1985; MADER et al. 2006; NIENABER, HAHN 2007) and improves the change of apparent temperature by Comprehensive Climate Index (CCI) (MADER et al. 2010). This study aims to test this hypothesis and to find out the effect of indirect evaporative cooling on microclimatic parameters in stable for sows in hot days during summer time.

MATERIAL AND METHODS

The experiment was conducted in relatively hot summer of 2012 (29–34°C) in the stable for mated and pregnant sows. Animals were housed in strawless gestation crates, which were arranged in 13 transverse rows with a total housing capacity of 120 sows. The housing also included 4 pens for boars, which were located in the alley next to the longitudinal peripheral wall oriented to the northwest. Feed was metered into a continuous trough, which also served for watering. Water level was maintained there by valve. Extract cross-ventilation was used in the house. Air was exhausted by 7 fans installed in the south-eastern outdoor wall with the total capacity of 4,000 m^3/h. Ten inlet flap-regulated openings, 2 × 600 × 200 mm each, were situated in the opposite wall of the building. Outside air cooled by sprayed water was drawn into the building, so indirect evaporative cooling process was used.

High-pressure water nozzles (11 units) provided spray. They were installed outside the building on a plastic pipe, located at the northwestern wall, at the end of the eaves, 650 mm above upper edge of the flap. Water jet sprayed out of nozzle by an angle of 45° downward.

During the experiment the air was cooled only in one half of the house (section A) and in the other one not modified air was exhausted (section N). Indirect evaporative cooling system was activated since noon to 6:00 p.m. Measurements were carried out from 1:00 to 6:00 p.m. Air temperature, relative humidity and air velocity were continuously recorded at 12 locations in each section in the zone of animals (500 mm above the floor) and at one place outdoor. Universal device ALMEMO 2290-4 (Ahlborn Mess und Regelungstechnik GmbH, Holzkirchen, Germany) and anemometer Testo 435-2 (Testo AG, Lenzkirch, Germany) were used for recording of measured parameters.

Corresponding temperature-humidity index (THI) was calculated according to the following equation recommended by NOAA (1976):

$$THI = 0.8\ T_a + (RH/100) \times (T_a - 14.3) + 46.4 \quad (1)$$

where:

T_a – ambient air temperature (°C)

RH – relative humidity (%)

THI values were classified as a safe if THI ≤ 74, critical, if 74 < THI < 79, dangerous if 79 ≤ THI < 84 and emergency if THI ≥ 84.

Comprehensive Climate Index (CCI), which takes into account other relevant factors, was calculated according to MADER et al. (2010) equation as follows:

$$CCI = T_a + RH_{cf} + WS_{cf} + RAD_{cf} \quad (2)$$

where:

T_a – ambient air temperature (°C)

RH_{cf} – correction factor of air humidity

WS_{cf} – correction factor of wind speed

RAD_{cf} – correction factor for radiation influence

Computed following equations:

Obtained climate parameters (temperature, relative humidity, air flow, THI and CCI) were statistically processed and compared among the cooled (A), not cooled (N) sections and outdoor environment (E). Basic statistic parameters (mean values and standard deviations) were calculated, data were analysed by One-Way AOV, and significant differences were tested by Tukey HSD All-Pairwise Comparisons by the STATISTIX, version 9.0 (Analytical Software, Tallahassee, USA).

RESULTS AND DISCUSSION

During the evaluated summer period, the outdoor air temperature ranged from 21.5°C to 34.8°C and relative air humidity ranged from 32.2% to 84.2%. Air temperature in the stable for mated and pregnant sows ranged from 23.4°C to 33.3°C and the relative humidity ranged from 35.7% to 76.4%. In the section without activated evaporative cooling the temperatures 32°C and higher were registered, which represented the proportion 21.53% of the whole observation time. Such values did not occur in the section with activated cooling.

When the outside air temperature was 31.54 ± 0.66°C, the indoor temperature in the section with inactive cooling (N) was the highest 32.88 ± 0.71°C, and in the section with active cooling (A) the lowest 29.96 ± 0.77°C (Table 1). Temperature in section A was lower by 2.92°C than in section N and lower by 1.58°C than ambient temperature. In section N, the temperature was higher by 1.34°C than the outdoor temperature. The differences in all cases were on a very highly significant level ($P < 0.001$; Table 2)

Relative air humidity in section A was higher by 18.52% than in section N and in comparison with the outdoor humidity it was higher by 21.85% (Table 1). Relative air humidity in section N was higher only by 2.80% compared with the outdoor air humidity. However, similar to the temperature also in relative air humidity very highly significant differences were recorded in all cases ($P < 0.001$; Table 2).

$$RH_{cf} = e^{[(0.00182 \times RH) + (1.8 \times 10^{-5} \times T_a \times RH)]} \times (0.000054 \times T_a^2 + 0.00192 \times T_a - 0.0246) \times (RH - 30) \quad (3)$$

$$WS_{cf} = \left[\frac{-6.56}{e^{\left(\left(\frac{1}{(2.26 \times WS + 0.23)^{0.45}} \right) \times (2.29 + 1.14 \times 10^{-6} \times WS2.5 - \log_{0.3}(2.26 \times WS + 0.33) - 2) \right)}} \right] - 0.00566 \times WS^2 + 3.33 \quad (4)$$

$$RAD_{cf} = 0.0076 \times RAD - 0.00002 \times RAD \times T_a + 0.00005 \times T_a \times \sqrt{RAD} + 0.1 \times T_a - 2 \quad (5)$$

Table 1. Mean values (± SD) of climate parameters at the period of cooling (n = 576)

Parameter of air	Outdoor environment	Section with non-active cooling	Section with active cooling
Temperature (°C)	31.54 ± 1.20	32.88 ± 0.71	29.96 ± 0.77
Relative humidity (%)	45.85 ± 10.85	48.65 ± 5.10	67.17 ± 3.00
Flow velocity (m/s)	1.226 ± 0.919	0.113 ± 0.066	0.175 ± 0.030
THI (–)	79.42 ± 0.73	81.75 ± 1.27	80.85 ± 1.21
CCI (°C)	41.03 ± 3.22	40.12 ± 0.99	38.18 ± 1.05

THI – temperature-humidity index; CCI – Comprehensive Climate Index; SD – standard deviation; n – number of measurements

The average air flow velocity in animal zone in section N was 0.113 ± 0.066 m/s, and in section A it was 0.175 ± 0.030 m/s (Table 1). The difference between the sections N and A was not significant (Table 2). The average outdoor wind speed (1.226 ± 0.919 m/s, $P < 0.001$) was significantly higher compared to air flow in both sections.

Outdoor temperature-humidity index had the lowest value of 79.42 ± 0.73 (Table 1). In both observed sections it was significantly higher ($P < 0.001$; Table 4), in section N by 2.33 and in section A by 1.43. These average values could be classified as dangerous (79 < THI < 84; NOAA 1976; HAHN 1985; NIENABER, HAHN 2007).

The average outdoor Comprehensive Climate Index was higher than both indoor sections (41.03 ± 3.22°C; Table 1). In section N (without cooling) CCI was 40.12 ± 0.99°C and in section A (with cooling) it was 38.18 ± 1.05°C. The differences in all cases were on a very highly significant level ($P < 0.001$; Table 2.)

According to MYER and BUCKLIN (2001), sows begin to feel the negative effects of heat stress at a temperature of 20°C, and temperatures 26°C and higher are critical for them (CHRISTIANSON et al. 1982; QUINIOU et al. 2001).

All indoor air temperatures exceeded 20°C, the upper value of the optimum. Average indoor relative humidity was in the optimum range recommended by SEEDORF et al. (1998) and HAEUSSERMANN et al. (2007).

The combinations of two cooling systems (water bath and sprinkling) were evaluated by HUYNH et al. (2006). The authors, who decided to test cooling systems in pens with or without an additional outdoor yards, found out that the bath and sprinkling reduced respiration rate of pigs by 4.2 and 5.2 min^{-1}, respectively ($P < 0.01$), and their surface body temperature by 0.3 and 0.4°C, respectively, ($P < 0.05$). Rectal temperature was not influenced by any treatment. An important finding in this study was that pigs in pens without an additional outdoor yard with sprinkling achieved greater weight gain. These pigs had limited space and had a high frequency of huddling. The pigs in pens with sprinkling not only benefited from sprinkling by showering but also by lying on the floor wetted by sprinklers. With 12 sprinkling periods at 30 min intervals, the floor stayed wet almost for the whole period between 10:00 a.m. and 4:00 p.m. In our experiment a wet floor was sporadically detected in windy climate and animals did not feel uncomfortably. A cooling system with sprinkling should avoid introducing surplus water into the air of barns. The main limitations of vapour cooling system is a heavy water use, increase of air humidity and the

Table 2. Differences of climate parameters among outdoor environment (E) and indoor sections (N) and section with active cooling (A) (n = 576)

Parameter of air	Section N–E	Section A–E	Sections N–A
Temperature (°C)	1.34*	–1.58*	2.92*
Relative humidity (%)	2.80*	21.32*	–18.52*
Flow velocity (m/s)	–1.113*	–1.051*	-0.062^{ns}
THI (–)	2.33*	1.43*	0.90*
CCI (°C)	–0.91*	–2.85*	1.94*

*significant at the level of $P < 0.001$; ^{ns}not significant ($P > 0.05$); CCI – Comprehensive Climate Index; n – number of measurements

subsequent problems with slurry dilution if the water is collected in the slurry.

The analysis of period with frequent occurrence of both high temperature and low relative humidity during the heat stress periods is an indication that evaporative cooling systems may be a feasible and cost-effective solution for minimizing the effect caused by such high thermal stressors in pig production. A computer simulation of the psychrometric process predicted that most periods of heat stress can be eliminated by using an evaporative cooling pad system with an efficiency of 80% (Lucas et al. 2000). If we apply the Lucas theory to results of our measurements, it would be possible to decrease the dry bulb indoor temperature by 7.5°C. The described system of indirect evaporative cooling is easier from service and economy view points, but it is not possible to achieve adequate results at cooling without additional construction and technological arrangements.

In pig husbandry was developed a lot of technical solutions with direct and indirect elimination of heat stress of animal with different breeding effect and economy. Some cooling systems involve high investments and some can cause adverse effects like increased humidity. It is known that high relative humidity depresses pig production (Lucas et al. 2000).

Silva et al. (2006) found positive effects of sow cooling by using the floor cooling system. Although the results of this method of cooling are interesting in view of the breeding results, its implementation in existing pig husbandry is difficult.

In experiment carried by Pang et al. (2010) a significant decrease of respiration rate and surface body temperature of sows in individual boxes with water-cooled cover was demonstrable. This construction consisted of a steel frame (in ground floor plane 600 mm × 1,500 mm, height 1,000 mm), galvanized steel water pipes (total length 57 m), an aluminium canopy and the heat insulating layer. Significant differences were found between lying time in cooling and non-cooling boxes.

The indirect evaporation cooling, realized in our climatic conditions, decreased significantly the air indoor temperature, however, from the Comprehensive Climate Index (Mader et al. 2010) analysis follows that the change in apparent temperature was only 1.94°C. Increase of air moving in animal zone may play a big role during critical hot summer days. No suitable change of air speed was found in our study between activated and non-activated state of cooling. In our study the average air velocity in the animal zone during non-activated and activated process of cooling (0.113 and 0.175 m/s) at indoor air temperatures above 26°C was insufficient. Technological equipment and method of ventilation design should allow not only sufficient air exchange but an increased airflow in the zone of the animals as well.

From the analysis of the measured data we found out, by simulated mathematical calculations in the section with activated cooling (A), that if air velocity increased to 1 m/s, the value of CCI would be reduced by 10.2%. Upon reaching the max. permissible air velocity 2.0 m/s in the zone of animals, the CCI reduction would be up to 19.8%. The environmental conditions for housed sows markedly improved in this way.

Bieda et al. (2001) designed another method of cooling. They prepared an experimental prototype of air-earth exchanger tube system, usable in the winter and summer period for modification of indoor air in extreme climate conditions. According to the results of their studies the temperature of piped air was by 11–14°C cooler during hot summer period.

Although our findings were positive only partly when analysing the thermal-humidity mode in treated compartment (marginal decrease of air temperature and THI improvement) the used system of indirect cooling has still some reserves. Vegetation or non-vegetation shielding of space, from which the modified air will be applied into building, would be appropriate at careful building projection. It is possible to use a manual sprinkling of animal body or lying floors, to cool the animals by contacting a wet concrete in extremely hot summer days.

CONCLUSION

The indirect evaporative cooling was tested by analyses of climate parameters in the experimental stable for sows. That system uses a method of spraying water into the hot outdoor air, outside the building, where it is cooled by evaporative effect of water sprayed from the jets under the roof. The air, conditioned by that way, is drawn into the building and improves the quality of the indoor environment. The air temperature and comprehensive climate index decrease but the relative humidity does not increase critically; the temperature-humidity index decreases slightly. The resulting temperature

difference with the application of cooling reached in our experiment cooling of the indoor air about 3°C. The system allows almost instantaneous declension of temperature curve from the risk of animals with a relatively low cost investment. A partial increase of internal relative humidity was within the range of recommended values. During the period with the higher relative humidity of ambient air, the air cooling system is not used. Running fans with higher output provided cooling at that time only by air flow. Due to low indoor air flow velocity (below 0.18 m/s), a change in apparent temperature by Comprehensive Climate Index was only 1.94°C. It would be possible to provide markedly better effectiveness of indirect cooling by increasing the air velocity up to 2 m/s in the zone of animals, which may improve the CCI by 19.8% and thus achieve better conditions for thermal comfort of housed sows. In capital-intensive cooling systems it is possible to achieve a greater impact; however, they cannot be usually installed additionally in full operation on farm. Efficiency of evaluated evaporative cooling system was moderate, because the nozzles were placed outdoors and only part of the humidified and cooled air was drawn into the building through inlet openings, and secondly because the indoor air flow velocity was low.

References

Aarnink A.J.A., van den Berg A.J., Keen A., Hoeksma P., Verstegen M.W.A., 1996. Effect of slatted floor area on ammonia emission and on the excretory and lying behaviour of growing pigs. Journal of Agricultural Engineering Research, *64*: 299–310.

Barbari M., Conti L., 2009. Use of different cooling systems by pregnant sows in experimental pen. Biosystems Engineering, *103*: 239–244.

Bieda W., Herbut E., Kozbial M., 2001. Preliminary results of studies on the heating of broiler house using aerial-earth tube heat exchanger. Annals of Animal Science, *1*: 195–202.

Black J.L., Mullan B.P., Lorschy M.L., Giles L.R., 1993. Lactation in the sow during heat stress. Livestock Production Science, *35*: 153–170.

Botto Ľ., Waldnerová S., Mihina Š., Brestenský V., Lendelová J., 1995. Podklady pre modernizáciu a rekonštrukciu objektov pre chov ošípaných. [Documentation for Modernization and Reconstruction of Stables for pig Rearing.] RIAP, Nitra: 61.

Brown-Brandl T.M., Eigenberg R.A., Nienaber J.A., Kachman S.D., 2001. Thermoregulatory profile of a newer genetic line of pigs. Livestock Production Science, *71*: 253–260.

Brouček J., Novák P., Vokřálová J., Šoch M., Kišac P., Uhrinčať M., 2009. Effect of high temperature on milk production of cows from free-stall housing with natural ventilation. Slovak Journal of Animal Science, *42*: 167–173.

Bull R.P., Harrison P.C., Riskowski G.L., Gonyou H.W., 1997. Preference among cooling systems by gilts under heat stress. Journal of Animal Science, *75*: 2078–2083.

Christianson L., Hahn G.L., Meador N., 1982. Swine performance model for summer conditions. International Journal of Biometeorology, *26*: 137–143.

Dong H., Tao X., Li Y., Xin H., 2001. Comparative evaluation of cooling systems for farrowing sows. American Society of Agricultural Engineers, *17*: 91–96.

Frančák, J., Mihina Š., Angelovič M., Gálik R., Korenko M., Simoník J., Botto Ľ., Jobbágy J., Žitňák M. 2012. Technika v Agrosektore. [Technic in Agrosector.] 1st Ed. Nitra, SUA in Nitra: 199.

Hahn G.L., 1985. Management and housing of farm animals in hot environmentals. In: Yousef M.K. (ed.), Stress Physiology in Livestock. Vol. II. Boca Raton, CRC Press: 151–174.

Haeussermann A., Hartung E., Jungbluth T., Vranken E., Aerts J.-M., Berckmans D., 2007. Cooling effects and evaporation characteristics of fogging systems in an experimental piggery. Biosystems Engineering, *97*: 395–405.

Huynh T.T.T., 2005. Heat stress in growing pigs. [Ph.D. Thesis.] Wageningen, Wageningen University: 167.

Huynh, T.T.T., Aarnink A.J.A., Verstegen M.W.A., Gerrits W.J.J., Heetkamp M.J.W., Kemps B., Canh T.T., 2005. Effects of increasing temperatures on physiological changes in pigs at different relative humidities. Journal of Animal Science, *83*: 1385–1396.

Huynh T.T.T., Aarnink A.J.A., Truong C.T., Kemp B., Verstegen, M.W.A., 2006. Effects of tropical climate and water cooling methods on growing pigs' responses. Livestock Science, *104*: 278–291.

Le Dividich J., Noblet J., Herpin P., Van Milgen J., Quiniou N., 1998. Thermoregulation. In: Wiseman J., Varley M.A., Chadwick J.P. (eds), Progress in Pig Science. Nottingham, Nottingham University Press: 229–263.

Lucas E.M., Randall J.M., Meneses J.F., 2000. Potential for evaporative cooling during heat stress periods in pig production in Portugal (Alentejo). Journal of Agricultural Engineering Research, *76*: 363–371.

Mader T.L., Davis M.S., Brown-Brandl T., 2006. Environmental factors influencing heat stress in feedlot cattle. Journal of Animal Science, *84*: 712–719.

Mader T.L., Johnson L.J., Gaughan J.B., 2010. A comprehensive index for assessing environmental stress in animals. Journal of Animal Science, *88*: 2153–65.

Mihina Š., Cicka A., Brouček J., 2011. Animal welfare as an important factor of food quality. Potravinarstvo, *5* (Special Issue): 156–163.

Myer R., Bucklin R., 2001. Influence of hot-humid environment on growth performance and reproduction of swine. Document AN107, Extension, Institute of Food and Agricultural Sciences, University of Florida. Available at http://edis.ifas.ufl.edu/an107

Nienaber J.A., Hahn G.L., 2007. Livestock production system management response to thermal challenges. International Journal of Biometeorology, *52*: 149–157.

NOAA, 1976. Livestock Hot Weather Stress. Operations Manual Letter C-31-76. Kansas City, National Oceanic and Atmospheric Administration.

Pang Z., Li B., Xin H., Lee I.B., Xi L., Cao W., Bitog J.P., Wang Ch., Li W., 2010. Effect of a water-cooled cover on the thermal comfort of pregnant sows in hot and humid climate. In: CIGR XVIIth World Congress, June 13–17, 2010, Québec City: 11.

Pogran Š., Bieda W., Gálik R., Lendelová J. Švenková J., 2011. Kvalita vnútorného prostredia ustajňovacích objektov. [Quality of Internal Environment in Animal Housing.] 1st Ed. Nitra, SUA in Nitra: 242.

Quiniou N.J., Renaudeau D., Milgen J., Dubois S., 2001. Modelling heat production and energy balance in group-housed growing pigs exposed to cold or hot ambient temperatures. British Journal of Nutrition, *85*: 97–106.

Renaudeau D., Noblet J., Dourmad J.Y., 2003. Effect of ambient temperature on mammary gland metabolism in lactating sows. Journal of Animal Science, *81*: 217–231.

Seedorf J., Schröder M., Linkert K.-H., Wathes C.M., 1998. Concentrations and emissions of airborne dust in livestock buildings in Northern Europe. Journal of Agricultural Engineering Research, *70*: 59–77.

Silva B.A.N., Oliveira R.F.M., Donzele J.L., Fernandes H.C., Abreu M.L.T., Noblet J., Nunes C.G.V., 2006. Effect of floor cooling on performance of lactating sows during summer. Livestock Science, *105*: 176–184.

Souza L., 2009. How Can Heat Stress Affect your Production? The Pig Site (the website for the global pig industry). Available at http://www.thepigsite.com

Suriyasomboon A., Lundeheim N., Kunavongkrit A., Einarsson S., 2006. Effect of temperature and humidity on reproductive performance of crossbred sows in Thailand. Theriogenology, *65*: 606–628.

St-Pierre N.R., Cobanov B., Schnitkey G., 2003. Economic losses from heat stress by US livestock industries. Journal of Dairy Science, *86* (E. Suppl.): E52–E77.

Xin H., Mcfadden V.J., 1995. Tunnel ventilation to alleviate animal heat stress. In: Livestock Industry Facilities & Environment, Pm-1606, Ames, Iowa State University. Available at http://www.extension.iastate.edu

Webster A.J.F., 1991. Metabolic Responses of Farm Animals to High Temperature. EAAP Publication, No. 55: 15–22.

Zhang H., Wang Z., Liu G., He J., Su Ch., 2011. Effect of dietary fat supplementation on milk components and blood parameters of early-lactating cows under heat stress. Slovak Journal of Animal Science, *44*: 52–58.

Zumbach B., Misztal I., Tsuruta S., Sanchez J.P., Azain M., Herring W., Holl J., Long T., Culbertson M., 2008. Genetic components of heat stress in finishing pigs: Development of a heat load function. Journal of Animal Science, *86*: 2082–2088.

Received for publication April 18, 2013
Accepted after corrections July 27, 2013

Corresponding author:

Ing. Jana Lendelová, PhD., Slovak University of Agriculture in Nitra, Faculty of Engineering, Department of Structures, Tr. A. Hlinku 2, 949 76 Nitra, Slovak Republic
phone: +421 37 641 5777, e-mail: jana.lendelova@uniag.sk

Technical exploitation parameters of grinding rolls work in flour mill

R. Opáth

Department of Production Engineering, Faculty of Engineering, Slovak University of Agriculture in Nitra, Slovak Republic

Abstract

Opáth R., 2014. **Technical exploitation parameters of grinding rolls work in flour mill**. Res. Agr. Eng., *60* (Special Issue): S92–S97.

The proposed research paper analyses power consumption in grinding rolls of a flour mill. The observed mill has 15 grinding passages. The hourly efficiency of grinding roll on the first passage is 3,006.72 kg/h. The specific power consumption of individual grinding rolls ranges from 4.955 to 24.26 kWh/t. The thesis also contains results of research of grinding effects on grist. The greatest effect on grist was observed on the first grinding passage, where particle size after grinding was only 12% of the original grain size, as determined by sieve analysis. On the second through fifth passage, it was 85–96% (or 78–85% with shelling) of the original size. It was discovered during scouring that, in some cases, the sieve size of particles after grinding increased from 101 to 104% of the original size. This is due to shear force causing trituration of grist.

Keywords: milling; machines; performance; energy consumption

Milling grain in flour mills is an important first step in producing such products as breads and cakes. The key machine in a flour mill is the grinding roll. Its function is to separate as much endosperm from the grain as possible. Because of this, the effect of grinding rolls on grist, as well as efficiency and power consumption are of permanent interest to grinding roll designers. The stimulus for development in the flour milling process is the flour miller's requirement to produce the highest quality products at minimum cost. In the past, this was achieved through investment in new technologies and strategies (Owens 2001).

The aim of this research was to analyse the efficiency and power consumption on individual grinding passages, including the effect on grist, in the process of grinding of wheat by grinding rolls. The subject of research was the process of semolina and flour production as a whole on all grinding passages of the observed mill.

The importance of measuring the grist dispersity is necessary to assess the final disintegration processes quality in relevant processing equipment and to detect individual properties of the mixtures produced (Smejtková et al. 2011). Particle size was assessed as one of the most important physical properties which affect the flowability of wheat flours. (Kuakpetoon et al. 2001).

Grain milling technologies involve size reduction procedures in which grain kernels are broken into pieces of various sizes by the machinery. One of the estimations of the efficiency of the milling process is based on energy required to create new surfaces. Size reduction is one of the least energy-efficient one of all the unit operations and the cost of power is a major expense in crushing and grinding, so the factors that control this cost are important (McCabe et al. 2005).

MATERIAL AND METHODS

The observed flour mill consists of five scrapping, two shellings, one transitional and seven scouring

Table 1. Technical parameters of grinding rolls

Passage	Grinding rolls					Drive of rolls		
	length (mm)	number of grooves/cm	position	grooves inclination (%)	facet width (mm)	revolutions (min^{-1})	gearing	power capacity (kW)
1S	1,250	3.2	CH-CH	6	0.2	620	1:2.5	45
2S	1,250	4.8	CH-CH	6	0.2	620	1:2.5	30
3S	1,250	6.4	CH-CH	8	0.1	560	1:2.5	22
4Sf	1,000	8.9	O-O	10	0.1	500	1:2.5	15
4Sc	1,000	10.2	O-O	10	0.1	500	1:2.5	11
5S	1,000	11.5	O-O	12	0.11	500	1:2.5	11
1L(a)	1,250	11.5	CH-CH	10	0.1	560	1:1.23	15
1L(b)	1,000	–	–	–	–	560	1:1.23	11
2L(a)[1]	1,000	–	–	–	–	560	1:1.23	15
2L(b)[1]	1,000	–	–	–	–	560	1:1.23	15
Pr	1,000	–	–	–	–	500	1:1.23	15
1V	1,000	–	–	–	–	500	1:1.23	15
2V	1,250	–	–	–	–	470	1:1.23	15
3V	1,000	–	–	–	–	470	1:1.23	11
4V	1,000	–	–	–	–	470	1:1.23	11
5V	1,000	–	–	–	–	440	1:1.23	11
6V	1,000	–	–	–	–	440	1:1.23	7.5
7V	1,000	12.7	O-O	12	0.1	440	1:2.5	7.5

[1]grinding rolls with joint inlet and outlet openings, set so that the first one processes 45% and the second 55% of the material

passages. Grinding is done by nine doubled grinding rolls, two entoleters and four triturators. Technical parameters of grinding rolls and auxiliary machines are listed in Table 1.

Processed wheat was analysed in the mill laboratory. Wheat was of standard quality with a density of 790 kg/m and moisture of 14%. It was moistened to 16.5% before grinding.

Real efficiency determination. Measurements were done on all grinding rolls during operation. The real efficiency of all grinding rolls Q_s was calculated from the measured weight of grist samples and the time of their sampling using the equation:

$$Q_s = \frac{m}{t} 3{,}600 \quad \text{(kg/h)} \tag{1}$$

where:

m – average weight of grist sample (kg)

t – average time of sampling (s)

Specific power consumption determination. Digital electrometer DIZ W1E4 (Schrack Technik, s.r.o., Czech Republic) was used to measure the power consumption of grinding rolls drive.

The specific power consumption of grinding rolls (A_m) was calculated according to the equation:

$$A_m = \frac{A}{m_s} 3{,}600 \quad \text{(kWh/t)} \tag{2}$$

where

A – electric work of grinding roll (kWh)

m_s – weight of grist at time t (h)

$$m_s = \frac{Q_s \times t}{1{,}000}(t) \quad \text{(kWh/t)} \tag{3}$$

where:

Q_s – real efficiency of grinding roll (kg/h)

t – work time of grinding roll (h)

Degree of grist disintegration determination. Samples of grist were taken on both sides of the observed grinding machine. Samples were sifted using a laboratory sifter with a mesh size of 850, 500, 355, 250, 160, 125 μm (Fig. 1). The material captured in sieves was weighed and results recorded. From these results, the weight of throughs was determined.

For determination of grist disintegration degree by individual grinding rolls, weight values of throughs of individual sieves of the sifter were used.

The weight of through of the sieve f, labelled m_{xf}, was measured. Through of other sieves were calculated according to the following equations:

through of sieve e $$m_{xe} = m_{xf} + m_{pf} \quad (4)$$

through of sieve d $$m_{xd} = m_{xe} + m_{pe} \quad (5)$$

through of sieve c $$m_{xc} = m_{xd} + m_{pd} \quad (6)$$

through of sieve b $$m_{xb} = m_{xc} + m_{pc} \quad (7)$$

through of sieve a $$m_{xa} = m_{xb} + m_{pb} \quad (8)$$

where:

$m_{x(a \text{ to } f)}$ – weight of through of sieve a to f (g)

The weighted average of particle size $\bar{x}$ was calculated from values of throughs of individual sieves of the laboratory sifter:

$$\bar{x} = \frac{m_{xa} \times r_a + m_{xb} \times r_b + m_{xc} \times r_c + m_{xd} \times r_d + m_{xe} \times r_e + m_{xf} \times r_f}{m_{xa} + m_{xb} + m_{xc} + m_{xd} + m_{xe} + m_{xf}} \quad (\mu m) \quad (9)$$

where:

$r_{a \text{ to } f}$ – mesh size (μm)

The degree of grist disintegration is a non-dimensional number, calculated using the formula:

$$S = \frac{\bar{x}_p}{\bar{x}_N} \quad (10)$$

where:

$\bar{x}_p$ – average particle size after grinding (μm)

$\bar{x}_N$ – average particle size before grinding (μm)

RESULTS AND DISCUSSION

Measurements were done under usual working conditions in the flour mill, which was put into service in 2002.

Real efficiency determination

Results of the real efficiency of individual grinding rolls are listed in Table 2. The efficiency of the mill stated by the manufacturer is 80 tons per day. Its real efficiency during the research was 3,006.72 kg/h, which means that it only treated 72.16 t of wheat in 24 hours. This means that the operator only used 90.2% of the mill's capacity and could treat 7.84 more tons of wheat per day.

The hourly efficiency of grinding rolls on grinding passages spanned from 3,006.72 to 1,113.92 kg/h. The only exception is the fourth grinding passage, which is divided into two passages, one of which, labelled 4Sc, treats the coarse fraction of grist, and the other, labelled 4Sf, treats finer grist. Because of this, the grinding roll on passage 4Sh had relatively low efficiency of 539.64 kg/h.

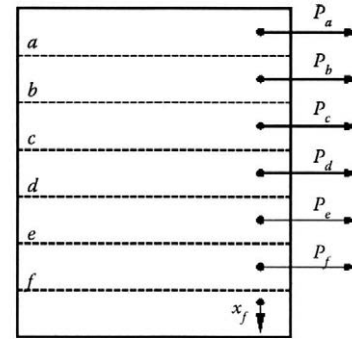

Fig. 1. Schema of laboratory sifter

a to f – sieves; p_a to p_f – material retained in sieve; x_f – through of sieve f

The grinding roll efficiency of 1,553.76 kg/h was determined on the first shelling passage. Other shelling passages had lower efficiency, spanning from 990.36 to 801.72 kg/h. The efficiency of transitional passage was 493.2 kg/h.

Grinding rolls on scouring passages had efficiency spanning from 725.40 kg/h on passage 1V to 200.52 kg/h on passage 5V.

The percentage of weight of wheat treated by individual grinding rolls can also be gathered from the results of the research. If the grinding roll on passage 1S treats 100% of ground wheat, then the second most loaded grinding roll is the one on passage 2S, treating 79.86% of all wheat. The third most loaded grinding roll is on passage 1L(a), which shells 51.68% of all treated material. The smallest amount of wheat goes through the grinding roll on passage 5V, which scours only 6.67% of treated wheat.

Specific power consumption determination

Measured and calculated values characterizing the power consumption of grinding rolls in grinding of wheat are listed in Table 3.

It can be seen from the results that the power consumption of grinding rolls individual electromotor on all passages was even. The results also show that the motor with a performance of 11 kW on the fifth grinding passage was permanently overloaded, while motors on other passages were overloaded, meaning that the usage of their performance capacities is low.

Table 2. Efficiency of grinding rolls measurement

Passage	Average sample weight (kg)	Average time of sampling (s)	Grinding roll efficiency (kg/h)	Processed wheat percentage (%)
1S	11.4	13.65	3,006.72	100.00
2S	12.2	18.29	2,401.20	79.86
3S	4.9	15.57	1,113.92	37.05
4Sc	3.4	22.68	539.64	17.95
4Sf	7.6	21.51	1,271.88	42.30
5S	11.1	27.67	1,444.32	48.04
1L(a)	12.3	28.50	1,553.76	51.68
1L(b)	6.2	22.54	990.36	32.94
2L(a)	7.3	32.78	801.72	26.66
2L(b)	9.0	32.78	988.56	32.88
Pr	3.8	27.73	493.20	16.40
1V	6.2	30.77	725.40	24.13
2V	5.6	31.41	641.88	21.35
3V	2.5	32.00	281.16	9.35
4V	2.3	31.14	266.04	8.85
5V	1.6	28.70	200.52	6.67
6V	2.0	29.35	245.16	8.15
7V	5.7	40.2	510.48	16.98

Specific power consumption on individual passages under conditions of observation varied from 4.955 to 24.26 kWh/t.

For comparison, results of the research done by Opáth et al. (2004) were used. Their research showed the lowest specific power consumption

Table 3. Specific power consumption measurement

Passage	Effective power (kW)	Utilization (%)	Power consumption (kWh)	Grist weight (t)	Specific power consumption (kWh/t)
1S	36.17	80.4	36.17	3.007	12.029
2S	23.56	78.5	23.56	2.401	9.813
3S	20.11	91.4	20.11	1.133	17.749
4Sf	9.60	64.0	9.60	0.540	17.778
4Sc	9.35	85.0	9.35	1.272	7.351
5S	12.31	111.9	12.31	1.444	8.525
1L(a)	7.70	51.3	7.70	1.554	4.955
1L(b)	7.57	68.9	7.57	0.990	7.646
2L(a)	7.32	48.8	7.32	0.802	9.127
2L(b)	8.68	57.9	8.68	0.989	8.777
T	11.96	79.7	11.96	0.493	24.260
1V	5.51	36.7	5.51	0.725	7.621
2V	5.59	37.3	5.59	0.642	8.707
3V	3.45	31.4	3.45	0.281	12.278
4V	5.68	51.6	5.68	0.266	21.353
5V	3.70	33.6	3.7	0.201	18.41
6V	4.27	56.9	4.27	0.245	17.429
7V	3.93	52.5	3.93	0.511	7.691

Table 4. Size of particles before and after grinding and the degree of grist disintegration

Passage	Size of grist particles (μm)		Degree of grist disintegration
	before grinding	after grinding	
1S	4,750	579	0.12
2S	651	554	0.85
3S	608	582	0.95
4Sf	685	621	0.91
4Sc	779	645	0.83
5S	673	645	0.96
1L	677	528	0.78
2L	531	435	0.85
1V	458	452	0.99
2V	443	456	1.03
2V entoleter 1	457	432	0.95
3V	448	446	0.99
3V entoleter 2	446	416	0.93
4V	487	494	1.01
4V triturator 1	494	480	0.97
5V	502	525	1.04
6V	467	482	1.03
6V triturator 2	488	481	0.98
7V	491	497	1.01
7V triturator 3	498	487	0.89
T	584	505	0.86
T triturator 4	503	478	0.95

(3.31 kWh/t) on the third and fifth grinding passage and the highest specific power consumption (7.27 kWh/t) on the fifth and sixth scouring passage of the mill on which the research was conducted.

Achieved results are also comparable with the results of CARLSSON-KANYAMA and FAIST (2010), who stated that energy consumption ranges from 0.32 to 2.58 MJ per kg of wheat flour.

Degree of grist disintegration determination

Results of disintegration of grist measurements (Table 4) show that the degree of disintegration on the first grinding passage was 0.12, which means that the average particle size after grinding was only 12% of the original size of wheat grain. This passage had the greatest grinding effect. This result is comparable with results of research done by KAŽIMÍROVÁ and OPÁTH (2007), with the degree of disintegration of 0.13 on passage 1S in the mill observed by them. The lowest degree of disintegration was found on scouring passages using smooth rolls. This is also comparable with the results gathered by KAŽIMÍROVÁ and OPÁTH (2007).

On the second through fifth grinding passages of the observed mill, the degree of disintegration spanned from 0.85 to 0.96.

The degree of disintegration of 0.78 was found on the first shelling passage. On the second shelling passage, it was 0.85, the same as on the second grinding passage.

During the second, fourth, fifth, sixth and seventh scouring, the degree of disintegration varied from 1.01 to 1.04, which means that particles increased their size transition through the grinding machine. This was caused by the use of smooth rolls, their advance and greater pressure. This was also the case on passage 7V, where rolls with fine grooves were used. Under these conditions, shear force causing trituration of grist also has a greater effect. The integrity of endosperm was disrupted, but individual grist particles were immediately pressed together and agglutinated into larger particles. This issue was dealt with by the installation of an auxiliary grinding machine on passage 5V. A greater amount of fine flour was created in grinding.

CONCLUSION

The mill was only used at 90.2% of its full capacity. Results show that the work of grinding rolls was even, and observed properties did not change significantly during the research period. The efficiency of grinding rolls on grinding passages varied from 539.64 to 3,006.72 kg/h. The lowest value was found on passage 4Sh, which treated more robust grist brought to the fourth grinding passage. The efficiency of grinding rolls on shelling passages gradually declined, which is considered optimal. The efficiency of the grinding roll on shelling passage 1L was 1,553.76 kg/h. The efficiency of the second shelling passage was 988.56 kg/h. The efficiency of scouring passages was the lowest, varying from 725.40 kg/h on passage 1V to 200.52 kg/h on passage 5V. This means that the efficiency of all grinding machines on grinding passages was greater than the efficiency of machines on other passages of the observed mill.

Specific power consumption for the same degree of grist disintegration was not the same on individual passages. Only a portion of electromotor

capacity was used on most of the passages of the observed mill. The only exception was the electromotor on passage 5S, which was permanently overloaded.

Over-equipped electromotors increase investment costs unnecessarily and require more effective compensation of mill's power factor. Based on this, it is recommended to take the expected efficiency of grinding rolls into account when designing flour mills and propose more adequate performance of the installed electromotor. Power consumption in grinding was even. This is caused by the steadiness and evenness of material flow onto individual passages.

The analysis of degree of grist disintegration showed that the mill produces very fine flour, with a min. gradual decrease of individual particle size. The only exception was the first grinding passage, where the size of ground material was only 12% of the original grain size. The degree of decomposition observed on the second, fourth, fifth, sixth and seventh scouring passage was higher than 1.0, which means that the size of ground particles increased. Smooth grinding rolls are used on these passages, with an exception of passage 7V, where rolls with fine grooves are used. The increase of particle size, discovered by sieve analysis, was caused by increased shear and pressure forces and lack or sharp decrease of cutting force on ground grist particles.

Presented results can be used as groundwork for designers and for optimization of parameters of grinding rolls and technical systems of flour mills as a whole. In practice, the results gathered are usable for adjustment of exploitation parameters of grinding and sifting machines, allowing for more exact division of final products on individual mill passages and power savings.

References

Carlsson-Kanyama A., Faist M., 2010. Energy use in the food sector: 1–36. Available at: www.comuv.com

Kažimírová V., Opáth R., Tóth P., 2003. Analýza spotreby elektrickej energie na výrobu pšeničnej múky. [Analysis of energy consumption in the production of wheaten.] In: Proceedings Progresívna technika v živočíšnej, potravinárskej výrobe a v odpadovom hospodárstve, September 10–11, 2003. Nitra,: 39–43.

Kažimírová V., Opáth R., 2007. Technické aspekty výroby pšeničnej múky. [Technical Aspect of Wheat Flour Production.] Nitra, SUA in Nitra: 110.

Kuakpetoon D., Flores R.A., Milliken G.A., 2001. Dry mixing of wheat flours: Effect of particle properties and blending ratio. Lebensmittel-Wissenschaft & Technologie, *34*: 183–193.

McCabe W.L, Smith J.C., Harriott P., 2005. Unit Operations of Chemical Engineering. 7th Ed. New York, McGraw-Hill International: 984–1000.

Opáth R., Kažimírová V., 1998. Analýza spotreby energie na mletie pšenice. [Analysis of energy consumption for grinding of wheat.] Acta Technologica Agriculturae, *1*: 24–27.

Opáth R., Kažimírová V., Tóth P., 2004. Energetická náročnosť procesu mletia pšenice. [Energy consumption during the milling process of wheat grain.] Acta Technologica Agriculturae, *7*: 106–108.

Owens G., 2001. Cereals Processing Technology. Cambridge, Woodhead Publishing: 248.

Smejtková A., Vaculík P., Passian L., 2011. Stanovení disperzity meliva pšenice, ječmene a ječmenného sladu. [Determination grist dispersity – wheat, barley and barley malt.] Agritech Science, *3*: 1–4.

Received for publication April 23, 2013
Accepted after corrections June 17, 2014

Corresponding author:

Doc. Ing. Rudolf Opáth, CSc., Slovak University of Agriculture in Nitra, Faculty of Engineering, Department of Production Engineering, Trieda A. Hlinku 2, 949 76 Nitra, Slovak Republic, phone: +421 37 641 4304, e-mail: rudolf.opath@uniag.sk

Verification of the working life of a ploughshare renovated by surfacing and remelting in the operation

I. Kováč, N. Vanko, M. Vysočanská

Department of Quality and Engineering Technologies, Faculty of Engineering, Slovak University of Agriculture in Nitra, Nitra, Slovak Republic

Abstract

Kováč I., Vanko N., Vysočanská M., 2014. **Verification of the working life of a ploughshare renovated by surfacing and remelting in the operation**. Res. Agr. Eng., *60* (Special Issue): S98–S103.

The most common way of renovation of the working parts of agricultural machinery is surfacing by hardfacing coated electrodes and piped hardfacing wires. Another way to prolong the working life of the machinery is the chemical heat treatment of the material surface by nitriding. By nitriding, high hardness is obtained of the surface affected by a suitable environment and by raised temperature. This paper deals with the possibilities of increasing the lifetime of the functional area of a ploughshare by the surfacing piped wire and hardfacing electrodes and reshaping the surface layer in an argon and nitrogen environment by using a welding rectifier and the Tungsten Inert GAS method, and by validation of these methods of renovation in operating conditions.

Keywords: equipment wear; renovation; weld deposit; saturation; soil processing tool

The wear of the cutting edges of tillage machinery in operating conditions significantly affects the quality of work and energy demands of land cultivation. With a greater thickness of the ploughshare cutting edge, the traction force and fuel consumption significantly increase while the working intensity and depth of tillage decrease. Also, the quality of tillage greatly decreases with a greater thickness of the ploughshare cutting edge. Therefore, the renovation of individual tools is performed so that the cutting edge is resistant against wear and the self-sharpening effect is created. This can be achieved through the thickness of the layer applied and the hardness of the additional and basic material (Žitňanský, Žarnovský 2005; Mikuš et al. 2006).

The size and intensity of wear can be measured by using quantitative methods, monitoring the weight loss and linear dimensions of a unit circuit in laboratory and operating conditions (Daňko et al. 2011; Kotus et al. 2011).

The user's sphere looks for different ways of prolonging the technical life of these tools. One of the potential possibilities is the application of a surfaced layer of hard material on the working part of the tool. The most common way of the renovation of the working parts of agricultural tools is surfacing by hardfacing coated electrodes and piped hardfacing wires. However, the metal inert gas (MIG) and metal active gas (MAG) technologies have recently been put in use for surfacing with piped hardfacing wires, mainly due to a higher labour productivity, the increase of surfacing performance, and the economy and quality of the weld deposit. High wear resistance and significant savings are achieved

Supported by the Scientific Grant Agency VEGA of the Ministry of Education of the Slovak Republic and the Slovak Academy of Sciences, Grant No. 1/0576/09.

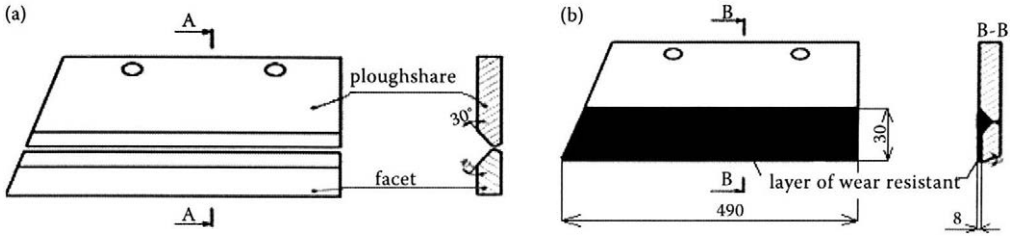

Fig. 1. Modification of the ploughshare (a) preparation of the facet and ploughshare, (b) weld deposit and creating the edge

by these procedures as evidenced by the works of authors Chotěborský et al. (2009a,b), Čičo and Bujna (2011), Kotus and Čičo 2011, and Kovaříková et al. (2011).

The structure of the weld deposit very significantly changes the characteristics of the weld deposit, weight losses, and relative wear resistance (Tolnai, Čičo 2001; Chotěborský et al. 2009a,b).

Another option to increase the resistance of the functional areas is the heat and chemical heat treatments, for example boriding and nitriding. The required hardness for nitriding is achieved already during the saturation of the surface by nitrogen, i.e. without further heat treatment. The essence of the higher hardness is the formation of very hard chemical compounds of nitrogen with iron and some ingredient elements. Hard layers with a thickness of up to 0.5 mm are formed by nitriding. Nitriding is conditioned by the presence of atomic nitrogen on the metal surface. Atomic nitrogen is able to penetrate through the surface absorption layer of nitride at an increased temperature of the basic metal lattice, and further to diffuse into the steel (Pulc et al. 2004).

In conditions of arc remelting in the gaseous atmosphere, a dissociate environment is created, which allows to create a stable structure with better mechanical properties and mainly with a higher wear resistance.

By this contribution we would like to highlight the possibilities of improving the lifetime of agricultural machinery working tools, especially by increasing the abrasion resistance of the surface layer due to nitrogen diffusion applied on the surface by remelting the material – the facet from the material class according to standard STN 41 5230 (1977), and by surfacing the facet from the material class according to standard STN 41 2050 (1976), followed by comparing these technologies in operating conditions. Surfacing was done by hand arc surfacing (MMAW) with hardfacing electrode and by using the MAG method (FCAW) of hardfacing wire electrode.

MATERIAL AND METHODS

A six-furrow plough Lemken EuroDiamant (Lemken GmbH & Co., Alps, Germany) was used for conducting the operating test. Ten worn-out ploughshares were renovated; the cutting blades of worn-out ploughshares were cut off with the laser and in their place a belt (facet) from the material of size 490 × 30 × 8 mm was welded on so that all ploughshares were of the same size (Fig. 1). Two ploughshares were used as etalons, one with the facet from the material according to STN 41 2050 (1976) without a weld deposit, and one from the material according to STN 41 5230 (1977) without remelting. The welding of the facet was done by using the welding semi-automatic machine Uni MIG 450p (Billik s.r.o., Nitra, Slovakia). The facet for hard-welds was produced from steel according to STN 41 2050 (1976). The facet for nitriding was made from steel according to STN 41 5230 (1977), the composition and properties of which contributed at the best to meeting our desired final quality parameters. The piped welding wire (referred to in the text as No. 1; Table 1) was used as an additional material for three ploughshares, and the hardfacing coated electrode (referred to in the text as No. 2; Table 1) was used for the remaining two ploughshares.

The welding parameters with the coated electrode No. 1: Ø d =1.6 mm, U = 25.5 V, welding speed v_n = 0.35 m/min, wire passing speed v_d = 0.3 m/min. Wire electrode No. 2: Ø d = 2.5 mm, current I = 75 A, voltage U = 28V. The protective atmosphere Ferromix C18 in the flow amount of 16 l/min.

Table 1. Chemical composition (%) of material No. 1 – WELCOVARE 1736 and No. 2 – WELCO 1707 S

Material	Component						
	C	Mn	Si	Cr	S, P, Mo, Cu		Fe
No. 1	0.45	1.6	0.6	5.5	up to 0.5		residue
	C	Mn	Si	Cr	Mo	V	Fe
No. 2	0.4	0.3	0.8	8.0	1.0	0.6	residue

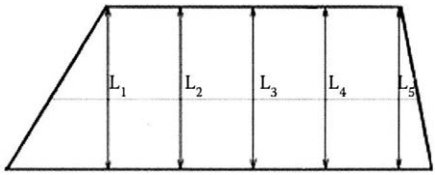

Fig. 2. Positions of the measurement of wear

Remelting using the TIG (GTAW) technology was done on five ploughshares by the application of the mixture of gases Ar + N_2 in mixing ratios 10:5, 10:6, and 10:7 l/min. It was accomplished by a welding source Invertig 360 GV (Rehm GmbH & Co., Baden-Württemberg, Germany) with the parameters I = 100 A, voltage U being regulated by the welding device. Argon performed the function of carrier gas, the flow quantity was adjusted to the value of 10 litres. Only the flow quantity of nitrogen was changed. The converter of gasses was used for blending. The output of the converter was connected to the welding torch.

RESULTS AND DISCUSSION

Operating tests were conducted at the AG H-N Nevidzany, s.r.o. (Červený Hrádok, Slovakia) company premises. The first measurement was done after treating 76 ha and the final measurement after treating 700 ha. When measuring the wear, the ploughshares were removed and evaluated based on the loss of linear dimensions which describe more reliably the extent of the wear; the ploughshare width plays an essential role in the quality of tillage, however, a weight loss was also detected (Fig. 2). The measured points of the ploughshare were marked as notches. The measurements were done on one plough.

The measurement locations on the ploughshares were strictly identified. The measured losses due to wear on the individual ploughshares and in particular areas of are shown in Table 2. The ploughshares dimensions before and after tillage as well as the linear decrease are graphically illustrated in Fig. 3.

Operating tests were continuously evaluated. The dry conditions and compacted soil layers also contribute to the increased wear (Kollárová et al. 2007). The most intensive wear occurred after processing 76 ha of soil, when the ploughshares were working in extremely dry conditions. The resistance against wear was seen on the ploughshares which had been remelted from the material of class 15 by the gas atmosphere Ar + N_2. This increase was not too great, it showed only 57.8% when compared with standards. When talking about the remelted ploughshares, the ploughshare that was the most intensively worn out was that in the measurement location L_1 on the tip, an equal wear was seen in other measured locations. The ploughshares renovated by surfacing reached several times higher resistance against wear and remelting, as well as against the standard. The ploughshares surfaced by the additional material marked as No. 2 reached the best resistance results, on average 3.6 times higher resistance compared with the standard; the ploughshare most intensively worn was that in the measurement location L_1 on the tip and the measurement decreased gradually in other measurement locations. The ploughshare surfaced by the additional material marked No. 1 reached on average 2.6 times increased resistance against the standard from the material of class 12, and we can see equal wear in the measured locations.

Čičo and Bujna (2011) say that ploughshares surfaced with electrodes labelled as Fidur 10/60 and 10/65 revealed lower wear as compared to untreated ploughshares, on average 2.2 times smaller.

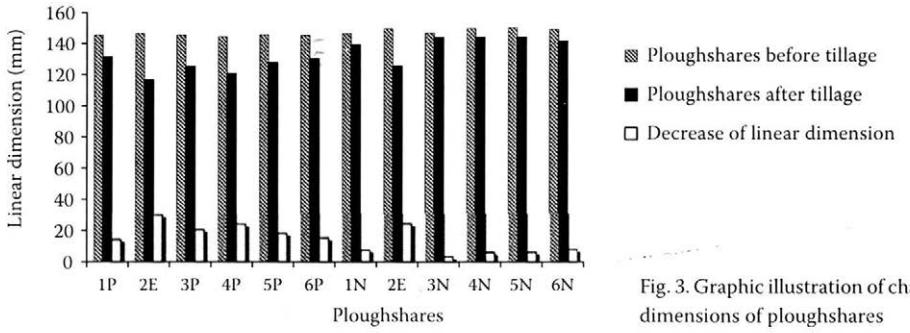

Fig. 3. Graphic illustration of changes in linear dimensions of ploughshares

Table 2. The loss of linear dimensions of ploughshares after tillage (76 ha)

Ploughshare identification	Ploughshare	ΔL_1 (mm)	ΔL_2 (mm)	ΔL_3 (mm)	ΔL_4 (mm)	ΔL_5 (mm)	ØΔL (mm)
L1	remelted 10:6	18.2	15.6	13.9	12.3	10.8	14.16
L2	etalon	26.2	28.1	29.5	31.9	34.2	29.98
L3	remelted 10:7	18.3	19.3	20.4	20.7	23.0	20.34
L4	remelted 10:7	20.2	22.0	23.6	25.4	27.9	23.82
L5	remelted 10:5	17.7	18.4	18.8	17.1	17.0	17.8
L6	remelted 10:5	14.7	15.1	15.0	15.2	16.0	15.2
	Ø remelting	21.46	18.08	18.34	18.14	18.94	–
P1	remelted MMAW	8.4	6.8	7.2	6.5	7.3	7.24
P3	remelted MMAW	4.4	4.7	3.8	1.7	1.6	3.24
	Ø surfacing MMAW	6.4	5.75	5.5	4.1	4.45	–
P2	etalon	19.6	22.9	24.9	25.8	27.0	24.04
P4	remelted FCAW	6.2	6.1	7.7	5.7	5.0	6.14
P5	remelted FCAW	5.2	6.4	6.2	6.6	6.5	6.12
P6	remelted FCAW	8.7	8.1	5.8	7.4	8.6	7.72
	Ø FCAW surfacing	6.7	6.87	6.57	6.57	6.7	6.68

MMAW – manual metal arc welding; FCAW – flux-cored arc welding; L1–L6 – left side; P1–P6 – right side

The results were favourable with the ploughshares which we tested. This also depends on the choice of the additional materials.

Ploughshares – etalons demonstrated the highest loss of wear, the best results having been achieved with the ploughshare with the welded facet from the material of class 12. The content of the alloying elements significantly affects the structural composition of the weld deposit and properties of the structures, perhaps even phases (Tolnai, Čičo 2001). In our case, the weld deposit with carbides freely distributed in matrix (Fig. 4) showed greater resistance than the weld deposit with carbides which had a needle-shaped structure (Fig. 5).

The structure of the remelted area is made by upper bainite, martensite, and ferrite (Fig. 6). In it, a grainy texture is observable. The grains are composed of dark heterogeneous phase which is a mixture of bainite and martensite. The white phase excluded on the edges of the grains is ferrite in the form of netting. The presence of bainite and martensite in steel structure 15 230 after remelting was shown by relatively increased hardness.

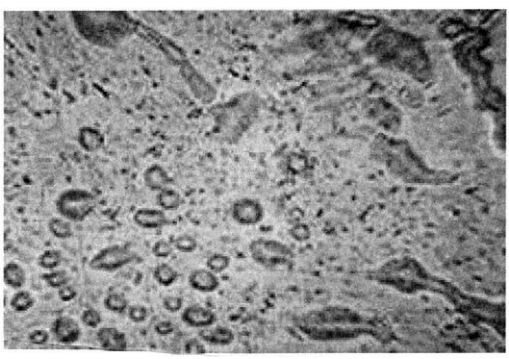

Fig. 4. Detail structure of the weld deposit of material No. 2, carbides freely distributed in basic matrix (etching by nital)

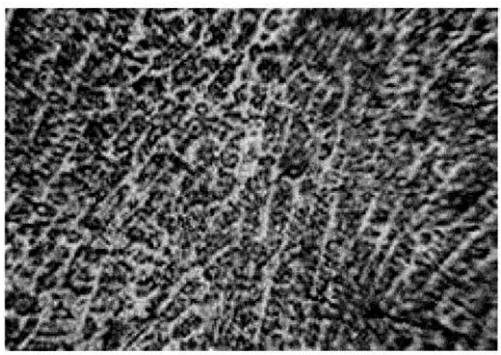

Fig. 5. Detail structure of the weld deposit of material No. 1, acicular structure of chromium carbides with the typical elongated shape (etching by nital)

Table 3. Weights of ploughshares before and after the test and the loss of weight of ploughshares after tillage (76 ha)

Ploughshare identification	Ratio of immixture of gases Ar and N_2 (l/min)	Weight of ploughshare before test (g)	Weight of ploughshare after test (g)	Loss of weight Δm (g)	Average loss of weight (g)
5P (remelted)	10:5	3,912	3,462	450	406.5
6P	10:5	3,418	3,055	363	
1P	10:6	3,920	3,540	380	380
3P	10:7	3,830	3,300	530	567.5
4P	10:7	3,830	3,225	605	
2E (etalon)	etalon 15 230	3,850	3,120	730	730
Surfacing material					
1N (surfacing)	1707 S	4,272	4,100	172	156
3N	1707 S	4,170	4,030	140	
4N	1736	4,170	4,056	114	
5N	1736	4,268	4,175	93	99.3
6N	1736	4,362	4,271	91	
2E (etalon)	etalon 12 050	4,015	3,596	419	419

The presence of nitrides and carbonitrides in the said structures was not proven at the given magnification. The fact that in the given structure nitrides and carbonitrides are probably not present is also confirmed by a small increase in hardness (Table 3).

The weight losses that are indicated in this paper correspond (Fig. 7) with the linear losses. Operating test results confirmed that, despite the higher wear of the remelted ploughshares, this technology allows to extend the technical life, is very simple, and it must also be realised that without the welding of the facets and the follow up renovation the worn ploughshares would go to the scrap. The utilisation of the results obtained must be preceded by farmer's interest. Irrespective of that, the operating tests continued later on under optimal soil conditions. The wear gradually grew while the ploughshares processed 700 ha of soil.

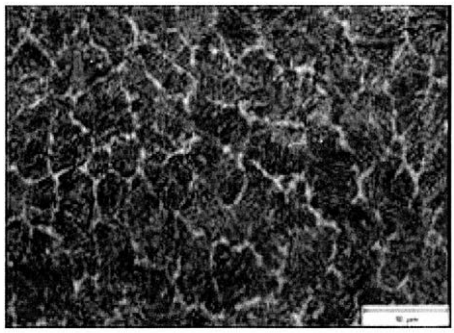

Fig. 6. The microstructure of the remelted layer of steel 15 230 in the mixture of 10 l Ar and 5 l N_2 is represented by upper bainite, martensite, and ferrite

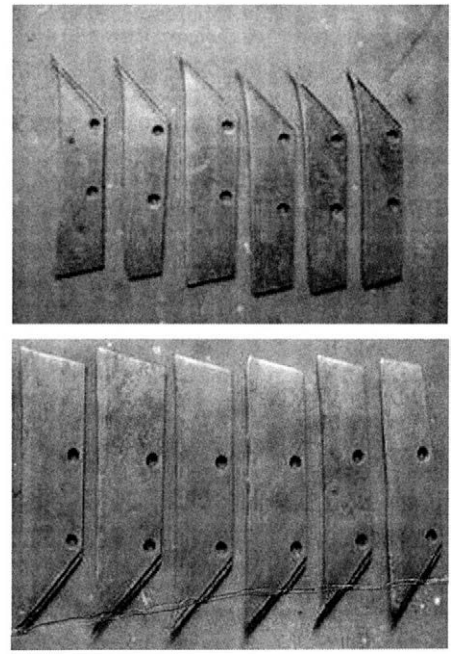

Fig. 7. Wear of ploughshares after operating test

CONCLUSION

Ploughing is one of the most demanding operations in agricultural production in terms of tillage machinery wear; therefore the ways of increasing the working life of this machinery must be sought. One means is the renovation of the worn ploughshares. The most used is the renovation by surfacing as preventive weld deposit, which proved in this case to be the optimal one but it can also be used as renovation described in this paper.

The effect of the surfacing renovation prolonged in our case the technical life 2.6–3.6 times. When alloying by gas mixture Ar + N_2 remelting using the TIG technology, the technical life was prolonged by 56% over the standard, and by renovation the technical life was given back to the ploughshare. The achieved results are only partial results; it is necessary to conduct further operating tests using these technologies. In this paper, we intended to point out other possibilities of renovation in operating conditions.

References

Čičo P., Bujna M., 2011. Odolnosť tvrdonávarových materiálov v prevádzkových podmienkach. [Wear Resistance of Hardfacing Materials in Operating Conditions.] Nitra, SUA in Nitra: 119.

Daňko M., Čičo P., Kotus M., Pauliček T., 2011. Odolnosť materiálov vytvorených laserovým naváraním proti abrazívnemu opotrebeniu. [Abrasive wear resistance of materials produced by laser deposit welding.] In: Proceedings Quality and Reliability of Technical Systems, 16. Nitra, SUA in Nitra: 101–105.

Chotěborský R., Hrabě P., Müller M., Savková J., Jirka M., Navrátilová M., 2009a. Effect of abrasive particle size on abrasive wear of hardfacing alloys. Research in Agricultural Engineering, *55*: 101–113.

Chotěborský R., Hrabě P., Müller M., Válek R., Savková J., Jirka M., 2009b. Effect of carbide size in harfacing on abrasive wear. Research in Agricultural Engineering, *55*: 149–158.

Kotus M., Čičo P., 2011. Vplyv parametrov MIG/MAG navárania na tvorbu návaru. [Effect of MIG/MAG Parameters by Surfacing on the Creation of Weld.] Nitra, Slovak University of Agriculture: 112.

Kotus M., Andrássyová Z., Čičo P., Fries J., Hrabě P., 2011. Analysis of wear resistent weld materials in laboratory conditions. Research in Agricultural Engineering, *57* (Special Issue): S74–S78.

Kollárová K., Simoník J., Švarda R., Žitňák M., 2007. Soil moisture as a surrogate factor to characterize the variability of soil conditions in precision farming system. In: Proceedings from Advances in Labour and Machinery Management for a Profitable Agriculture and Forestry – XXXII CIOSTA-CIGR section V, September 17–19, 2007. Nitra, Slovak University of Agriculture: 389–399.

Kovaříková I., Šimeková B., Hodúlová E., Ulrich K., 2011. Properties of composite wear resistant layers created by laser beam. In: Annals of DAAAM and Proceedings of 22nd DAAAM Symposium, November 23–26, 2011. Vienna: 1193–1194.

Mikuš R., Balla J., Žernovič M., 2006. Formovanie tvaru ostria spevneného tvrdou vrstvou počas opotrebenia. [Formation of blade shape strengthen by hard layer during wear process.] In: Intertribo: tribologické problémy v exponovaných trecích sústavach: IX. medzinárodné sympózium. [Tribological Problems in Exposed Friction Systems: IX. International Symposium.] Bratislava, Kongres Management s.r.o: 119–123.

Pulc V., Hrnčiar V., Gondár E., 2004. Náuka o materiáli. [Material Science.] Bratislava, Slovak University of Technology in Bratislava: 333.

STN 41 2050, 1976. Oceľ 12 050. [Steel 12 050.] Bratislava, Slovak Office of Standards, Metrology and Testing.

STN 41 5230, 1977. Oceľ 15 230 Cr-V. [Steel 15 230 Cr-V.] Bratislava, Slovak Office of Standards, Metrology and Testing.

Tolnai R., Čičo P., 2001. Oteruvzornosť návarových materiálov novej koncepcie. [Wear resistance of hardfacing materials of a new concept.] Acta Technologica Agriculturae, *4*: 99–102.

Žitňanský J., Žarnovský J., 2005. Renovačné procesy a vplyv rezných podmienok. [Renovation processes and effect of cutting conditions.] In: Proceedings Quality and Reliability of Technical Systems, 13. Nitra: 184–187.

Received for publication July 12, 2012
Accepted after corrections May 29, 2013

Corresponding author:

Ing. Ivan Kováč, Ph.D., Slovak University of Agriculture in Nitra, Faculty of Engineering, Department of Quality and Engineering Technologies, Tr. A. Hlinku 2, 94976 Nitra, Slovak Republic
phone: + 421 37 6414308, e-mail: ivan.kovac@uniag.sk

CZECH ACADEMY OF AGRICULTURAL SCIENCES

Těšnov 17, 117 05 Prague 1, Czech Republic
workplace: Slezská 7, 120 00 Prague 2, Czech Republic
e-mail: redakce@cazv.cz
Tel.: + 420 227 010 427, Fax: + 420 227 010 116
Account No. 86634011/0100 KB
IBAN CZ41 0100 0000 0000 8663 4011; SWIFT KOMBCZPPXXX

The Czech Academy of Agricultural Sciences publishes scientific journals dealing with the problems of agriculture, forestry and food sciences and technology. The periodicals are published in English.

Journal	Number of issues per year	Yearly subscription in USD
Plant, Soil and Environment	12	720
Czech Journal of Animal Science	12	720
Agricultural Economics (Zemědělská ekonomika)	12	680
Journal of Forest Science	12	580
Veterinární medicína (Veterinary Medicine – Czech)	12	790
Czech Journal of Food Sciences	6	620
Plant Protection Science	4	175
Czech Journal of Genetics and Plant Breeding	4	175
Horticultural Science	4	195
Research in Agricultural Engineering	4	155
Soil and Water Research	4	175

Subscription to these journals be sent to the above-mentioned address.

The journal publishes results of basic and applied research from all fields of agricultural engineering. Original scientific papers, short communications, review articles, and selectively book reviews from the disciplines concerned are published in the journal. Papers are published in English (British spelling). The author is fully responsible for the originality of the paper and formal correctness. The paper and its content must not be published previously elsewhere. The Board of Editors decides on the publication of papers, taking into account scientific importance, peer reviews and manuscript originality, quality and length. Standard size of paper (A4 format), type size 12 font, double-space lines, 2.5 cm margins on each edge of the page. **Scientific papers** and **review articles** shall not be longer than 15 standard pages, including tables and figures. **Short communications** should not be longer than 6 standard pages and book reviews should not be longer than 3 standard pages. Manuscripts must be submitted in MS Word text editor to the electronic editorial system (http://www.agriculturejournals.cz/web/rae.htm).

Tables should be placed at the end of the manuscript. Word editor should be used to create tables; each item should be placed into a separate cell. Tables are to be numbered with Arabic numerals in the order in which they are referred to in the text. **Figures**. Figure captions should be placed after the tables. Autotypes should be submitted in TIFF or JPG format in minimal resolution 300 dpi. Graphs should be provided in MS Excel and they should be stored with original data. All graphs and photos should be numbered, continually according to the order in which they are included in the text, using Arabic numerals. **Abbreviations and units**. If any abbreviations are used in a paper, they shall be explained appropriately when they are used in the text for the first time. It is not advisable to use any abbreviations in the paper title or in the abstract. The SI international system of measurement units should be used.

Title page must contain title of paper, complete name(s) of the author(s), the name(s) and address(es) of the institution(s) where the work was done.

Abstract is a short summary of the whole paper (as a single paragraph). It should describe all essential facts of a scientific paper. The abstract should not go to more than 170 words. The abstract is an important part of the paper because it is published and cited in world databases. No references are to be cited. **Keywords** (recommendation 5 words) should be different from words mentioned in the title.

Introduction should outline the main reasons why the research was conducted; describe a brief review of literature consisting of refereed periodicals, journals and books, and the goal of the authors.

Material and Methods. All preliminary material, experiments conducted, their extent, conditions and course should be described in detail in this section. All original procedures that were used for the processing of experimental material and all analytical methods used for evaluation should also be detailed. Data verifying the quality of acquired data should be indicated for the used methods. The whole methodology is only to be described if it is an original one; in other cases it is sufficient to cite the author of the method and to mention any particular differences. Methods of statistical processing including the software used should also be listed in this section.

Results and Discussion. More than one-year results should be published in the paper. The results obtained from the experiments including their statistical evaluation and any commentary should be presented graphically or in tables in this section. Each phenomenon should be commented and explained, using scientific arguments. The author should confront partial results with data published by other authors, whose names and year of publication are to be cited by including them in the text directly, e.g. ... as published by Lowe (1981), Novák and Šídlo (2002) found ..., or citing authors and years of publication in parenthesis (Lowe 1981; Novák, Šídlo 2002; Jakl et al. 2003).

Conclusion. In the conclusion it is necessary to mention briefly the most important results presented in article, the key points of next research and experimental work and recommendation for utilization in practice.

References should be preferably a list of refereed periodicals arranged in alphabetical order according to the surname of the first authors. The surnames and initials of all authors should be followed by the year of publication cited, the original title of the paper (if the cited source is not in English, it should be translated in brackets behind of the original title), the name of the periodical, the relevant volume and page number, in the case of a book or proceedings the title should be followed by the name of the publisher and the place of publication. Names of authors should be separated by commas, not by & or and. Examples:

Journal article: Litak G., Longwic R., 2009. Analysis of repeatability of diesel engine acceleration. Applied Thermal Engineering, 29: 3574–3578.

Monographs: Bouman A., 1995. Mechanical Damage in Potato Tubers – Enquiry of the EAPR Engineering Section. Wageningen, Institute of Agricultural and Environmental Engineering: 29.

Papers published in collections and proceedings: McClements D.J., 1994. Ultrasonic NDT of foods and drinks. In: McGonnagle W.J. (ed.), International Advances in Nondestructive Testing. Yverdon, Gordon and Breach Science, *17*: 63–95.

Toscano G., Riva G., Pedretti E.F., Corinaldesi F., 2008. Evaluation of solid biomass for energy use in relation to the ash qualitative and quantitative characteristics. In: International Conference on Agricultural Engineering, Agricultural and Biosystems Engineering for a Sustainable World, June 23–25, 2008. Hersonissos – Crete, Greece.

Dissertation: Vančurová P., 2008. Podmínky konkurenceschopnosti výroby bionafty v České republice. [Conditions of Competitiveness of Biodiesel Production in the Czech Republic.] [Ph.D. Thesis.] Prague, Czech University Life Sciences Prague: 1 – 159.

Internet publications: George G.C., 2001. Solids flowability. University of Akron. Available at www.ecgf.uakron.edu/chem/fclty/chase/solidsNote.PDF (accessed August 2, 2007).

Contact address should include the postal address, telephone and fax numbers, and e-mail of the corresponding author in English.

Proof-sheets will be sent to the corresponding author by e-mail. Your response, with or without corrections, should be sent within 48 hours.

Offprints: Corresponding author will receive a free "electronic reprint" in Portable Document Format (PDF).

Compliance with these instructions is obligatory for all authors. If a manuscript does not comply with the above requirements, the editorial office will not accept it for a consideration and will return it to the authors without reviewing.

Research in **AGRICULTURAL ENGINEERING**

Volume 60 **2014**

Research in AGRICULTURAL ENGINEERING • Published by the Czech Academy of Agricultural Sciences • Editorial Office: Slezská 7, 120 00 Prague 2, Czech Republic, phone: + 420 227 010 606, fax: + 420 227 010 116, e-mail: rae@cazv.cz •
Distribution: Czech Academy of Agricultural Sciences, Slezská 7, 120 00 Prague 2, Czech Republic, phone: + 420 227 010 427, fax: + 420 227 010 116, e-mail: redakce@cazv.cz